Development of a dosing system for individualized therapy with oral films

Inaugural-Dissertation

zur Erlangung des Doktorgrades
der Mathematisch-Naturwissenschaftlichen Fakultät
der Heinrich-Heine-Universität Düsseldorf

vorgelegt von

Svenja Niese
aus Bad Soden am Taunus

Düsseldorf, Januar 2019

aus dem Institut für Pharmazeutische Technologie und Biopharmazie
der Heinrich-Heine-Universität Düsseldorf

Gedruckt mit der Genehmigung der
Mathematisch-Naturwissenschaftlichen Fakultät der
Heinrich-Heine-Universität Düsseldorf

Berichterstatter:

1. Prof. Dr. Jörg Breitkreutz

2. Prof. Dr. Dr. h.c. Peter Kleinebudde

Tag der mündlichen Prüfung: 04.04.2019

Publications

Parts of this thesis have already been published in peer reviewed journals or at conferences:

Original publications

- Niese, S. and Quodbach, J., 2018. *Application of a chromatic confocal measurement system as new approach for in-line wet film thickness determination in continuous oral film manufacturing processes.* Int J Pharm. 551, 203-211.
  DOI: 10.1016/j.ijpharm.2018.09.028

The idea was defined in collaboration by Svenja Niese and Julian Quodbach. The study design was mainly developed by Svenja Niese and optimized based on the advice of Julian Quodbach. Svenja Niese performed the experimental work and data evaluation. The manuscript was written by Svenja Niese and revised by Julian Quodbach.

Evaluation of the authorship I: "Application of a chromatic confocal measurement system as new approach for in-line wet film thickness determination in continuous oral film manufacturing processes".
Parts of contribution in %.

author	idea	study design	experimental	evaluation	manuscript
Svenja Niese	50	80	100	90	80
Julian Quodbach	50	20	0	10	20

- Niese, S. and Quodbach, J., 2019. *Formulation development of a continuously produced orodispersible film containing warfarin sodium for individualized dosing.* Eur J Pharm Biopharm. 136, 93-101.
  DOI: 10.1016/j.ejpb.2019.01.011

Svenja Niese was responsible for the idea and the study design of this research paper. Julian Quodbach gave helpful advice in the conceptualization of the idea and the development of the study design. The experimental work and data evaluation were performed by Svenja Niese. The manuscript was written by Svenja Niese and revised by Julian Quodbach.

Evaluation of the authorship II: "Formulation development of a continuously produced orodispersible film containing warfarin sodium for individualized dosing". Parts of contribution in %.

author	idea	study design	experimental	evaluation	manuscript
Svenja Niese	80	80	100	90	80
Julian Quodbach	20	20	0	10	20

- Niese, S., Breitkreutz, J. and Quodbach, J., 2019. *Development of a dosing device for individualized dosing of orodispersible warfarin films.* Int J Pharm. 561, 314-323. DOI: 10.1016/j.ijpharm.2019.03.019

The initial idea for this study was defined by Jörg Breitkreutz and developed by Svenja Niese in course of this work. The study design was mainly developed by Svenja Niese and optimized based on the advice of Jörg Breitkreutz and Julian Quodbach. Julian Quodbach also gave helpful advice for the conceptualization of the idea. The experimental work and data evaluation were performed by Svenja Niese. The manuscript was written by Svenja Niese and revised by Jörg Breitkreutz and Julian Quodbach.

Evaluation of the authorship III: "Development of a dosing device for individualized dosing of orodispersible warfarin films". Parts of contribution in %.

author	idea	study design	experimental	evaluation	manuscript
Svenja Niese	40	80	100	90	80
Jörg Breitkreutz	50	10	0	0	10
Julian Quodbach	10	10	0	10	10

Oral presentations

Niese, S., Breitkreutz, J. and Quodbach, J., *Development of a continuously produced orodispersible film for individual dosing of warfarin sodium,* 11th PBP World Meeting, Granada (Spain) 2018.

Niese, S. and Quodbach, J., *Critical evaluation of the tensile test for oral films,* 11th Annual Meeting of the PSSRC, Graz (Austria) 2017.

Poster presentations

Niese, S., Breitkreutz, J. and Quodbach, J., *Introducing a device for flexible dosing of oral films,* 2nd European Conference on Pharmaceutics, Krakow (Poland) 2017.

Niese, S., Breitkreutz, J. and Quodbach, J., *Investigating the suitability of release liners for solvent casting of oral films,* 10th PBP World Meeting, Glasgow (United Kingdom) 2016.

Table of Contents

Abbreviations and non-SI units

α	significance level
API	active pharmaceutical ingredient
ASTM	American Society for Testing and Materials
AV	acceptance value (Ph.Eur. 2.9.40)
CAD	computer aided design
CI	confidence interval
CMC	sodium carboxymethyl cellulose
CV	coefficient of variation
FDA	US Food and Drug Administration
FDM™	Fused Deposition Modeling
FINAT	Féderation internationale des fabricants et transformateurs d'adhésifs et thermocollants sur papiers et autres supports
HPC	hydroxypropyl cellulose
HPLC	high performance liquid chromatography
HPMC	hydroxypropyl methylcellulose
Hz	Hertz
ICH	International Council for Harmonisation of Technical Requirements for Pharmaceuticals for Human Use
INR	international normalized ratio
MCC	microcrystalline cellulose
n	number of samples
N	Newton
ODF	orodispersible film
ODT	orodispersible tablet
PE	polyethylene
PEG	polyethylene glycol

pH	negative decimal logarithm of the hydrogen ion activity
Ph.Eur.	European Pharmacopoeia
pk_a	negative decimal logarithm of the acid dissociation constant
PLA	polylactic acid
PVA	polyvinyl alcohol
R^2	coefficient of determination
RP	rayopeel
rpm	revolutions per minute
sd	standard deviation
SFE	surface free energy
SFT	surface tension
STL	stereolithography
σ_l	surface tension of the liquid
σ_s	surface free energy of the solid
σ_{sl}	interfacial tension solid and liquid
USP	United States Pharmacopoeia
UV	ultraviolet
WFT	wet film thickness

1. Introduction

1.1 Individualized dosing as opportunity for patient centricity

Individualized medicine is gaining in interest and importance in the last years in different parts of the medical and pharmaceutical care system. It is a task of the complete healthcare system to enable a customized treatment to the patient's individual needs. The individualized medicine in general also affects the pharmaceutical industry from formulation development through production, regulatory affairs up to clinical testing (Sternberger-Rützel et al., 2018).

Individualized medicine can increase safety of a pharmacotherapy by treating a patient with the right medicine at the right dose. Diagnostic tests enable prediction of a possible drug response to make sure the patient is treated in the correct way. An example of treatment with the appropriate active pharmaceutical ingredient (API) is the initial testing for HER2 (human epidermal growth factor receptor 2) in breast cancer patients prior to a treatment with the monoclonal antibody trastuzumab (Aktories, 2005; Roche Registration, 2018). Tests to decide for the correct API dose are recommended from the US Food and Drug Administration (FDA) for e.g. warfarin sodium (hereinafter referred to as warfarin) because of genetic variations influencing the metabolism (Jones, 2007). The safety of a therapy is improved by personalizing the doses for a patient since side effects due to overdosing are reduced and insufficient dosing because of too low doses is avoided as well. Individualized dosing as a part of personalized medicine is the possibility to react on differences in the needed drug dose resulting from individual needs because of age, gender, health status, ethnic affiliation and drug response (Breitkreutz and Boos, 2007; Standing and Tuleu, 2005; Stegemann et al., 2010; Sternberger-Rützel et al., 2018). Besides inter-individual differences, also intra-individual differences in drug dose requirement may be possible for the same patient at different times because the health status can differ. A well-coordinated individualized therapy may improve the therapy outcome because of better compliance due to reduced side effects as well as that the patient feels better looked after.

The parenteral application of APIs is the most flexible delivery route but poorly accepted by patients for a daily medication regime and presenting disadvantages such as the risk of infections and inflammations at the injection site. There are only few parenteral therapies with a regularly dosing regime, which are fully established and accepted, e.g. insulin therapy for

diabetes patients, which is a model example for individualized therapy. The dose needed is determined with a blood glucose test and then flexibly adjusted for administration using syringes or specialized dosing devices.

The most acceptable route of drug delivery is the oral application (Thabet et al., 2018a; Walsh et al., 2011; Wening and Breitkreutz, 2011). Wening and Breitkreutz (2011) presented possible approaches to enable flexible dosing for different oral dosage forms. The investigated approaches were evaluated with regard to a potential benefit after classifying them regarding their dosing concept (Figure 1), practicability, costs and dose flexibility. The main differentiation was made by distinguishing the dosing process between accumulation of multiple drug carriers and partition of monolithical dosage forms. For the route of dosing via partition of a small unit from a bigger unit, the dosing flexibility of a dosage form is mainly dependent on the dosing device used. The smaller the steps of the device the more flexible the dosing process. When accumulating units of a dosage form to the total dose, the flexibility is mainly dependent on the dose of the smallest unit. The utilized dosing device only assists to receive the correct number of small units to get the demanded dose.

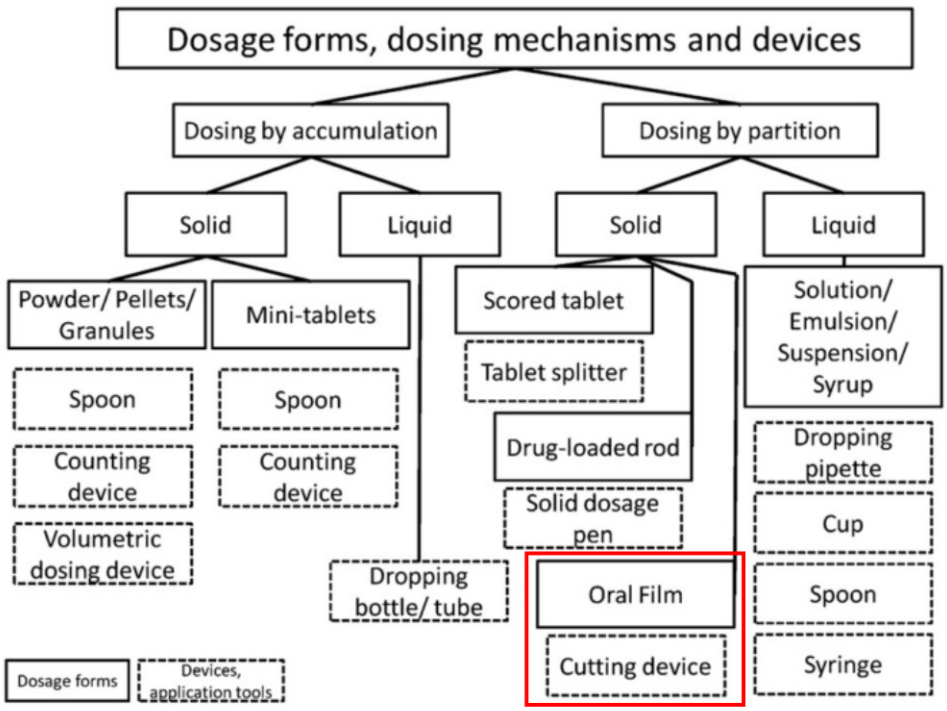

Figure 1: Classification system for oral dosage forms and their flexible dosing approaches (Wening and Breitkreutz, 2011). Used by courtesy of the International Journal of Pharmaceutics, Elsevier.

The most flexible oral dosage forms are liquids. However, disadvantages of liquids are the possible instabilities, drug solubility challenges, high costs, toxicological properties of excipients and short shelf-lives (Standing and Tuleu, 2005). Furthermore, the correct application of the dosing tools is essential for a safe use of liquid oral dosage forms but as shown in published studies the application of dosing tools is prone to error (Sobhani et al., 2008; Tanner et al., 2014). Therefore, solid dosage forms are of great interest for individual dosing for patients of all age groups. Inappropriate for individual dosing are tablets with common sizes since the practice of tablet splitting leads to risky dosing inaccuracies (Rosenberg et al., 2002; Teng et al., 2002; van Santen et al., 2002). An attempt to individualize the drug delivery with a tablet-like dosage form was made by introducing the concept of the Solid Dosage Pen, which cuts off individually dosed slices from a drug-loaded rod (Schoemakers and Grummel, 2002; Wening and Breitkreutz, 2010). A limiting factor of the dosage forms dispensed by the Solid Dosage Pen is the shape and size for patients with swallowing dysfunction and dysphagia (Stegemann et al., 2012). The slice obtained from the Solid Dosage Pen is similar to a conventional tablet and might show the same swallowing issues. A promising solid dosage form without swallowing difficulties for patients from neonates up to geriatrics are (orodispersible) mini-tablets. They show good acceptance (Klingmann, 2017; Klingmann et al., 2013; Spomer et al., 2012; Thabet et al., 2018a; van Riet-Nales et al., 2013) and allow flexible dosing by counting the mini-tablets with counting devices or by hand (Frampton, 2016; Mitra et al., 2017).

The acceptance studies on mini-tablets in neonates and children has facilitated the shift of paradigm from previously favored liquid formulations as syrups to flexible solid dosage forms (orodispersible tablets (ODTs), orodispersible films (ODFs), mini tablets) for the pediatric patient population (Stoltenberg and Breitkreutz, 2011; Thabet et al., 2018a). Besides mini-tablets, ODFs are a possible solid dosage form for flexible dosing not only for pediatrics but also for all patient age groups due to their easy intake without swallowing difficulties (Hoffmann et al., 2011; Visser et al., 2017b). Because of the need for solid dosage forms for safe and easy individualized dosing for pediatrics and geriatrics (Breitkreutz and Boos, 2007; Standing and Tuleu, 2005) as well as for all other patients with varying, individual health states (Schellekens et al., 2017), this work focuses on ODFs as an alternative to mini-tablets for flexible dose delivery.

The flexibility of drug therapy is not only dependent on the dosage form but can also be managed by different parties at varying stages during the life course of the drug. Individual

drug products can be manufactured already at the industry site, which might result in a "batch-size-of-one" scenario in future manufacturing concepts (Sternberger-Rützel et al., 2018). Closer to the patient would be hospitals or public pharmacies as well as compounding centers that provide patients with individualized drugs by preparing individual extemporaneous preparations from prefabricated materials after receiving a prescription from the doctor. This is possible for semi-solid formulations and capsules filled with an API, individual amounts of mini-tablets (Mitra et al., 2017) or with a printed substrate (Khinast et al., 2009). Customized provision might be possible as well for the preparation of ODFs (Steiner et al., 2018; Visser et al., 2015a; Visser et al., 2015b) or by cutting a premanufactured ODF into different sized pieces (Hoffmann et al., 2011). Furthermore, printing of one or more API-containing inks on a drug-free ODF is a possible customization of the film that might be feasible in a pharmacy (Alomari et al., 2015; Pardeike et al., 2011; Preis et al., 2015). The most flexible dosing is performed at the patient's home by a caregiver or the patient oneself. This enables a flexible dose adaption to the current health situation of the patient who may require different doses of a drug at different times. The patient would not rely on specialized personal in a pharmacy or the like to receive a different dose of the medication if the state of health would be about to change. This might be induced by the primary disease that can change for the better or the worse, as well as by additional medication with interaction potential or by the body condition e.g. changes in weight, nutrition or exercising. The independence of a further production step to receive a different dose can reduce costs for the drug therapy and treatment is not delayed for the patient reducing risk of failure of the therapy. Another dose is just received by flexible dosing from a stock dosage form instead of producing a new medicinal product and dispose the old one.

1.1.1 Warfarin sodium in need of true individualized dosing

An API that is in need of flexible dosing that is possible directly at the patient's home is the vitamin K antagonist warfarin. Due to a narrow therapeutic index and pronounced inter- and intra-individual variabilities in drug response because of genetic polymorphisms in people of different ages and ethnic groups (Aithal et al., 1999; Biss et al., 2012; Ma and Lu, 2011; Reynolds et al., 2007; Shastry, 2006; Yu et al., 1996) warfarin is an ideal model drug for individualized dosing.

The commentary of the European Pharmacopoeia proposes the individual dose adjustment of warfarin with help of an adequate test for the prothrombin time, most commonly the international normalized ratio (INR). The INR monitoring is advised for the duration of the

warfarin application to avoid adverse side effects as well as ineffectiveness of the antithrombotic therapy. The individualized therapy can be performed on the basis of INR blood measurements to decide for the appropriate API dose.

Warfarin was one of the first drugs for that pharmacogenomics testing was applied (PMC, 2017) to enable safe and effective therapy. A suitable test for variances in the pharmacogenomics influencing the effect of a drug is only beneficial if the following therapy can be adjusted to the result of the test. Hence, an urgent need to enable flexible dosing for this API exists, further supported by the fact that warfarin patients are also subject to intra-individual fluctuations in their demands on the daily dose.

Currently on the US market, where warfarin is mainly used, there are only tablets in varying strengths and a powder for reconstitution before injection. Although tablets are available in different strengths, patients probably will not have all necessary doses available at home to flexible adjust to the demanded dose if the API need changes. The previous dosed dosage form might be disposed, and a new dosed dosage form has to be purchased. The same problem exists for printing individual doses of warfarin on oral films (Vuddanda et al., 2018) or for preparing individual dosage forms via 3D-printing of filaments containing warfarin (Arafat et al., 2018) since all of these approaches are not performed by the patient. The British National Formulary for Children includes a so called “Special” for an oral suspension of 1 mg/ml warfarin (Paediatric Formulary Committee, 2014). This oral liquid formulation is the most flexible dosage form available for the patient at home but presents problems with a short shelf-life and lacking studies about pharmacokinetic and pharmacodynamics since the “Special” does not hold a marketing authorization (Standing and Tuleu, 2005).

Therefore, there is a gap to be filled for individualized dosing enabling flexible warfarin therapy directly at the patient’s home. No additional production steps ought to be necessary. Filling this gap is subject of this thesis and supposed to be approached by the use of oral films that will be flexibly dispensed with a dosing device (Figure 1, marked in red).

1.2 Opportunities and challenges for oral films in individualized therapy

Parts of this section have already been published in a peer-reviewed journal. The content was linguistically adapted, and data sets were partly extended.

- Niese, S., Breitkreutz, J. and Quodbach, J., 2019. *Development of a dosing device for individualized dosing of orodispersible warfarin films.* Int J Pharm. 561, 314-323. DOI: 10.1016/j.ijpharm.2019.03.019.

Oral films are defined in the European Pharmacopeia in the monograph of oromucosal preparations. The different film types were classified and discussed by Preis et al. (2013) presenting the main types as mucoadhesive buccal films and orodispersible films. Mucoadhesive buccal films are "intended for systematic absorption through the buccal mucosa over a prolonged period of time" (Ph.Eur 9.3, 2018a), whereas orodispersible films are "single- or multilayer sheets of suitable materials, to be placed in the mouth where they disperse rapidly" (Ph.Eur 9.3, 2018a). Since there are no large pieces left over after dissolution of ODFs that have to be swallowed, this solid dosage form suits the use for patients with swallowing difficulties, dysphagia or fear of choking (Hoffmann et al., 2011; Stegemann et al., 2012). An advantage for patients dealing with liquid restrictions due to illnesses is that the administration of oral films requires practically no consumption of water (Visser et al., 2017b). The easy administration of ODFs is a valuable benefit for patient compliance (Borges et al., 2015).

The most commonly used preparation method for oral films is the solvent casting procedure (Borges et al., 2015; Dixit and Puthli, 2009; Hoffmann et al., 2011) that can be performed in petri dishes (El-Setouhy and El-Malak, 2010), on small-scale film applicators (Garsuch and Breitkreutz, 2010; Preis et al., 2012) or on pilot-scale coating benches (Thabet and Breitkreutz, 2018; Thabet et al., 2018c) using a process liner as substrate to cast the film on. A similar process is used for large-scale production lines to manufacture oral films in the industries (Hoffmann et al., 2011). The polymer masses usually contain one or more polymers as matrix former, one or more APIs, solvent and additional optional ingredients like plasticizers, fillers or taste masking agents. The mass is cast on the process liner, dried and cut into pieces of the desired size and shape (Hariharan and Bogue, 2009; Lee et al., 2017). Another, less frequently used manufacturing method is the hot-melt extrusion of oral films (Repka et al., 2005; Repka

et al., 2003; Stanković et al., 2015) that might be an alternative manufacturing process for APIs, which are hard to handle in aqueous polymer masses but can withstand high temperatures. A promising manufacturing technique is the printing of an API ink onto (drug-free) oral films (Alomari et al., 2015; Janßen et al., 2013; Pardeike et al., 2011; Preis et al., 2015). The API containing ink may be printed on drug-free films or films containing another API in the polymer matrix (Thabet et al., 2018b) resulting in flexible drug-dose and drug-drug combinations. Another advantage is the prevention of toxic waste by reducing cutting waste of API containing film pieces when printing on drug-free films (Preis et al., 2015).

The option to be cut is an important advantage of oral films, which enables the flexibility of dosages that may be obtained. The manufactured film can be divided into flexible doses by cutting off pieces corresponding to the demanded drug dose (Hoffmann et al., 2011; Visser et al., 2015b). To ensure correct dosing of differently sized pieces, the height of the film has to be accurate and uniform throughout the whole film (Susarla et al., 2013). The dose of a film piece is then only dependent on the area of the piece, provided that the film was cast with a homogenous polymer/API mass (Jansen and Horstmann, 2014). Because of fast disintegration of ODFs, the flexible dosing does not influence the efficacy of the product by revealing different dissolution behaviors for differently sized pieces. Cutting may be performed for example in pharmacies preparing individualized film pieces for different patients depending on a prescription of a physician. For improved personalization it should be possible that the patient cuts the film into the required size according to the present dosage need (Wening and Breitkreutz, 2011). This requires a special dosing device to ensure correct and precise dispensing of the oral film (Figure 1, marked in red). There is currently no such device available although several patents can be found in literature. The following section will give an overview of the patent situation for oral film dispensers.

1.2.1 Patent situation of technologies for dispensing film shaped materials

A patent search revealed many results for devices that dispense some kind of a film shaped material. Starting from paper, foils and wrap film (Denter et al., 1986; Labrecque, 1990) over stamps (Groeneweg, 1998) and labels (Avery, 1942), office materials (Messina, 2004; Sakanishi, 2006) and adhesive tape (Blum, 2000; De Man and Boes, 1999; Lee, 1999) up to medical supplies such as strip bandages (Damikolas, 1998; Ross, 2003) and wound dressings (D'Angelis, 2006), or food products (Kind and Dorfman, 1995). Dispensing devices can be found in different areas, but also in the field of pharmaceutical products. Devices to dispend

strips containing single packed tablets or powder units (Anderson et al., 2003; Arens, 1953) were developed and patented as well as inhalation devices working on a similar principle by delivering single packed powder doses to the patient when inhaling form the device (Davies et al., 1990).

For dispensing a long oral film strip, different ideas were filed as patents, which have partially already expired and some of them have never been granted. However, the state of the art is available and shall therefore be mentioned here. The following list makes no claim for completeness since it shall only give a summary of the possible ideas. For non-pharmaceutical oral film strips, used as breath fresheners, multi-dose containers are patented and on the market that comprise multiple stamp-sized film pieces (Evans and Gieda, 2002). This kind of packaging is difficult for pharmaceutical products since the stability regarding climatic conditions and possible microbial contaminations is not guaranteed. An advancement that solves this problem is the so called “Rapidcard”, which is a multi-dose container for pharmaceutical flat administration forms that are individually packed and therefore stability is ensured (Lehrke et al., 2004). However, this invention is only a packaging unit for films with predefined size and cannot dispense flexible pieces of a long film strip. A selection of patents found of devices that work as dispensers for oral film strips is shown in Figure 2. These examples show some ideas how to enable dosing of an oral film strip to individualize drug therapy. Nevertheless, they show also points that have to be criticized and that ought to be improved in course of this work.

The first patent that is presented in Figure 2 a was filed by Leichter and Blake (2003) and shows a dispenser that contains a film strip that is coiled up with a base layer that serves as a separator between the layers of the oral film. By pushing down the upper housing of the dispenser a piece of the film is dispensed in front of the device. When the upper housing is pushed down completely, a knife that is positioned in the upper housing cuts the dispensed film piece right after the exit slot. The film is unrolled by a rack and pinion drive where the rack is fixed to the upper housing and the pinion is the outer shell of the drum where the coiled-up film strip is located in. While the rack moves the drum, the base layer is separated from the film and collected in the bottom of the device so that only the film is dispensed. A positive development of this patented device is the idea to store the base layer in the device so the patient is not able to ingest it accidentally. However, negative points to consider are that only a predefined length of the film strip can be dispensed, determined by the length of the rack and pinion drive. This is not suitable for the intended flexible dosing of different lengths.

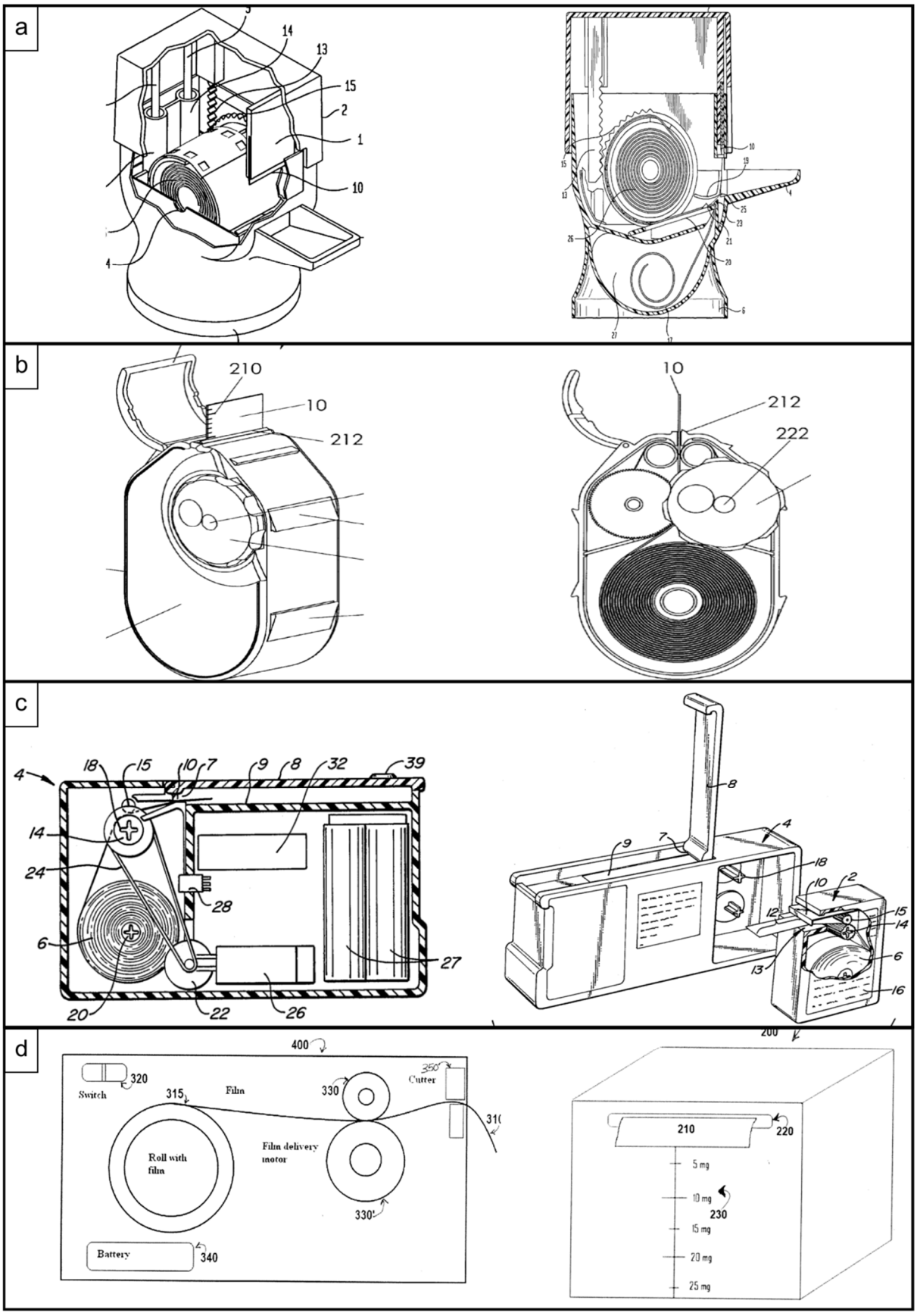

Figure 2: Selection of oral film strip dispensing devices described in patents.
a: Leichter and Blake (2003), b: Sheffield (2011), c: Allen et al. (1985), d: Yuan (2013).
Used by courtesy of the International Journal of Pharmaceutics, Elsevier (Niese et al., 2019).

Furthermore, the single base layer provides not enough protection to ensure stability of the film strip.

The next patent presented in Figure 2 b was filed by Sheffield (2011). A dispenser is described that houses a long coiled-up film strip that is packed between two packaging layers. The film strip is dispensed through an opening at the front and the packaging layers are coiled up in the device after releasing the film strip. The device can be closed with a cap positioned in front of the opening. The dispensing process is driven by a rotary knob at the outside of the housing that is connected to one of the rolls collecting the packaging layers. The dosing steps are marked directly on the film that then can be teared off at the desired dose. Beneficial features of this invention are the packaging of the film strips from both sides to ensure stability and the cap that closes up the device from the outer surroundings. The packaging layers are collected in the device as well as in the previous presented dispenser, which avoids accidental intake by the patient. Furthermore, this device enables a flexible dosing of the long film strip by rotating the knob as long as necessary until the desired dose is dispensed. Positive as well, is the fact that the device is not powered electrically. The movements are produced by the power spent by the user. Negative is the fact that no cutting unit is included and that the film is only detached by tearing it off. The tearing procedure might lead to a deformation of the thin film strip and therefore to a change in the dispensed dose since the dose is dependent from the length of the film. Likewise, the applied dosing scale on the film is very small and might be difficult to read, which might cause dosing errors because of miscounting the marked steps.

Another patent shown in Figure 2 c was filed by Allen et al. (1985) already more than three decades ago. The battery-operated device consists of two main parts. The reusable housing that contains the power unit and two rotating pins with a cross-shaped axis and the disposable cartridge that contains two rolls with a cross-shaped slot. The lower roll is used to coil up the film strip whereas the upper roll is positioned to guide the film strip to the outside of the cartridge and the device. The guiding roll is connected to the power unit to receive the motion that is conveyed by a belt. When the cartridge is inserted in the device the film is dispensed through an opening at the top of the housing. When closing the cover after dispensing the film, it is used to press down a blade on the dispensed film strip to cut it off behind the opening. The electrical power unit makes some interesting features possible that are described in the patent. The device may be customized to dispense a set dose, or a time can be set when the next dose is dispensed or an alarm sets off. The remaining doses can be monitored on the display as well as the current time. Although the electrical power unit enables interesting features providing

extended patient safety it is also prone to errors. Furthermore, it is expensive to produce, which is balanced out a little with the reuse option by providing a disposable cartridge that can be replaced. The film strip is not packed within this device, which necessitates a very tight design of the cartridge and the housing to ensure stability of the film. Advantages of the presented device are the flexible dosing and the included cutting blade that is positioned in a safe place to avoid risk of injury.

The last presented patent in Figure 2 d that was filed by Yuan (2013) is also an battery-operated device (left). The film strip is coiled up on a roll and delivered to the outside between two motor rolls. At the opening, where the film leaves the device, a cutter is located to cut off the film after the dispensing process. The length of the dispensed film piece is measured by the revolutions of the motor rolls and has to be calibrated to the dose per length of the used film. Another embodiment of the dispenser presented in this patent is run without battery power (Figure 2 d, right). This device is actually only a container that houses a coiled-up film that is pulled out by the patient. The dispensed length is determined by either marks on the housing or by marks applied on the film. The main disadvantage of both approaches is the missing packaging of the film strip risking stability issues. Whereas the electronically-driven device shows the disadvantage of higher susceptibility to failure without any additional features as for example presented in the previous patent, the second approach only presents a container without cutting unit or dispensing unit. The film is dispensed by pulling and therefore the risk of deformation of the film is present, which might lead to dosing inaccuracies. Favorable is the flexible dosing of different lengths of the film strip and the cutting unit in the electronical approach.

The presented patents all show positive and negative features that ought to be improved for a successful implementation into individualized therapy according to pharmaceutical requirements. The most important property is the option of flexible dosing in steps as small as possible for the incorporated API since this is the benefit of a dosing device compared to single-dosed oral films. The dosing steps have to be clearly noticeable by the patient to avoid dosing failure due to miscounting. A suitable cutting unit has to be incorporated in the device to ensure proper cutting of the film without deformation due to pulling stresses applied by the user. The storage of the long film in the device calls for a good packaging of the film to ensure stability over the time of usage or storage. The device has to be as tight as possible towards the outer surrounding moisture conditions to avoid stability issues for the parts of the film that might already be unpacked due to the working mechanism of the device. The packaging has to be

stored in the device after releasing the film to the outside of the device. This avoids accidental intake of the waste material and risk of injury for the patient. To reduce production costs of the device, the motion should be coming from a mechanical operating system rather than from an electrical power unit.

1.3 FDM™ 3D-printing as a tool for rapid prototyping

3D-printing is a rapid prototyping technique and also referred to as additive manufacturing, where a model is build (added) up layer by layer (Gardan, 2015). Additive manufacturing enables the fast and easy production of parts that are highly customized without the need of specialized equipment like machinery or molds except of the 3D-printer (Berman, 2012; Ligon et al., 2017). All kind of shapes can be printed with a 3D-printer that are difficult or impossible to produce with common manufacturing processes due to complicated hollow (Figure 3, left) or lightweight structures (Figure 3, right) that need complex cross sectional areas to reduce the overall weight but maintain stability (Wong and Hernandez, 2012).

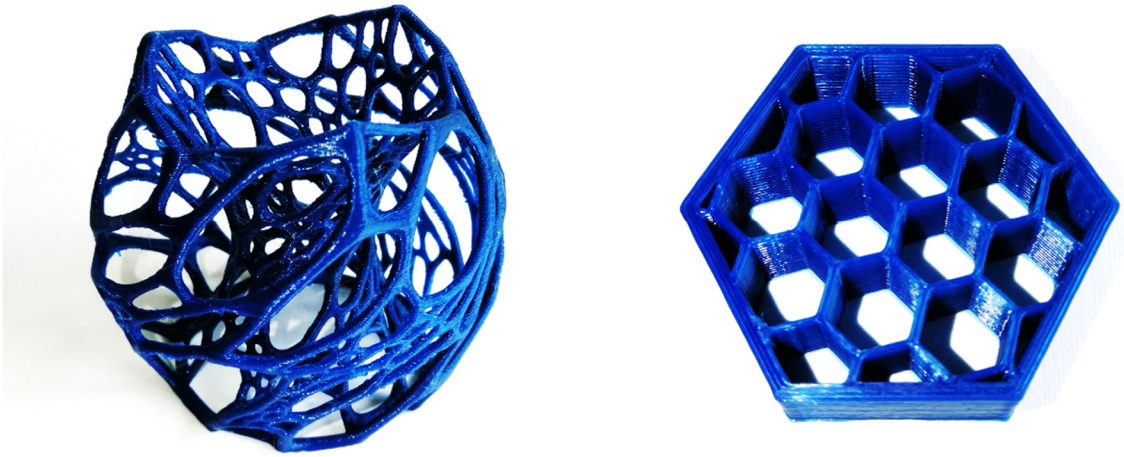

Figure 3: 3D-printed objects showing sophisticated hollow structures (left, model by user "nervoussystem" at www.thingiverse.com/thing:19104) and lightweight structures with a honeycomb infill pattern (right).

3D-printing can be applied to generate prototypes in the course of product design processes. A prototype is a model that enhances the development of a product by speeding up the design process. The virtual designed product becomes tangible in a 3D-object and product properties can be tested and evaluated already in early development stages (Berman, 2012; Gebhardt, 2016). Depending on the development stage the prototype can be used to just get an idea of the shape and the appearance of the object or in advanced stages the prototype may serve as a working model with functional parts (Gebhardt, 2016). The working model is used to prove functionality of the designed product. The prepared prototype may be printed from cheap materials to get an idea of the product, whereas the finished object can be produced from a more expensive material for example metal. The expensive manufacturing of metal parts at different stages of product development is avoided and the costs of the development can be

reduced (Berman, 2012). Furthermore, it might not be necessary to prepare the prototype with the exact identical properties as the final product, e.g. regarding the inner structure if the prototype shall just illustrate the three-dimensional design. The principal idea of rapid prototyping for product cycle development is pictured in a summarized form in Figure 4. If the prototype is not meeting the design criteria in the first step the design process can be repeated until the prototype meets the criteria. If the designed prototype matches with approval, the final product can be produced with an adequate manufacturing method. For all the steps before the final production of the product, no specialized machinery or staff is needed, which massively reduces time and costs (Gardan, 2015; Upcraft and Fletcher, 2003).

There are different techniques referred to as 3D-printing or additive manufacturing that can be classified into liquid-, solid-, semi-solid- and powder-based techniques depending on the materials used as starting materials (Alhnan et al., 2016; Gardan, 2015; Wong and Hernandez, 2012). In the present thesis, the FDM™ technology (fused deposition modeling), also called fused filament fabrication, was used as rapid prototyping technique. The filament, a thin polymer strand, is molten in a heated print head and delivered through a nozzle that positions the molten polymer strand on the print bed according to the X- and Y-coordinates provided to the 3D-printer. When one layer (X-Y-directions) is finished, the Z-axis moves vertically for exact one layer height and the next layer is positioned on the first, building up the three-dimensional object (Gardan, 2015; Ligon et al., 2017; Upcraft and Fletcher, 2003). The coordinates for the movements are provided to the 3D-printer in form of the so-called G-code. This code is obtained from the slicing software that processes the 3D-file coming from the

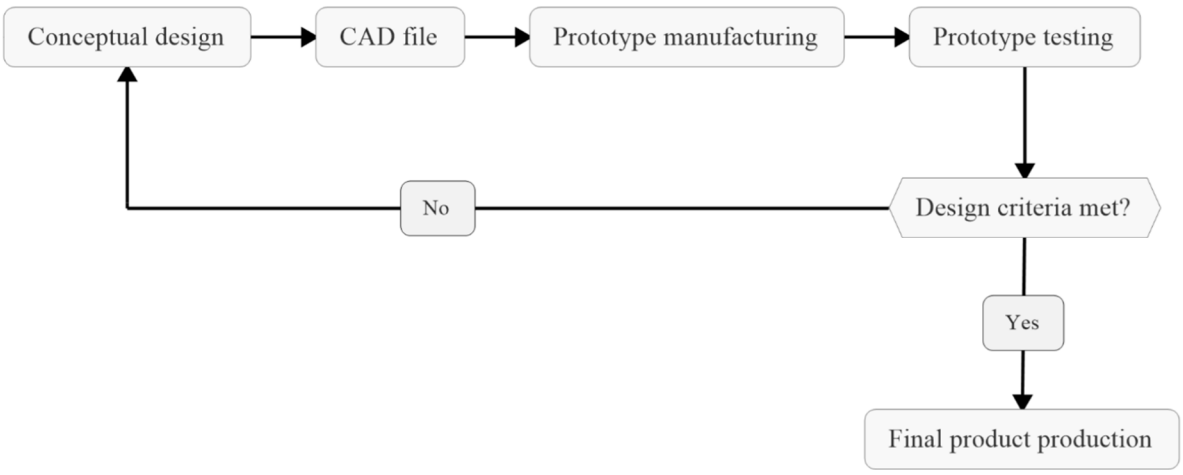

Figure 4: Rapid prototyping for improved product development. Adapted from Wong and Hernandez (2012).

CAD (computer aided design)-software. The slicing software converts the object from the 3D-file into a layered object (refer to Figure 66 and section 5.5.1) and assigns coordinates that have to be performed by the 3D-printer to manufacture this object layer by layer. After the object has been printed it can be post-processed to improve the surface appearance or to remove scaffolds that are used to support overhangs that would not be printable out of nothing.

The prepared CAD-files are further beneficial as virtual prototypes to get a first impression, e.g. whether different parts fit together when assembled, or whether the developed movement might be possible. The CAD-files can be used to simulate movement processes to ensure that no component of the product fails to work with the other components. This might save more time and costs if performed before manufacturing of the first three-dimensional prototypes.

2. Aims and Outline

This work focuses on the development of a novel dosing system enabling the individualized therapy with oral films. A prototype shall be developed to be compliant with the specifications given by the European Pharmacopeia. The approaches presented in the overview of patents of film strip dispensers in the introduction of this work showed already some beneficial ideas as well as some items that have to be improved. The beneficial features shall be combined with the improved negatively rated points to develop a dosing device that enables successful flexible dosing of an oral film strip to improve individualized therapy with this solid dosage form for patients of all age groups, especially including children. The device and, therefore the step of dose individualization shall be manageable by the patient or the caregiver. No additional production step shall be necessary that would require specialized equipment.

Furthermore, the development of an appropriate ODF for the use in the dosing device was part of the dosing system design and development. The manufacturing of the ODF is supposed to be performed by a pilot-scale manufacturing process to obtain long oral films that can be coiled up for the use in the device. The formulation development shall start on a small-scale coating bench and suitable formulations shall be scaled up to the pilot-scale coating bench afterwards. The formulation development shall be conducted as a systematic approach considering the manufacturing process and the requirements given by the use of the ODF in the dosing device and the handling by the patient. Therefore, properties like the viscosity of the polymer solution, the mechanical resistance, content uniformity and the physical and chemical stability of the dried film shall be investigated.

The pilot-scale manufacturing process shall be optimized by implementing a process analytical technology tool to determine the wet film thickness of the produced film during the process. The novel in-line measurement of the film thickness as critical parameter for the content uniformity of the produced oral film will improve the film production using the solvent casting technique. Until now, the control of the process was not feasible regarding the film thickness.

Warfarin has been chosen as model drug, as it is a reasonable drug substance for individualized therapy with oral films. There is a current need for flexible dosing in adults as well as children. The usually required daily doses and the physicochemical properties of warfarin allow the incorporation in an oral film.

The prototype of the dosing device will be produced via 3D-printing as rapid prototyping technique using an FDM™ printer. By this means, the developed device can be easily improved by redesigning and reprinting individual parts. The 3D-printed prototype of the dosing device will be used to perform proof of concept studies for the functionality of the intended use to demonstrate the correct working within the specifications given by the European Pharmacopoeia.

3. Results and Discussion

3.1 Formulation development of drug-free orodispersible films

3.1.1 Introduction and objectives

The first aim of this work was to conduct a pharmaceutical excipient screening to manufacture orodispersible films and to find basic drug-free formulations for further investigations. For this purpose, film manufacturing with a small-scale coating bench was considered due to small batch sizes. This approach saved material and time compared to the film manufacturing process on the pilot-scale coating bench, which was supposed to be used for film manufacturing of the final long ODFs. In the end, the developed ODFs were supposed to be suitable for the use in a dosing device for their flexible dosing. The dosing device should be developed in course of this work.

Therefore, some requirements had to be considered during the preliminary formulation development approach for drug-free ODFs. On the one hand, the film forming mass was supposed to be processible on the pilot-scale coating bench in later experiments. For this process the most critical parameter was identified as the viscosity (Thabet and Breitkreutz, 2018). The viscosity must neither be too low nor too high to form a satisfying film on the process liner during the film manufacturing process (Hariharan and Bogue, 2009; Thabet and Breitkreutz, 2018). In addition, the sufficient formation of a homogenous film on the process liner is of great relevance for the ODF production as well as that the dried film can be separated from the liner without spontaneous delamination (Hariharan and Bogue, 2009). On the other hand, the dried ODFs shall withstand the use in a potential dosing device, which may be handled by the patient as operator. Sufficient mechanical properties are essential, especially great resilience to the tensile stress, as the patient might apply high forces onto the film utilizing the dosing device. Since the film is supposed to be dosed by length, a deformation of the film due to mechanical stress will lead to unacceptable dosing inaccuracies. The oral film should act orodispersible, which means that the disintegration time was a factor that had to be assessed as well during this part of the work (Ph.Eur 9.3, 2018a). Furthermore, common critical attributes of oral films were investigated and evaluated.

3.1.2 Excipient screening on the small-scale coating bench

The excipient selection was performed after screening the literature for the preparation of ODFs. Commonly used film forming polymers and plasticizers were chosen for the use in this work. Since the developed ODF is supposed to be suitable for the use in children, the formulation should consist of as few as possible excipients without critical components not suitable for the use in pediatric formulations (EMA, 2013). Therefore, for example no propylene glycol was used as plasticizer since higher doses of this substance are not recommended for children under the age of four years (Breitkreutz et al., 2002; Thabet et al., 2018a). Because of a limitation in the metabolism, propylene glycol can accumulate in the children's body, which can lead to seizures, irregular heartbeats and in the worst case to death (MacDonald et al., 1987). In case of unsatisfying film properties, the first approach was to change the polymer concentration, the polymer itself or the plasticizer rather than adding new excipients to the formulation.

Water-soluble film forming polymers were selected for the preparation of orodispersible, and therefore, water-soluble films. The uncharged cellulose derivatives hydroxypropyl methylcellulose (HPMC) (El-Setouhy and El-Malak, 2010; Garsuch and Breitkreutz, 2010; Janßen et al., 2013; Kulkarni et al., 2010) and hydroxypropyl cellulose (HPC) (Boateng et al., 2009; Thabet and Breitkreutz, 2018) show good film forming properties and are available in various grades enabling a variable adjustment of the viscosity for the film forming mass. As alternative polymers polyvinyl alcohol (PVA) (El-Setouhy and El-Malak, 2010; Hariharan and Bogue, 2009; Kulkarni et al., 2010), the polysaccharide pullulan (Kulkarni et al., 2010; Panchal et al., 2012) and the charged cellulose derivative sodium carboxymethyl cellulose (CMC) (Lee et al., 2017) were taken into consideration.

To optimize the mechanical properties, the addition of a plasticizer was evaluated. Glycerol as the probably most commonly used plasticizing agent in oral film preparation was selected for the development of the basic formulation (Garsuch and Breitkreutz, 2010; Kulkarni et al., 2010; Patel et al., 2010; Thabet and Breitkreutz, 2018). Glycerol was not added to HPC films because the manufacturer specifications stated that the polymer does not require plasticizer addition because of its elastic nature (Ashland, 2017). Table 1 gives an overview of the formulations investigated in this part of the work.

Table 1: Drug-free formulations for small-scale coating bench trials. Percentages referred to total weight (w/w). Dynamic viscosity measured at $4s^{-1}$ (mean ± sd, n = 3). HPMC: Pharmacoat® 606; HPC: Klucel™ (type); CMC: Walocel® C30 PA 09.

Formulation	Polymer [%]		Glycerol [%]	Viscosity [Pa*s]
R	Listerine® Cool Mint® Breath Strips (marketed product)			
F1	HPMC	15	3	1.37 ± 0.01
F2	HPMC	17.5	3.5	2.94 ± 0,01
F3	HPMC	20	4	6.10 ± 0.04
F4	HPMC	25	5	---
F5	Pullulan	20	---	0.71 ± 0.02
F6	HPC (ELF)	15	---	0.77 ± 0.00
F7	HPC (ELF)	17.5	---	1.47 ± 0.01
F8	HPC (ELF)	20	---	2.85 ± 0.02
F9	HPC (ELF)	25	---	8.82 ± 0.13
F10	HPC (EXF)	14	---	1.45 ± 0.03
F11	HPC (EXF)	15	---	2.09 ± 0.01
F12	HPC (EXF)	17.5	---	4.03 ± 0.01
F13	HPC (JXF)	10	---	2.32 ± 0.01
F14	HPC (JXF)	12.5	---	5.77 ± 0.03
F15	CMC	8	3	2.43 ± 0.02

3.1.3 Formulation optimization

The aim of the preliminary formulation development was to optimize the polymer solutions with the selected polymers for the use on the pilot-scale coating bench. Thabet and Breitkreutz (2018) defined a threshold for the dynamic viscosity of the polymer mass, which it is required to comply with for a successful film manufacturing process. The formulations were supposed to surpass this threshold of a minimum viscosity of 1 Pa*s. Rheological measurements with the rheometer were performed for all the polymer solutions (refer to section 5.4.1). First, a shear rate ramp was recorded to examine the flowing properties of the polymer solutions and to identify possible time dependent flow characteristics like thixotropy, recognizable by a hysteresis between the curves of the measurement towards higher shear rates and the measurement back towards lower shear rates. The shear rate ramp was recorded for shear rates from 0 to 100 s^{-1} representing the range that includes the general reached shear rates during the film manufacturing process. The investigated polymer solutions showed no time dependent flow characteristics. A slight pseudoplastic flow behavior was observed for the polymer solutions. The higher the viscosity at low shear rates the more pronounced was the decrease in viscosity towards higher shear rates. For further comparison of the polymer solutions, the

viscosity at a shear rate of 4 s^{-1} was measured and considered since it represents the conditions during the coating process.

Different concentrations of polymers were chosen, and the viscosity was measured (Table 1). For formulation F4, no viscosity is presented since the HPMC mass did not form a completely dissolved solution in a sufficient time with the high amount of polymer. Therefore, further trials were focused on HPMC formulations with less than 25 % polymer content. Formulations with 20 % pullulan and 15 % HPC (ELF) show viscosities below the recommended threshold and were discarded. Pullulan was not further investigated due to high costs and because a high polymer content would be necessary to reach the threshold for the viscosity. To improve formulation F6, the content of the HPC (ELF) was raised to 17.5 %, 20 % and 25 %. These samples show acceptable viscosities above the threshold. Coating masses with high viscosities can lead to spreadability problems on the process liner during the film manufacturing process due to higher contact angles, and therefore should be avoided as well (Hariharan and Bogue, 2009). The viscosity of the polymer solutions, processible on the pilot-scale coating bench by Thabet and Breitkreutz (2018) ranged up to 5.66 ± 0.07 Pa*s. Therefore, formulations with viscosities higher than this were discarded for further investigations. This was the case for formulations F3 and F9.

3.1.4 Process liner selection

3.1.4.1 General considerations

Another relevant aspect of the film manufacturing process is the selection of the process liner, which is the substrate the film is coated onto. It is designated as process liner since it is only used during the manufacturing process and does not remain with the dry film as final dosage form. Depending on the properties of the liner, the casting mass might not spread sufficiently, and no homogenous film might be formed. Further, the dried film has to adhere to the liner until the user wants to take it off for further processing (Hariharan and Bogue, 2009). To select an appropriate process liner for further investigations and the production of oral films on the continuously working pilot-scale coating bench, a study comparing different polymer solutions and different process liners regarding their compatibility was conducted.

Three polymer solutions containing the polymers HPMC (Formulation F1, Table 1), CMC (Formulation F15, Table 1) and HPC (Formulation F10, Table 1) were cast on five different process liners (refer to Table 22 and section 5.1) with the small scale coating bench as explained in section 5.3.3. Different behaviors of the prepared films were observed during

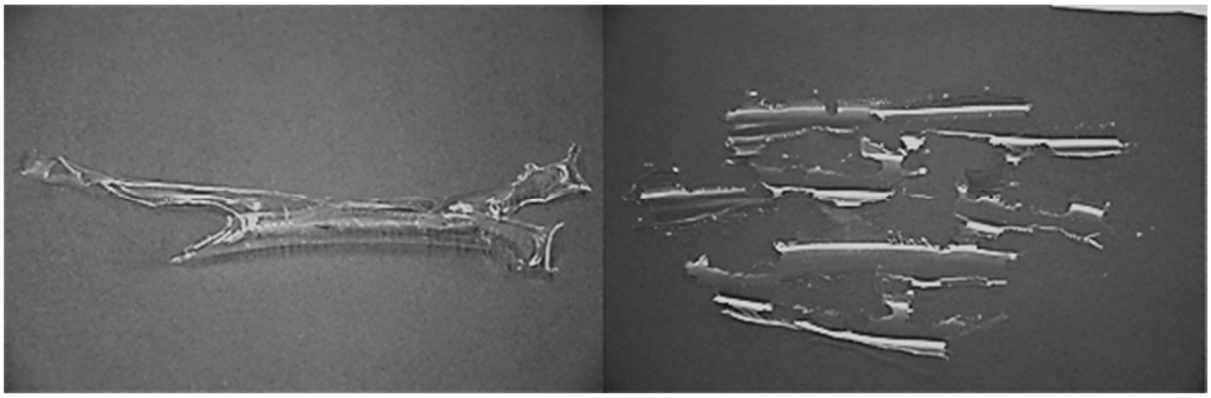

Figure 5: Dried films with unacceptable results from solvent casting.
Left: Fully retracted HPMC film on Liner 5. Right: Perforated CMC film on Liner 2.

the casting process and during the drying step (Table 2). Some films showed an acceptable casting process resulting in homogenous films while others retracted completely to the center of the liner (Figure 5, left). Some other films showed a casting behavior in between of these extreme examples. They were castable to a film and did not fully retract. However, they formed holes during drying and resulted in a perforated film (Figure 5, right). The aim of this study was to explain the different behaviors and investigate whether the compatibility between polymer mass and process liner can be determined beforehand to reduce trial and error approaches.

3.1.4.2 Surface properties

For better explanation of the different film forming behaviors, surface properties of the polymer solutions and of the process liners were determined and evaluated. The contact angle of the polymer solution on the process liner was measured (refer to section 5.4.14). Although the deposition of a drop of the solution on the liner with a syringe was not exactly comparable with the casting process of the film, the results underlined the visually observed solvent casting results of the polymer solution/liner combinations (Table 2). The polymer solutions that retracted on the liner showed contact angles above 90° representing bad wetting behavior (red). The polymer solutions that were castable on the liners showed contact angles lower than 90° and showed an acceptable wetting behavior in the first instance (Bauer et al., 2017). The problems on Liner 3 arose from the wavy manner of the very thin liner foil. The films could not adhere well to the liner because the movement of the liner was transferred to the film and caused delamination. The formation of the perforated films from CMC on Liner 2 and Liner 4 were not explainable with the contact angles measured as single parameter. Although contact angles were lower than 90° for both combinations, no homogenous films were formed. Therefore, another explanation needs to be found.

Table 2: Solvent casting results (green: acceptable films; light red: minor problems; dark red: retracted films) and contact angles of the polymer solutions on the process liners (mean ± CI, α = 0.05, n = 10).

rating / contact angle θ	**HPMC**	**CMC**	**HPC**
Liner 1	acceptable	acceptable	acceptable
	54.5 ± 1.3°	80.7 ± 1.8°	56.0 ± 2.7°
Liner 2	acceptable	perforated	acceptable
	70.7 ± 2.2°	81.9 ± 1.2°	65.0 ± 4.6°
Liner 3	no adhesion to liner	retracted, no adhesion to liner	acceptable, handling problems
	79.3 ± 5.8°	98.8 ± 1.0°	73.7 ± 0.9°
Liner 4	acceptable	perforated	acceptable
	72.1 ± 1.4°	69.3 ± 4.2°	63.9 ± 2.1°
Liner 5	retracted, no adhesion to liner	retracted, no adhesion to liner	retracted, no adhesion to liner
	90.7 ± 1.5°	107.4 ± 1.0°	93.2 ± 5.1°

For further investigations into the observed behavior, the surface free energy (SFE) of the process liners was determined. The SFE is the free energy of a solid against its saturated vapor (Owens and Wendt, 1969). It is the workload that is needed to create a new surface unit [J/m² = Nm/m² = N/m] (Rudawska and Jacniacka, 2009). Measuring this work is not directly possible since the work to increase the surface has to be differentiated from the work of deformation of the solid. Compared with this, the surface tension (SFT), as the surface free energy of a liquid is called, is easily measured using a tensiometer. As shown in the Young's equation (refer to Equation 9 and section 5.4.15) wetting is favored if the SFE of the solid is high whereas the SFT of the liquid should be low as well as the interfacial tension of the two phases (Bauer et al., 2017; Owens and Wendt, 1969; Young, 1805). This is explainable because materials with high SFE tend to enter a more favorable thermodynamic state. This state is reached by wetting the solid with a liquid showing a lower SFT. Calculations to determine the SFE of the process liners were performed as described in section 5.4.15. The contact angles of water and diiodomethane were measured on the process liners (refer to section 5.4.14) and are presented in Table 3. These contact angles together with the literature values of the absolute SFT and the polar and dispersive interacting parts of the SFT of the test liquids were used for the calculation of the SFE of the process liners.

Table 3: Contact angles of test liquids on the process liners (mean ± CI, α = 0.05, n = 20) and literature values of absolute SFT and dispersive and polar parts of the test liquids (Ström et al., 1987).

	Contact angle diiodomethane [°]	**Contact angle water [°]**
Liner 1	63.1 ± 1.9	76.9 ± 0.8
Liner 2	57.6 ± 1.4	83.0 ± 0.7
Liner 3	61.0 ± 1.4	100.3 ± 0.6
Liner 4	45.6 ± 1.8	80.9 ± 1.8
Liner 5	101.1 ± 1.7	107.3 ± 1.1

	Diiodomethane	**Water**
SFT [mN/m]	50.8	72.8
SFT(D) [mN/m]	50.8	21.8
SFT(P) [mN/m]	0	51.0

The calculated SFE values for the process liners are shown in Figure 6. The absolute SFE can be divided in dispersive interactions and polar interactions (Fowkes, 1962; Owens and Wendt, 1969). The bigger the polar interactions of the SFE, the better are the possible interactions with polar materials and vice versa.

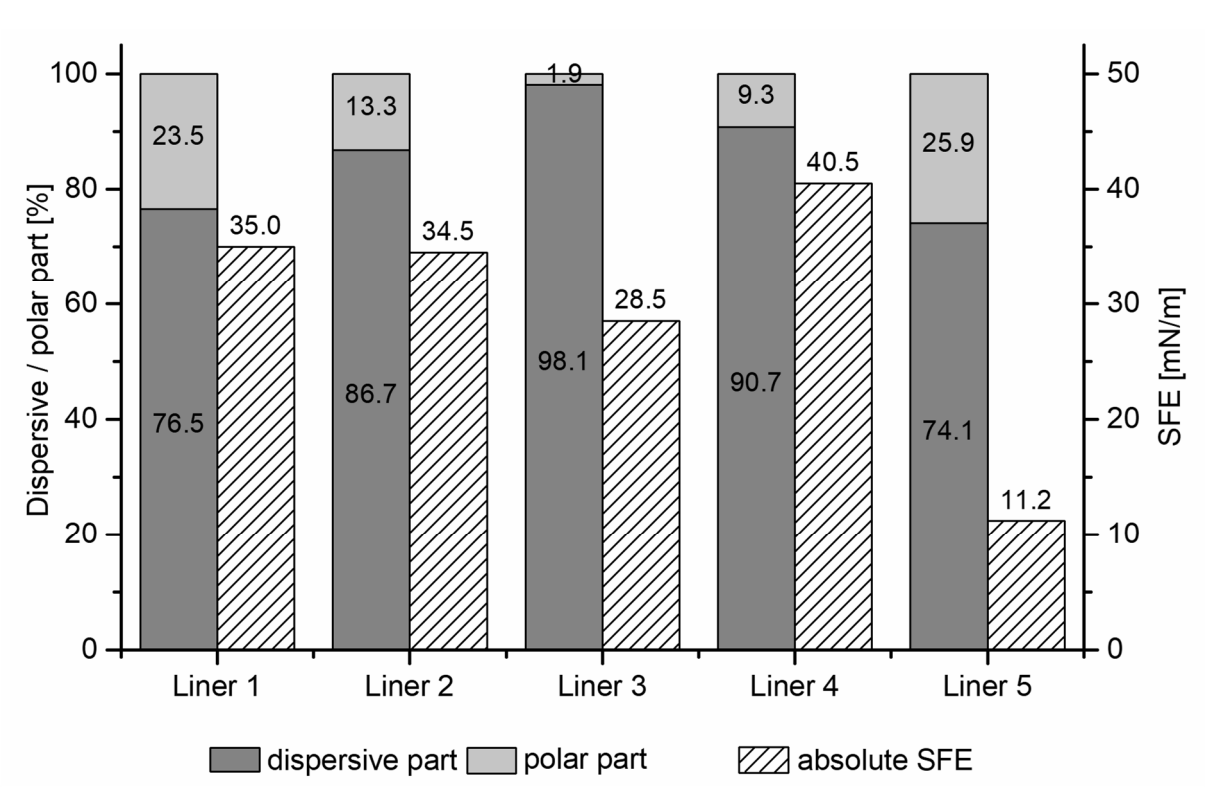

Figure 6: Surface free energy of the process liners. Absolute SFE (dashed columns) and the relative polar and dispersive parts of the SFE (filled columns). Calculated from the mean of 20 contact angles (Table 3).

The low SFE value of Liner 5 supported the observation made during the solvent casting trials of the polymer solutions on the liner. A process liner with a low SFE is not wetted easily because the thermodynamic state of the liner is already favorable and not improved by wetting with a liquid. This explains the high contact angles of the polymer solutions on Liner 5. Furthermore, Young's equation also provides evidence that the wetting of a solid material with a low SFE would not be favorable. Likewise, Liner 3 that also showed problems during the solvent casting of the polymer solutions revealed a lower SFE. However, for this liner the problems that occurred were likely an interplay between the poor wetting behavior and the wavy manner of the process liner. The easy movement of the foil assisted the poor adherence of the polymer film caused by the low SFE resulting in handling problems for this liner. The poor wetting behavior of the CMC solution on Liner 2 - 5 is explainable when taking the SFT of the polymer solution and their polar and dispersive parts into consideration (Figure 7).

The polar and dispersive interactions of the SFT were calculated according to section 5.4.15. For the calculations, the contact angle of diiodomethane and the contact angles of the three polymer solutions were measured on a Teflon® piece (refer to section 5.4.14) and are shown in Table 4. The absolute SFTs were measured (refer to section 5.4.13) and used as well (Table 4).

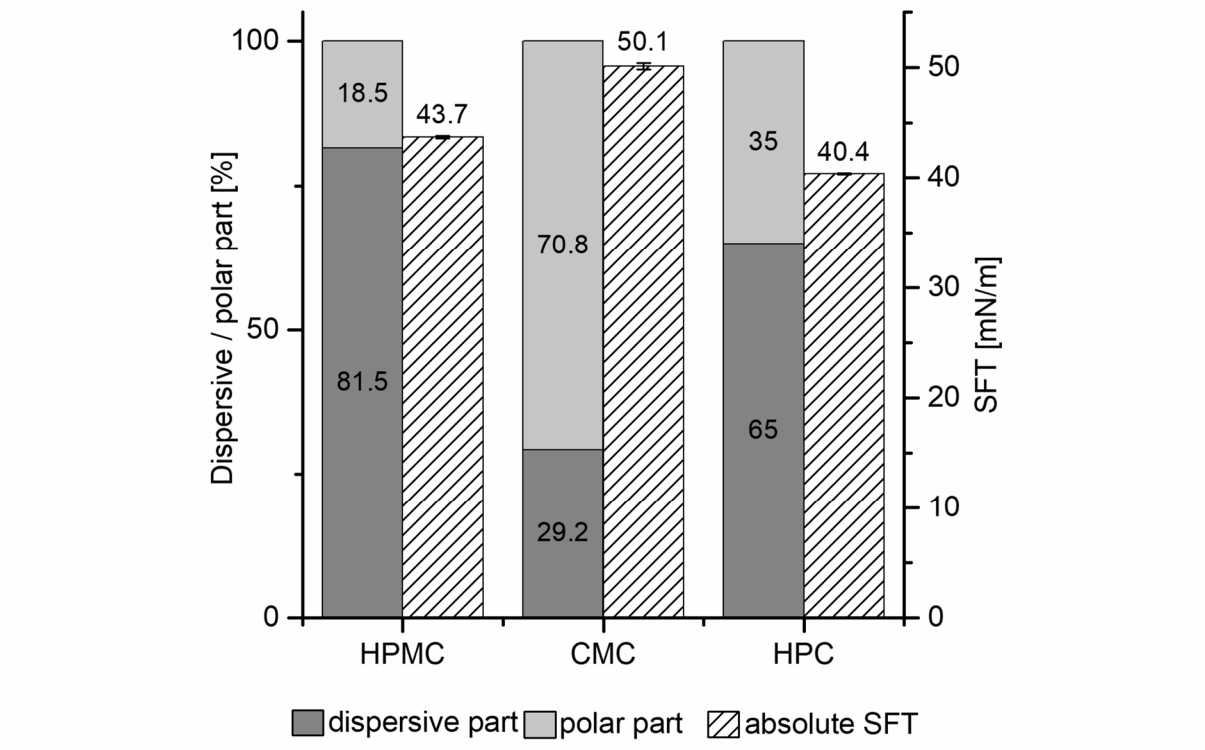

Figure 7: Surface tension of the polymer solutions. Absolute SFT (dashed columns, mean ± sd, n = 3) and the relative polar and dispersive parts of the SFT (filled columns).
Calculated from the mean of 10 contact angles and the mean of 3 absolute SFTs.

Table 4: Contact angles of the polymer solutions and diiodomethane on Teflon® (mean ± CI, α = 0.05, n = 10) and surface tension of the polymer solutions (mean ± sd, n = 3) and diiodomethane (Ström et al., 1987).

	Contact angle [°]	**Surface tension [mN/m]**
HPMC 15 %	75.5 ± 0.8	43.7 ± 0.1
CMC 8 %	107.5 ± 2.0	50.1 ± 0.3
HPC (EXF) 14 %	80.7 ± 2.0	40.4 ± 0.1
Diiodomethane	73.5 ± 0.9	50.8

First, the SFE of the Teflon® was calculated by substituting the SFT and the contact angle of diiodomethane on Teflon® into Equation 13 (refer to section 5.4.15). Since Teflon® only interacts on a dispersive level, the absolute SFE (σ_s) was equal to the dispersive part of the SFE (σ_s^D). In the next step, the polar and dispersive parts of the SFT of the polymer solutions were determined by inserting the contact angles of the polymer solutions on Teflon®, the absolute SFT and the dispersive part of the SFE of Teflon® into Equation 13.

The more the SFE of a solid and the SFT of a liquid resemble one another, the better the interactions can take effect. The two phases then adhere better to each other (Dataphysics, 2018). The polymer solution containing CMC showed a higher SFT than the other polymer solutions. This is the first reason that decreases the chance that the CMC solution is a well wetting solution since it does not favor a lower energy state of the liner as much as the solutions with lower SFT. This explains the wetting problems of CMC on Liner 3 and Liner 5 with low SFE well, but not the different behavior on the other liners showing higher SFEs. Although the SFE of Liner 1 and Liner 2 is almost the same, CMC formed an acceptable film on Liner 1 but not on Liner 2. This might be explained by the high part of polar interactions of the SFT of CMC. Liner 1 also showed higher polar interaction options than the other liners. The polar interactions might be the reason that CMC formed an acceptable film on Liner 1 but led to perforated films on Liner 2 and Liner 4. The higher absolute SFE of Liner 2 and Liner 4 might have prevented the CMC film from fully retracting and made the difference to the liners with lower SFEs. However, although showing high polar interaction possibilities it did not help the CMC film from retracting on Liner 5. The low absolute SFE seemed to be of greater relevance for the wetting behavior.

Liner 3 and Liner 5 were excluded for further investigation of the delamination behavior of the dried film since no acceptable films were obtained by solvent casting of the polymer solutions.

3.1.4.3 Peel adhesion

The delamination behavior of the dried film from the process liner is important for the handling of the film after the casting process. Further production steps have to be fulfilled with the film on the liner. The film is usually coiled up with the liner after casting and stored until cutting and packaging. If the film delaminates from the process liner spontaneously, the cutting and packaging process cannot be performed sufficiently. Therefore, after examination of the behavior of the polymer solution on the process liner, the delamination behavior of the dried film from the process liner was also investigated in this work.

The 90° peel adhesion test was applied to investigate the adhesion force of the dried film on the process liner. The test was conducted as explained in section 5.4.12. Since no acceptable films were formed on Liner 3 and Liner 5, no peel adhesion test could be performed for these samples. Furthermore, the samples with CMC on Liner 2 and Liner 4 were excluded since the films were perforated. The film of HPMC on Liner 1 was also not measurable in the peel adhesion test since it already delaminated from the liner spontaneously. It was not clearly identifiable for what reason the HPMC film delaminated from the liner spontaneously. It was assumed that it was rather due to handling errors than due to film properties.

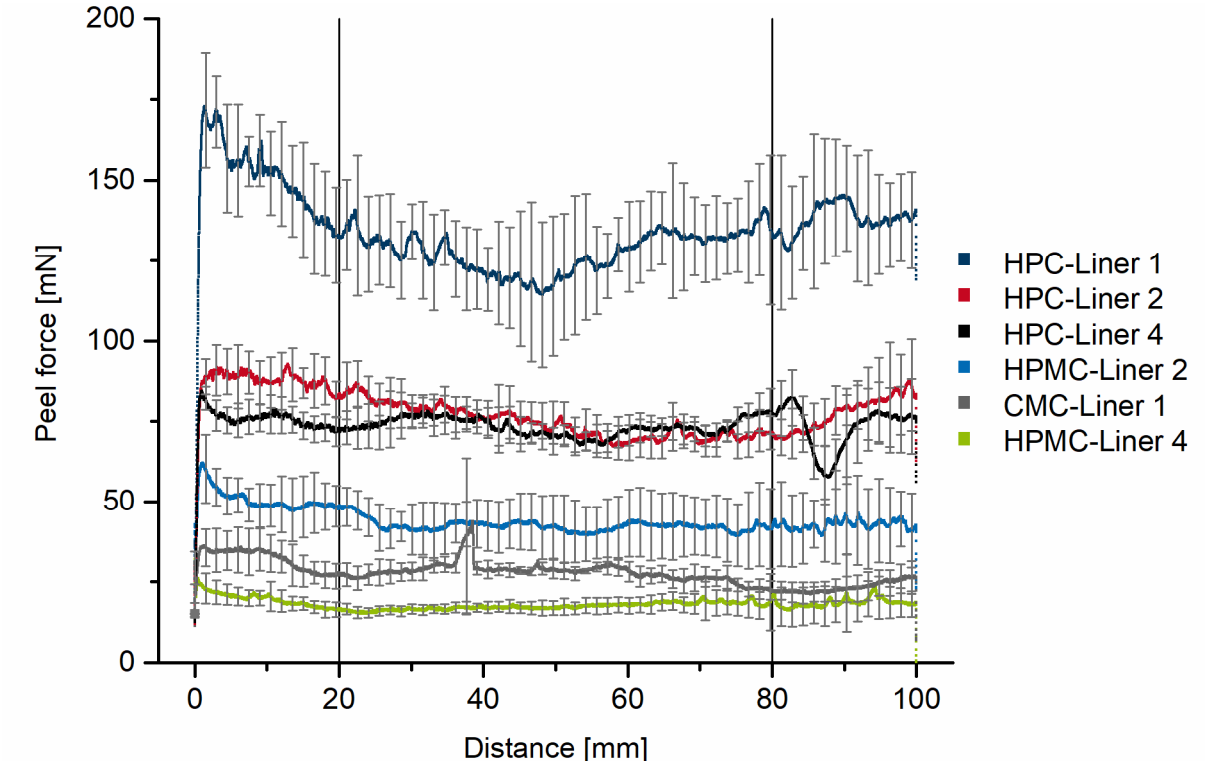

Figure 8: 90° Peel adhesion test results. Peel force recording over the test distance (mean ± CI, α = 0.05, n = 6). Marked interval between 20 and 80 mm used for calculation of the mean of six measured samples.

Figure 8 shows the measurement data of the peel adhesion test for the remaining samples. Since the peel forces show some variations at the beginning and at the end of the measurement, the mean value of the peel force (Figure 9) was calculated from the center section of the test (20 – 80 mm distance). A higher peel force in the initial area of the tested sample may originate from the force that needed to be overcome to obtain an even delamination of the sample. The changes for the peel force in the ending area of the sample, at higher distances is not that pronounced. But according to the standard method of the peel adhesion test from the adhesive industry, both the measurement data from the first 20 mm and the last 20 mm were excluded from further calculations (FINAT, 2001).

The length and width of the test samples were measured before and after the test was performed. No changes were observed between the start and the end of the test. Therefore, an elongation of the film was eliminated, and it was avoided that the evaluation of the peel force would falsely be affected by the deformation force applied. As it is shown in the results for the mechanical properties of the produced films (refer to section 3.1.5), the obtained peel forces in the peel adhesion test were far below the forces necessary to deform the film samples. While the highest peel force reached for the tested samples was less than 200 mN, the puncture forces were higher than 5.0 ± 0.8 N (calculated from the puncture strength of Formulation R in Figure 12). Due to these findings, it was obvious that deformation processes of the film did not disturb the peel adhesion test.

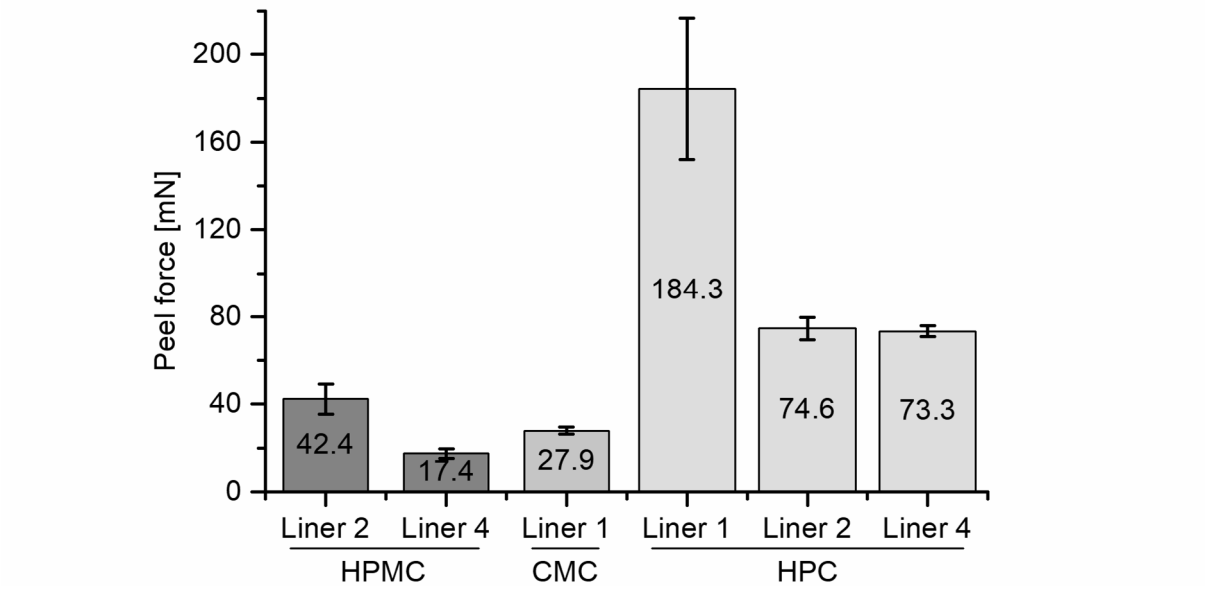

Figure 9: 90° peel adhesion test results. Peel force calculated from the mean value of the interval between 20 and 80 mm test distance from six samples (mean ± CI, α = 0.05, n = 6).

The mean peel forces of the samples are shown in Figure 9. Although no plasticizer was added to the HPC formulations, the films showed the highest peel forces from the process liners. It can be concluded that the recommendation of the manufacturer of the HPC, that no additional plasticizer is necessary for an HPC film, was correct for the purpose of this work. The high adhesion of the HPC films on the liner was described by Krampe (2015) as well and used as an explanation to prefer HPMC over HPC as film former for ODFs.

As presented in Figure 10, there was a weak correlation between the measured peel force of the dried film on the process liner and the contact angle of the corresponding polymer solution on the liner. The trend shows that the peel force was higher for samples that showed a lower contact angle in their solution stage. This seems comprehensible since a polymer solution that shows good wetting behavior (lower contact angle) would form a dry film that adheres better to the liner (higher peel force). Nevertheless, it may not be forgotten that the contact angle is a measurement value between the polymer solution and the process liner whereas the peel force is a value obtained from the interaction of the dried polymer film and the process liner. Especially the absolute SFT and the polar and dispersive interactions of the polymer solutions cannot be compared to the interaction possibilities of the dried films.

The investigation of the surface properties as an explanation of the interaction between polymer solutions and process liners during the solvent casting process is a promising method for a better understanding of the film manufacturing process. Furthermore, the determination of the

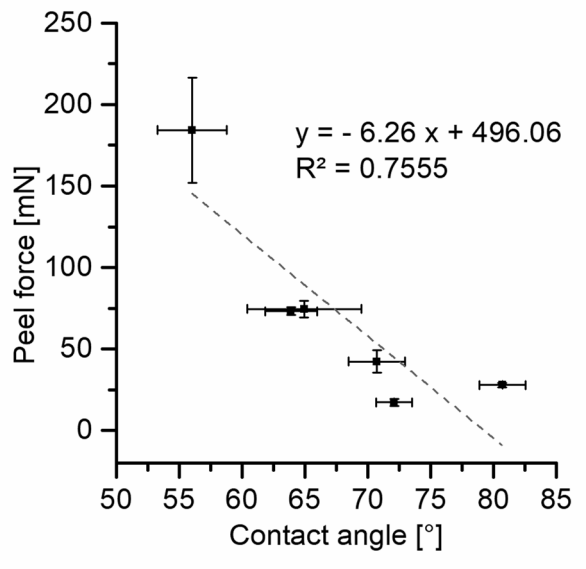

Figure 10: Correlation of the peel force (dried film on liner, mean ± CI, α = 0.05, n = 6) and the contact angle (polymer solution on liner, mean ± CI, α = 0.05, n = 10).

contact angles of the polymer solution on the liner as well as the SFT of the polymer solution and the SFE of the liner can be used for predictions of wetting behavior. The suitability of a process liner for casting a polymer solution can be tested without preparing a film. This may save time and resources since only low amounts of the polymer solution and the liner are needed for these investigations.

In this work, CMC as film forming polymer was excluded from further studies since it was not possible to prepare films with appropriate properties on most of the liners. Addition of other excipients such as surfactants would be necessary to improve the properties, which was not desired. The formulations should be kept as easy as possible with as few as possible excipients. Furthermore, Liner 3 and Liner 5 were not used for further film preparations due to handling and film casting problems.

3.1.5 Mechanical properties

The mechanical properties were investigated for the produced films since they are a critical value for oral films and should therefore be examined during formulation development. The mechanical properties have an impact on the production process as well as on further steps as cutting, packaging and even more important on the handling by the patient (Preis et al., 2014b; Thabet et al., 2018c). The test performed in this part of the work was the puncture test for oral films developed by Preis et al. (2014b), which is described in section 5.4.11.1. An exemplary graph that was obtained from the puncture test for formulation F8 (Table 1) is depicted in

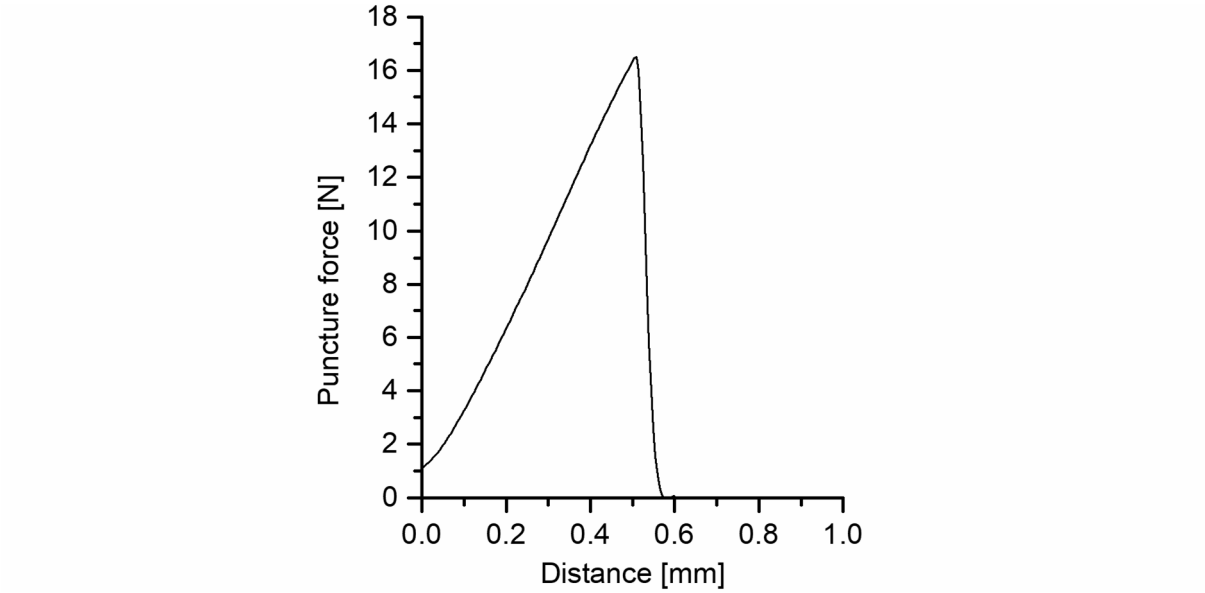

Figure 11: Exemplary force-distance diagram obtained from the puncture test for formulation F8.

Figure 11. The test records a force-distance diagram that is further converted into a stress-strain diagram for evaluation of the measurement values. The force-distance diagrams of the other formulations showed comparable shapes as the presented exemplary graph. The shape might be explained with a brittle behavior of the film (DIN, 2012) but it was also observed that due to the design of the sample holder the films rather broke than to deform over a longer distance. The reason may be that the films were placed between two plates in the sample holder, with a hole in the middle where the probe punctures the film (Preis et al., 2014b). When the probe punctures the film and moves forward, the film is bend over the edge of the hole in the metal plate. This exposes the film to a possible breaking point. Therefore, an interpretation of the force-distance curves must be treated with caution in this test, since it is not comparable with the example curves from the tensile test standard (DIN, 2012).

The results for the mechanical properties of the formulations that were processed to cast films are shown in Figure 12. Formulation R (Reference) is the marketed product Listerine® Cool Mint® Breath strips that was measured to obtain a reference of a manageable film. It was noticeable that the marketed product revealed the lowest puncture force and a very low elongation to break. The handling of this film confirmed a rather brittle behavior of the marketed product in comparison to the produced film samples, which might be because the film is not completely transparent, which suggests that some of the ingredients are not fully dissolved in the matrix. Crystalline structures may lead to lower mechanical resilience of the films and favor a brittle behavior. All formulations showed measured values above the

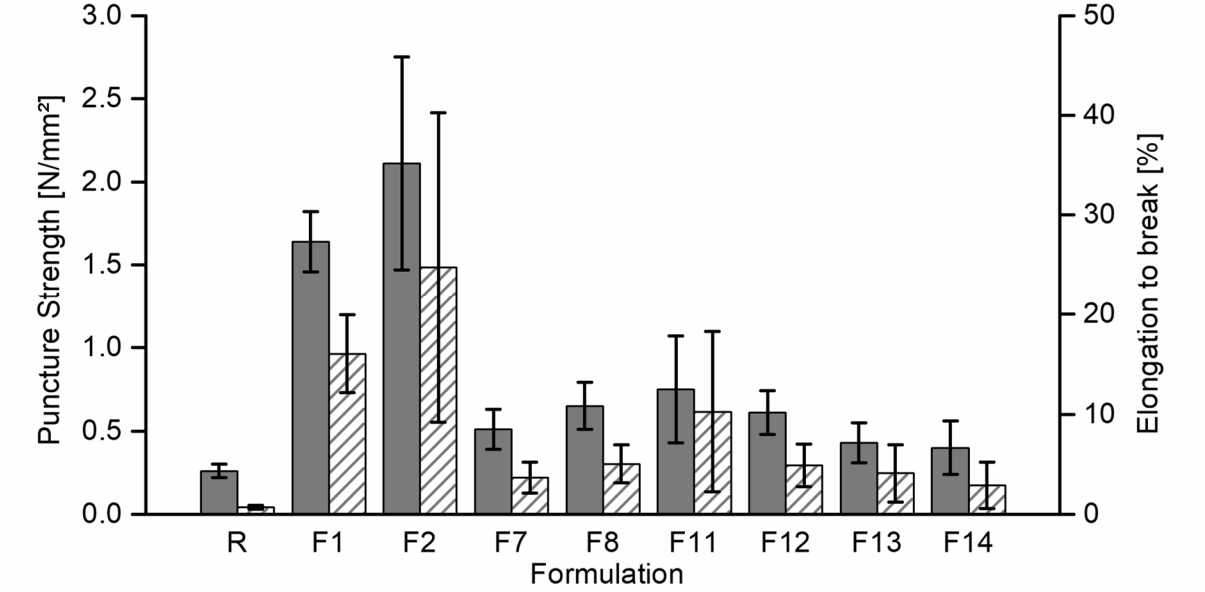

Figure 12: Mechanical properties determined with the puncture test. Formulations from Table 1 that were cast to a film. Filled columns: puncture strength; Dashed columns: elongation to break (mean ± sd, n = 6).

marketed product. The formulations containing HPMC (F1 and F2) showed higher puncture forces than the HPC formulations. The elongation to break also tended to be higher for HPMC than for HPC films. This can be an effect of the incorporated plasticizer in the HPMC films. Plasticizers have a huge impact on the mechanical properties and may reduce brittleness and increase flexibility (Patel et al., 2010). The results of the different HPC formulations showed no significant differences due to high scattering of the data. It was expected that the puncture strength would increase for higher polymer contents since a thicker film would be formed (refer to section 3.1.6).

The results showed high scattering, which was already recognized during the test because the recorded force-distance diagrams showed obvious differences. A possible reason may be that the position of the probe puncturing the film is not exactly defined. The sample holder table with the fixed film is manually moved below the probe at the central position above the cavity with the film. It may happen that the probe is not perfectly positioned every time and depending on the point where it penetrates the film, deviations may occur for the test results. Although there are no limits for the mechanical properties of ODFs stated in the European Pharmacopoeia, it requires sufficient mechanical strength of the film that it can resist handling without problems (Ph.Eur 9.3, 2018a; Thabet et al., 2018c). Preis et al. (2014b) concluded that the puncture strength has to reveal values above 0.08 N/mm² and that the films have to have slight ability to elongate. All prepared films can be categorized into these limits. The puncture forces are even much higher than desired whereby the film gains in mechanical resilience towards handling stress.

3.1.6 Further characterization

The prepared ODFs were further characterized regarding their masses and thicknesses (refer to sections 5.4.5 and 5.4.6), their disintegration time (refer to section 5.4.7) and their water vapor sorption behavior (refer to section 5.4.8). For all tests, the produced films were compared with the marketed product that was listed as Formulation R.

The mass and thickness result data are presented in Figure 13. Since all films were cast at the same gap height of 500 µm it was expected that the mass as well as the thickness increased with an increasing polymer content within the same polymer group. For the HPC films, it did not make a difference for the mass and the thickness which type of HPC was used for film preparation (Figure 14). The plot of the mass against the polymer content showed a good correlation ($R^2 = 0.9876$) although the two measurement points for a polymer content of

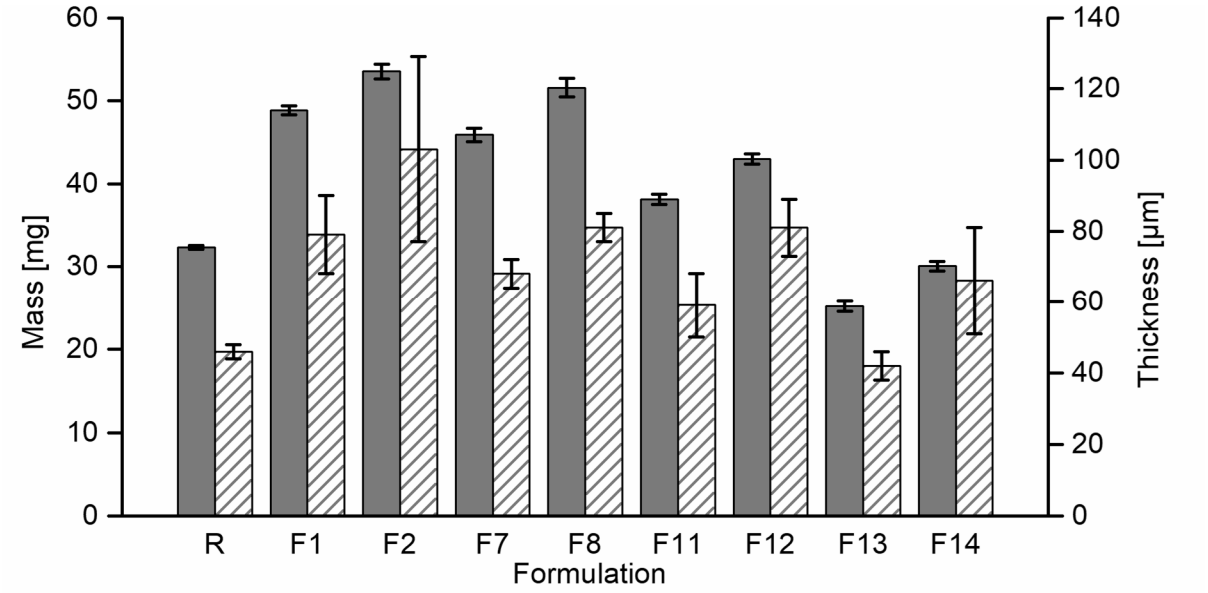

Figure 13: Masses and thicknesses of 6 cm² film pieces of the formulations from Table 1 that were cast to a film. Filled columns: mass; Dashed columns: thickness (mean ± CI, α = 0.05, n = 10).

17.5 % (F7 and F12) were not congruent. The regression line in Figure 14 (right) also indicates a weak correlation between the thickness of the dried film and the polymer content but scattering of the thickness values is very high. Therefore, no reliable statement can be made about the correlation. The HPMC films showed slightly higher masses and thicknesses compared to the HPC films with the same polymer contents. This was expected since the HPMC films additionally contained glycerol as plasticizing agent.

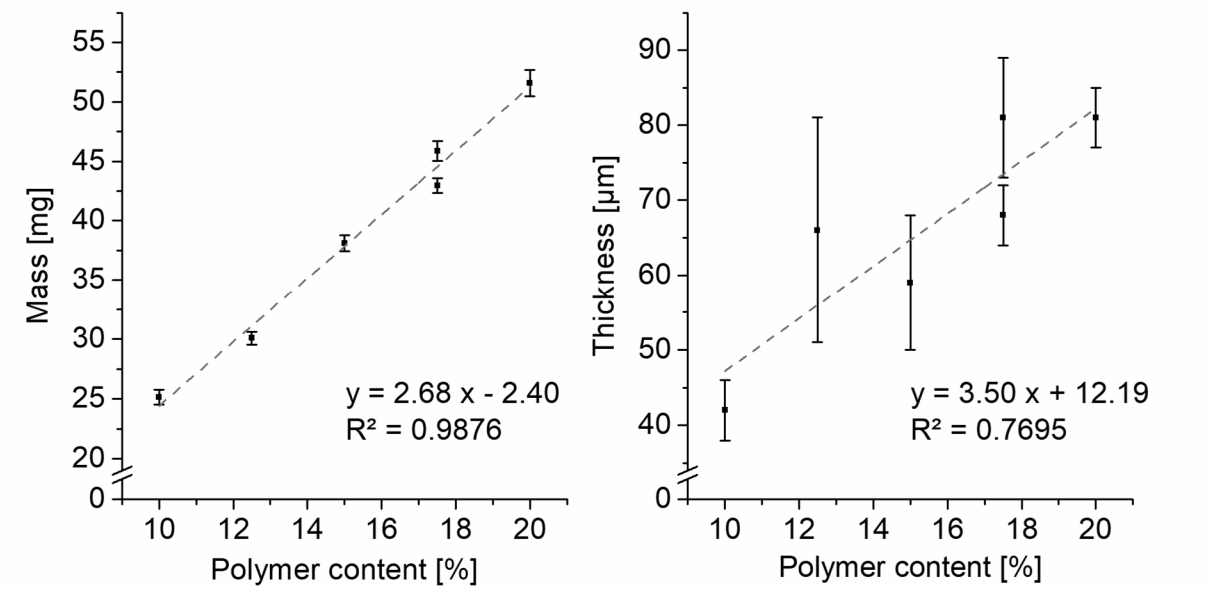

Figure 14: Correlation between the mass (left) or the thickness (right) of the dried HPC film pieces (mean ± CI, α = 0.05, n = 10) and the polymer content of the film forming solution.

The higher scattering of the thickness data compared to the mass data can be traced back to air bubbles entrapped in the film. They distorted the measurements and the highest scattering values were trackable to the films with the most air bubbles. The marketed product showed very consistent measurement data since no air bubbles were visible. The mean values were similar to the produced films (Figure 13). The thickness and the mass of ODFs have most relevance for a good handling, therefore they should not be too thin and for a good disintegration behavior they should not be too thick. The handling of the produced films was not a problem and the disintegration behavior was tested in this work as well.

The disintegration time of the dried films was measured using the "slide frame" method (refer to section 5.4.7) introduced by Garsuch and Breitkreutz (2010). The disintegration time of ODFs is of great relevance since the key feature of the ODFs is the rapid disintegration in the mouth (Ph.Eur 9.3, 2018a). Although the European Pharmacopoeia points out this important point, until now it does not give a specific method or a certain limit for an acceptable disintegration time for ODFs. The only thresholds available are recommendations for orally disintegrating tablets. According to the European Pharmacopoeia, ODTs ought to disintegrate within 3 min whereas the FDA recommends a disintegration time of not more than 30 s (FDA, 2008). Because there are no recommendations on disintegration times for ODFs from the regulatory side the thresholds for ODTs were applied.

The disintegration data from the produced films and the marketed product are shown in Figure 15. The disintegration times showed the same trend as the mass and thickness results: the higher the polymer content within the HPC films the longer the disintegration time of the films. The HPMC films showed longer disintegration times, which was not only explainable with the slightly higher thicknesses. Although the HPMC films contained the hydrophilic plasticizer glycerol, the pure HPC films showed better disintegration behavior. During the test, it appeared as that the HPMC film swelled in the area where the water drop was applied. This increased the disintegration times since for the swollen polymer/water drop mixture it took longer to dissolve the film and fall through the film in the beaker. All films were within the threshold of the European Pharmacopoeia for ODTs but only the marketed product was within the range recommended by the FDA. One more problem regarding the disintegration testing of oral films is the lack of an official testing method (Speer et al., 2018). There are many different approaches found in literature (Buanz et al., 2015; Garsuch and Breitkreutz, 2009, 2010; Preis et al., 2014a) but due to different test assemblies the results were hardly comparable. The disintegration time differs extremely depending on if there is a force applied on the film during

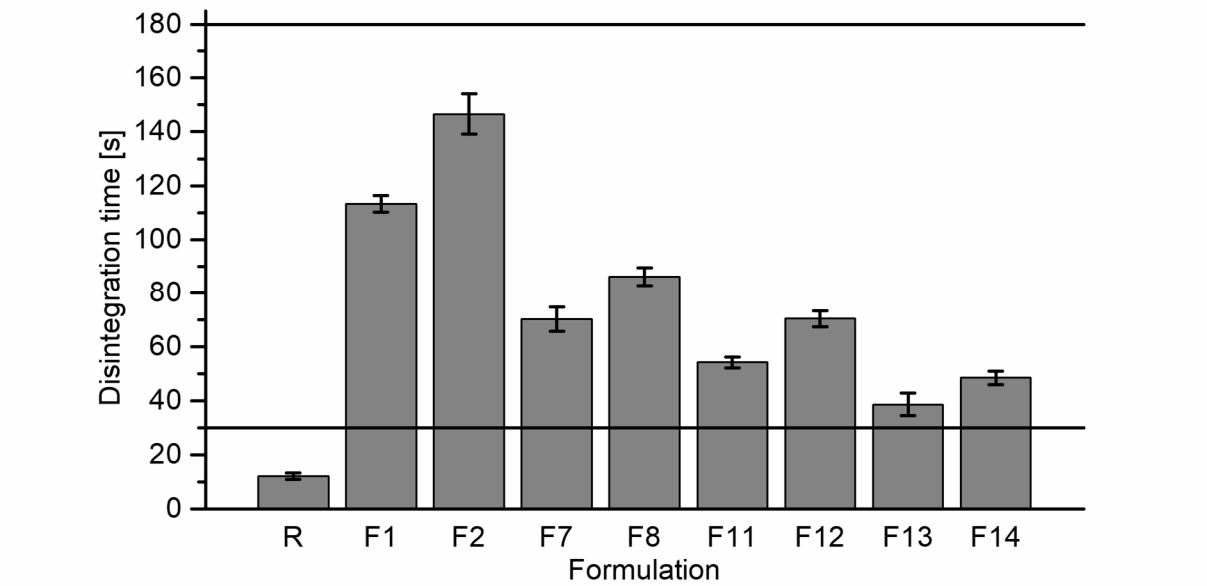

Figure 15: Disintegration time of a 6 cm² film piece of the formulations from Table 1 that were cast to a film (mean ± sd, n = 6). Marked thresholds at 30 and 180 s (see text).

testing or if the films is only put into a disintegration medium. Furthermore, the type of the medium, the temperature as well as the utilized volume also have an impact on the disintegration time. This might also be a reason for the rather high results for the prepared film formulations. The "slide frame" method does not apply any extra force on the film during testing. Only the water drop that is deposited on the film influences the disintegration time (Speer et al., 2018).

The water vapor sorption of the films was measured using dynamic vapor sorption (refer to section 5.4.8). The ability of the films to absorb water at different relative humidities was recorded and the results are pictured in Figure 16. It was obvious that the HPC films did not show any differences in their water sorption behavior. The isotherms overlap exactly in the graph. This was expected since the water sorption is not dependent on the different masses of the films since the measurement instrument weighed the starting mass of the films and then calculated the relative change in mass. The HPMC films showed higher water uptakes, which is likely due to the plasticizer incorporated since glycerol increases the water content of the films due to its hydrophilic character (Karlsson and Singh, 1998). The higher water uptake of HPMC in comparisons to HPC is also pronounced without the addition of plasticizer since the HPC is more lipophilic than other water-soluble cellulose ethers (Ashland, 2017; Saša et al., 2006). The isotherms of HPC and HPMC films show an exponential shape with increasing slopes for higher relative humidities because the first water molecules adsorbed to the samples enable better adsorption of the following water molecules (Saša et al., 2006). The marketed

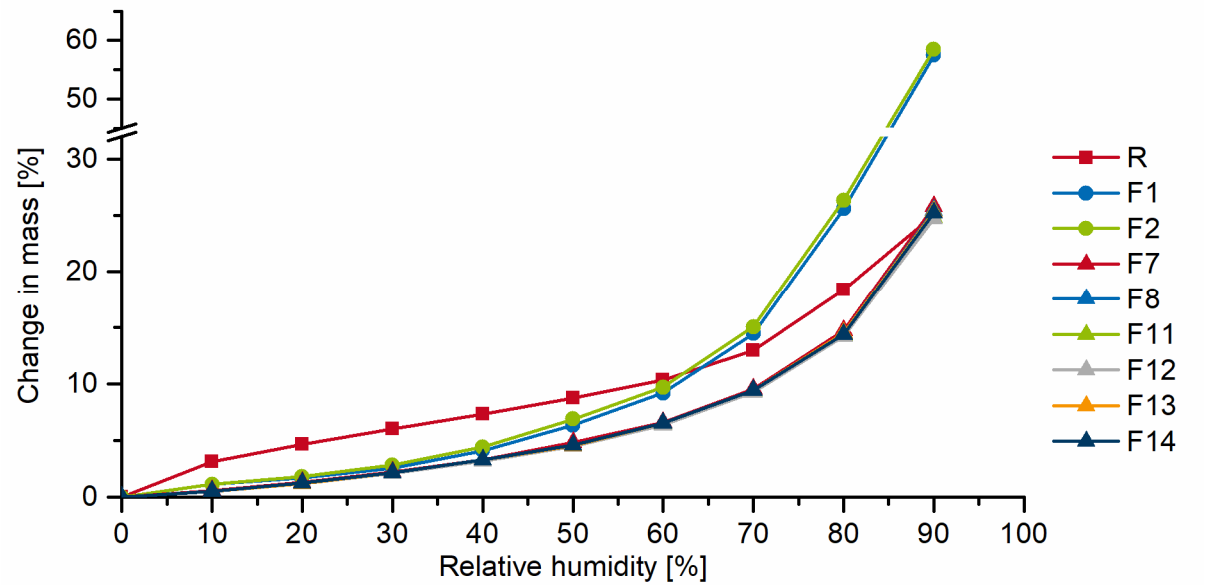

Figure 16: Water vapor sorption isotherms for the drug-free film formulations from Table 1 that were cast to a film at 25 °C (n = 1).

product shows a sigmoid shape for the isotherm. It rapidly absorbs water at 10 % relative humidity and then reduces the water uptake velocity until it increases again at high relative humidities. At 90 % relative humidity, it shows the same change in mass as the HPC films. Water in a dosage form is always a risk for stability issues of the films regarding the mechanical and microbiological stability.

The incorporated water especially is a risk for the mechanical properties of the films since water acts as plasticizer in the polymer matrix. The films get more flexible at higher water contents and might even get sticky if too much water is incorporated (Karlsson and Singh, 1998). This would lead to handling problems in regions with changing weather conditions. Furthermore, measurements of mechanical properties in laboratories without climate control could vary widely due to changing moisture in the air. Therefore, it would be important to pack and store the films under controlled conditions and use plasticizers less hydrophilic than glycerol to reduce the water uptake of the polymer matrix.

3.1.7 Summary

In this section, the preliminary formulation development of drug-free ODFs prepared with a small-scale coating bench using the solvent casting method was discussed. Different polymers were chosen, and the polymer solutions were investigated regarding their viscosities. This is a key factor for the application of the pilot-scale coating bench for further studies in this work. Formulations revealing viscosities below the stated threshold of 1 Pa*s (Thabet and

Breitkreutz, 2018) were excluded for further investigations. An integral part of this section was the determination of the surface properties of different process liners and different polymer solutions. It can be concluded that the selection of a suitable process liner for casting an ODF can be assisted by the determination of the SFE of the liner and the SFT of the solution. The absolute surface properties have to match but especially the polar and dispersive interactions shall be comparable. This improves the adhesion of the solution on the liner and therefore, the spreadability and formation of a homogenous ODF. The liners that revealed properties that were not supportive for forming satisfying ODFs were discarded as well as the polymer solution containing CMC. A correlation between the contact angle of the polymer solution on the process liner and the peel force of the dried film on the liner was detected but has to be confirmed by further experiments. The mechanical properties of the produced ODFs revealed higher puncture strengths and more flexibility expressed as the elongation to break compared to the marketed product Listerine® Cool Mint® Breath strips. Strong and flexible films are a good result but especially the flexibility has to be monitored well with regard of the use in a dosing device. A high flexibility might lead to deformation of the films that leads to inacceptable dosing inaccuracies. Therefore, the testing of the mechanical properties will be developed further in regard of the special handling in section 3.2 of this work. The disintegration test showed that the produced films revealed higher disintegration times than the marketed product, but they were all lower than 180 s as given by the European Pharmacopoeia as a limit for ODTs. The disintegration time could be reduced by varying the film manufacturing thickness and therefore the thickness of the dried film.

In the next part of this work, formulations will be optimized for the use on the continuously working pilot-scale coating bench. Since it was reported that an upscaling from the small coating benches to the continuously working pilot-scale coating bench is not expected to be without problems the formulation development on the small-scale coating bench was only a preliminary study (Thabet and Breitkreutz, 2018). The different processes have different requirements on the polymer solutions and the film, for example because of different application processes of the polymer mass onto the liner or the varying drying processes.

3.2 Formulation development of orodispersible films on a pilot-scale coating bench

Parts of this section have already been published in peer-reviewed journals. The content was linguistically adapted and data sets were partly extended.

- Niese, S. and Quodbach, J., 2018. *Application of a chromatic confocal measurement system as new approach for in-line wet film thickness determination in continuous oral film manufacturing processes*. Int J Pharm. 551, 203-211.
  DOI: 10.1016/j.ijpharm.2018.09.028.
- Niese, S. and Quodbach, J., 2019. *Formulation development of a continuously manufactured orodispersible film containing warfarin sodium for individualized dosing.* Eur J Pharm Biopharm. 136, 93-101.
  DOI: 10.1016/j.ejpb.2019.01.011.

3.2.1 Introduction and objectives

The aim of this section was the formulation development of orodispersible films containing warfarin sodium as model drug. The films were prepared using the continuously working pilot-scale coating bench to obtain a long oral film that can be coiled up on a roll. The produced oral film should be useable in the dosing device for safe and flexible dosing of the ODF. Since the film preparation processes on the small-scale coating bench and on the pilot-scale coating bench show major differences, the formulation development of the final ODF containing warfarin was not further performed with small batches on the small-scale coating bench. Relevant differences between the coating benches are the handling of the polymer mass up to the application site, the application technique of the polymer mass onto the process liner, the drying step of the coated mass as well as the drying time. For the small-scale coating bench, the polymer mass is poured onto the process liner manually and coated with a defined gap width using a coating knife that moves across the fixed liner. The drying is performed at room temperature or with a heated plate, the liner is fixed on. Drying time is therefore not limited. In contrast, the pilot-scale coating bench uses a pump to move the polymer mass from the reservoir to the coating knife where the knife is fixed with a defined gap width and the polymer mass is delivered onto the moving process liner. The liner moves across two heating plates within a drying tunnel equipped with exhaust air for the drying step and is coiled up at the end

of the process. The drying time is therefore dependent on the liner velocity and the length of the drying tunnel (Krampe et al., 2016; Thabet and Breitkreutz, 2018).

Formulations F2 and F8 that were investigated during the preliminary formulation development on the small-scale coating bench (refer to section 3.1) and considered as suitable were further examined and improved for the use on the pilot-scale coating bench. The formulation development started with drug-free formulations due to the toxicity of the model drug warfarin. The API was not incorporated into ODFs until suitable drug-free formulations were found that showed satisfying film properties.

Because of the intended use of the long oral film in the dosing device, it is important that the film withstands the handling in the device that will differ from the handling of the single-dosed ODF pieces. Especially the deformation behavior under tensile stress is of interest regarding the handling of the film. Therefore, the puncture test for investigating the mechanical properties was replaced by the tensile test, which better represents the handling in the dosing device. Different test specimens and different preparation methods of the samples were evaluated.

Furthermore, an in-line analytical method for the wet film thickness (WFT) was implemented into the continuous film manufacturing process. The WFT is the most critical parameter for the content of the produced oral film and therefore needs to be controllable. The new in-line WFT measurement method using a chromatic confocal optical probe was validated for the use in the continuous film manufacturing process. Caffeine was used as model drug in this part of the work.

The incorporation of the model drug warfarin into the drug-free formulation was the last step of this section. The films were characterized and the stability of the unpacked ODFs was tested over a time period of three months regarding the content uniformity and the mechanical properties. Since the use in the dosing device was intended for the developed ODFs, the packaging was considered and stability was also evaluated for the films packed in heat-sealed aluminum packages.

3.2.2 Formulation development of drug-free films

3.2.2.1 General considerations

For the formulation development of the long ODF containing warfarin, different polymers were used as film forming matrix. HPMC (F2) and HPC (F8) were continued to use since they showed promising results in the preliminary formulation development (refer to section 3.1). PVA as a third polymer was incorporated into the study at this point. These polymers were all discussed in several reviews and publications for fast dissolving oral films (Borges et al., 2015; Dixit and Puthli, 2009; El-Setouhy and El-Malak, 2010; Hariharan and Bogue, 2009; Shimoda et al., 2009). As alternative plasticizing agents to glycerol, citric acid and its ester triethyl citrate (Patel et al., 2010) were chosen and investigated in different concentrations. The aim was to reduce the high water vapor sorption of ODFs containing glycerol as plasticizer. Since the ODF is supposed to enable use in pediatric patients, the preparation was meant to be composed with as few excipients as possible. The considered drug-free formulations are shown in Table 5.

Table 5: Drug-free formulations for pilot-scale coating bench trials. Percentages referred to total weight (w/w).

Formulation	Polymer [%] (ratio)		Plasticizer [%]		Cast film
H1	HPMC	17.5	---		x
H2	HPMC	17.5	Glycerol	3	x
H3	HPMC	17.5	Glycerol	2	x
H4	HPMC	17.5	Triethyl citrate	3	x
H5	HPMC	17.5	Triethyl citrate	2	x
H6	HPMC	17.5	Citric acid	3	x
H7	HPMC	17.5	Citric acid	2	x
P1	PVA	10	---		---
P2	PVA	10	Glycerol	5	---
P3	PVA	12.5	---		---
P4	PVA	12.5	Glycerol	5	---
P5	PVA	12.5	Glycerol	2	---
PH1	PVA:HPMC	12.5 (1:1)	---		---
PH2	PVA:HPMC	12.5 (1:1)	Glycerol	2	---
PH3	PVA:HPMC	12.5 (2:1)	---		---
PH4	PVA:HPMC	12.5 (2:1)	Glycerol	2	---
PH5	PVA:HPMC	15 (2:3)	---		x
PH6	PVA:HPMC	15 (2:3)	Glycerol	1	x
PH7	PVA:HPMC	15 (2:3)	Triethyl citrate	1	x
PH8	PVA:HPMC	15 (2:3)	Citric acid	2	x
HPC	HPC (ELF)	20	---		x

3.2.2.2 Formulation optimization and manufacturing of long drug-free films

The different polymer masses were investigated regarding their dynamic viscosity as key parameter for the evaluation of the processability on the pilot-scale coating bench. As already described in section 3.1.3, Thabet and Breitkreutz (2018) reported a threshold value of 1 Pa*s for the viscosity of polymer masses that are processed on the continuously working coating bench. The polymer mass flows down at the wrong side of the coating knife without forming a film on the process liner when showing lower viscosities than the reported threshold value. A shear rate ramp was measured for all formulations to evaluate the flowing properties of the formulations (refer to section 3.1.3 and 5.4.1). All formulations revealed little pseudoplastic flow behavior that was stronger pronounced for the formulations with HPMC and PVA as combined polymer matrix. Formulations containing HPMC, PVA or HPC as polymer matrix showed no hysteresis and therefore no time dependent flow properties. The formulations containing HPMC and PVA as combined polymer matrix showed slight time dependent flow properties that were more pronounced with a higher HPMC fraction. Since the viscosity during the coating process is of interest for the formulation development, the viscosity at a shear rate of 4 s^{-1} was measured representing the conditions at the coating knife with a gap width of 500 µm and a liner velocity of 12.5 cm/min (refer to section 5.4.1). Figure 17 presents the measured viscosity values for the drug-free formulations. It was obvious that no adjustment for the HPMC formulations was required since they were based on published data (Thabet and Breitkreutz, 2018) and therefore sufficiently above the threshold value. An adjustment of the

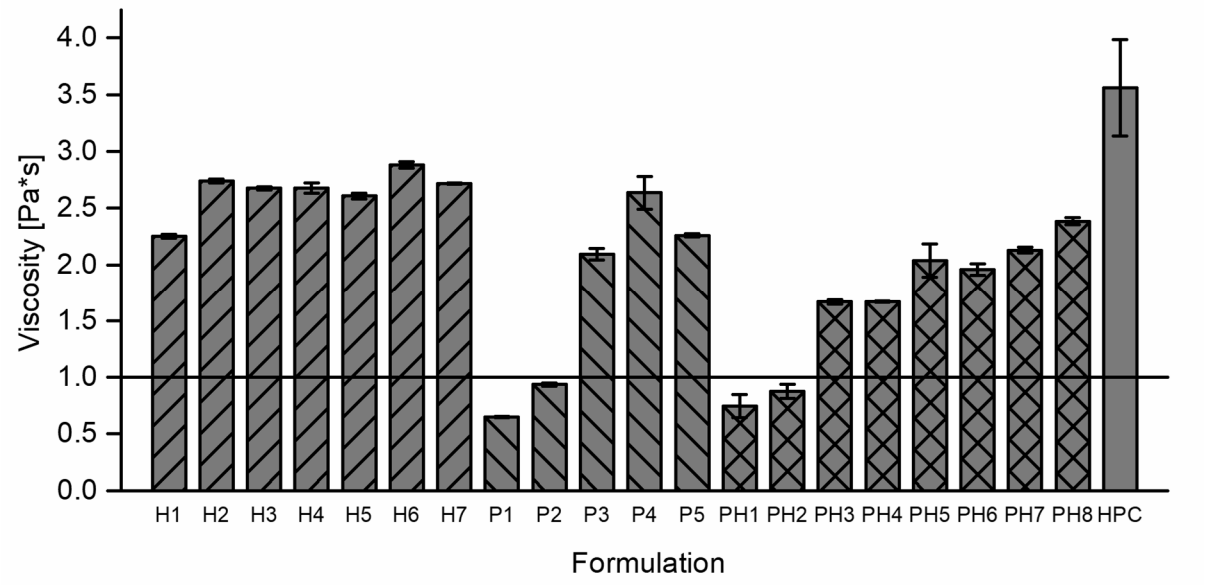

Figure 17: Dynamic viscosity of polymer solutions from Table 5 measured at a shear rate of 4 s^{-1} and 25 °C. The line represents the viscosity threshold (Thabet and Breitkreutz, 2018), patterns differentiate the polymer matrices of the solutions (mean ± sd, n = 3). Used by courtesy of the European Journal of Pharmaceutics and Biopharmaceutics, Elsevier (Niese and Quodbach, 2019).

concentration of the pure PVA formulations was necessary as P1 did not show an acceptable viscosity with a polymer content of 10 %. The threshold was not fulfilled for P2 as well, although additional glycerol slightly increased the viscosity. The increase of the polymer content to 12.5 % PVA resulted in satisfying viscosities for P3 – P5. Formulations PH1 and PH2 containing PVA and HPMC with a polymer content of 12.5 % and a ratio of 1:1 resulted in too low viscosities independent of additional plasticizer. The viscosity threshold was met after performing a change in the polymer ratio and a concentration increase (PH3 – PH8). The HPC formulation with a polymer content of 20 % exceeded the viscosity threshold by far. The polymer solutions that showed viscosities above the threshold of 1 Pa*s were processible on the pilot-scale coating bench in this work (refer to section 5.3.4.1), whereas the formulations with a lower viscosity could not be cast without the aforementioned problems. The published threshold therefore was confirmed with these results.

The identification of processible formulations for the film manufacturing on the continuously working pilot-scale coating bench was the first step in the formulation development. The next step was the assessment of the dried ODFs after manufacturing. For further investigations, only films that showed satisfying properties were taken into consideration. Satisfying films were defined as homogenous films with a constant coating width and without holes. They should be dry at the end of the manufacturing process and neither should they separate from the liner spontaneously nor should they stick and deform when separating them from the liner. The HPMC formulations did all form satisfying films without adjustment of the basic process settings. Formulation H1, though, separated easily from the process liner while cutting the film with the cutting plotter (refer to section 5.3.5). This led to uncontrolled cuts since the cutting template referred to exact coordinates on the cutting map and the blade of the cutting plotter rather pushed the film ahead of itself than cutting through it. The film had to be firmly held down on the cutting map during the cutting process to receive acceptable cuts. Therefore, H1 was rejected and the formulation improved by adding plasticizers. The stickiness of the film onto the liner was increased by the plasticizer addition and the following HPMC films were sufficiently adhering and cuttable with the cutting plotter. Formulation P3 formed holes throughout the film during the film manufacturing process resulting in unsatisfying films. Potentially, a higher SFT not matching the SFE of the liner might be the cause (refer to section 3.1.4) (Owens and Wendt, 1969). This behavior could not be improved by adjusting the settings of the film coater. The addition of a plasticizer did not change this aspect as well but additionally made the films P4 and P5 very elastic and hard to handle. They adhered strongly

to the liner and were highly deformable, changing the length and therefore the dose per length of a potential incorporated API. The separation from the liner was only feasible under deformation and destruction of the films. These observations led to the rejection of PVA as individual polymer matrix in this work. The formulations containing PVA and HPMC in combination as film forming matrix showed too low viscosities for PH1 and PH2. Therefore, at first the polymer ratio was changed from 1:1 to 2:1. PH3 and PH4 then formed adequate films but were very elastic hampering the handling of the films. They deformed extremely while separating them from the liner and were therefore discarded and the formulation further optimized. At this point, the ratio of the film formers was changed in advantage of HPMC to 2:3. This lowered the elastic contribution of the PVA. To stick with an adequate viscosity, the polymer content was raised to 15 % (PH5 – PH8). Satisfying films were produced by these formulations. The formulation with HPC as film former showed acceptable film forming properties after increasing the pump setting due to its high viscosity.

3.2.2.3 Critical investigation of the tensile test for oral films

The long ODF that is developed in course of this work for usage in a dosing device is intended for individualized dosing of ODFs (refer to section 3.3). Thus, the prepared film must meet other requirements than the well-known single-dose ODFs. The mechanical properties of the film are a critical parameter for the handling of the dried film. The film strip has to be flexible enough to withstand the coiling-up on the stock roll of the dosing device. Rupture of the film is not acceptable. Likewise, the film must be robust enough not to deform by the pulling stress while being delivered through the device and during handling by the patient. Neither an elastic nor a plastic deformation is acceptable since the dosing is based on the film length in the device.

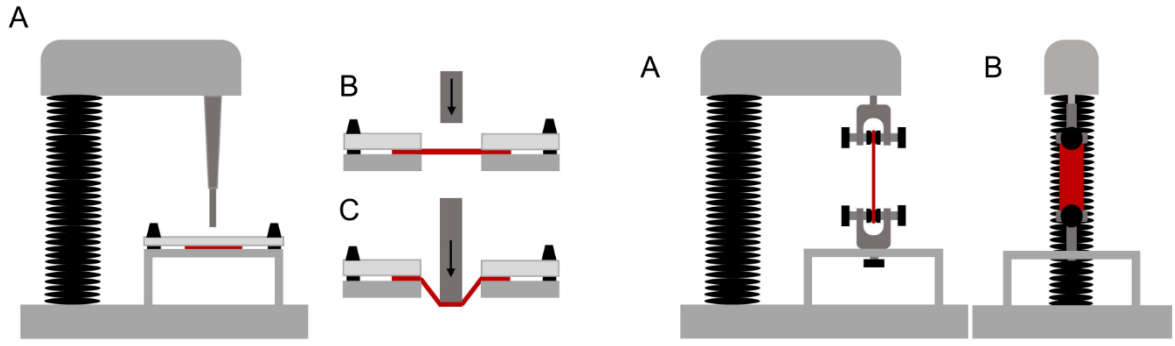

Figure 18: Schematic drawings of the test for mechanical properties of oral films:
Left: Puncture test (A: side view, B: close-up view before test, C: close-up view during test).
Adapted from Preis et al. (2014b) and used by courtesy of the International Journal of Pharmaceutics, Elsevier.
Right: Tensile test (A: side view, B:front view) (DIN, 2003, 2012).

A deformation of the film changes its length and leads to unacceptable dosing errors. During the formulation development it became obvious that the test for mechanical properties, which is used as standard for oral films, the puncture test (refer to section 3.1.5 and 5.4.11.1) does not reflect the stress applied to the ODF during the use of the dosing device. The normally used puncture test applies a puncture force on the horizontally fixed film (Figure 18, left). This kind of force is at no time applied on the film in the dosing device or the manufacturing process of the long film. Therefore, a different characterization method was needed and hence, the tensile test (refer to section 5.4.11.2) was chosen to be used for the mechanical characterization of the long films. The applied tensile force (Figure 18, right) better reflects the tensile stress that may be applied in the device.

In most published works the tensile test for oral films was performed using dumbbell-shaped test specimens to ensure breakage of the film in the middle of the specimen and not at the clamps (Boateng et al., 2009; Garsuch, 2009; Hoffmann, 2012; Visser et al., 2015b; Wörtz, 2015). The preparation of a dumbbell-shaped specimen from the oral film is complicated and entails the risk of incorrectly cut samples or breakage points that might distort the test results. Thus, two different test specimens stated by the DIN EN ISO 527-3 (2003) for tensile properties of films and sheets were investigated and compared in this study. The dumbbell-shaped specimen (Figure 19, Specimen 4: further referred to as “dumbbell”) and the rectangular-shaped specimen (Figure 19, Specimen 2: further referred to as “rectangle”). The

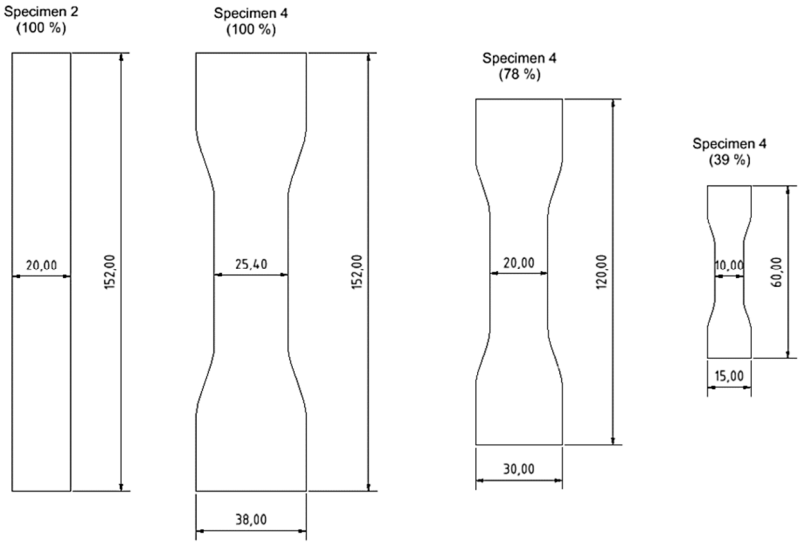

Figure 19: Test specimens for the tensile test according to DIN (2003). Specimen 2 = Rectangle, Specimen 4 = Dumbbell (length specifications in mm). By courtesy of the DIN Deutsches Institut für Normung e.V. (German Institute for Standardization). Decisive for the application of the DIN-standard is the latest version that is available at the Beuth Verlag GmbH, Burggrafenstraße 6, 10787 Berlin.

aim was to evaluate whether the use of the harder to handle dumbbell-shaped specimen is reasonable. The rectangular-shaped specimen was chosen as comparison because, on the one hand, the international standard for the determination of tensile properties for films and sheets states this specimen as the recommended one (DIN, 2003). On the other hand, the rectangular shape with a width of 20 mm reflects the exact width of the oral film strip that will be used in the dosing device. The dumbbell specimen was modified to match the test equipment of the texture analyzer (Figure 19). The clamps only have a width of 25 mm. Therefore, the original width of the ends with 38 mm was too wide for the used equipment. The specimen was scaled down to present the same width in the middle part than the film (20 mm, Figure 19 (78 %)). Nevertheless, the ends were still too wide for the clamps and the sample was scaled down again to the half of the width (10 mm, Figure 19 (39 %)) resulting in an end width of 15 mm fitting the used clamps.

Furthermore, two different preparation methods for the samples were compared in this study. The samples were once cut with a knife as it was done in previous works. The other option was to cut the samples with an automatic cutting plotter that was expected to cut more precisely (refer to section 5.3.5).

Different drug-free films were prepared with the continuously working pilot-scale coating bench and were investigated in this part of the work (H1, H2, H4, PH5, PH6, PH7 and HPC, Table 5). Two other formulations with citric acid as plasticizer were also used that are not shown in Table 5. They contained 5 % (w/w) citric acid for an HPMC film (17.5 % w/w) and a film with a matrix of PVA and HPMC (2:3, 15 % w/w), hereafter referred to as HCA5 and PHCA5. The tensile test was performed for each of these nine films (refer to section 5.4.11.2) for both test specimens and both cutting methods. The obtained stress-strain curves were evaluated regarding different measurement values. The commonly used values from literature are the tensile strength, the tensile strain at break and the Young's modulus (Bala et al., 2013; Borges et al., 2015; Dixit and Puthli, 2009; Garsuch and Breitkreutz, 2009; Visser et al., 2015b). These measurement values were critically reviewed. The Young's modulus was excluded since the international standard clearly points out that the definition of the Young's modulus does not apply for the testing of films and sheets (DIN, 2003, 2012). Therefore, the secant modulus, which is similar to the Young's modulus but accepted as parameter in the American Society for Testing and Materials (ASTM) standard (ASTM, 2012), was applied. The tensile strength was not used as parameter because the information given by this value does not represent the actual handling of the film. The tensile strength is defined as the

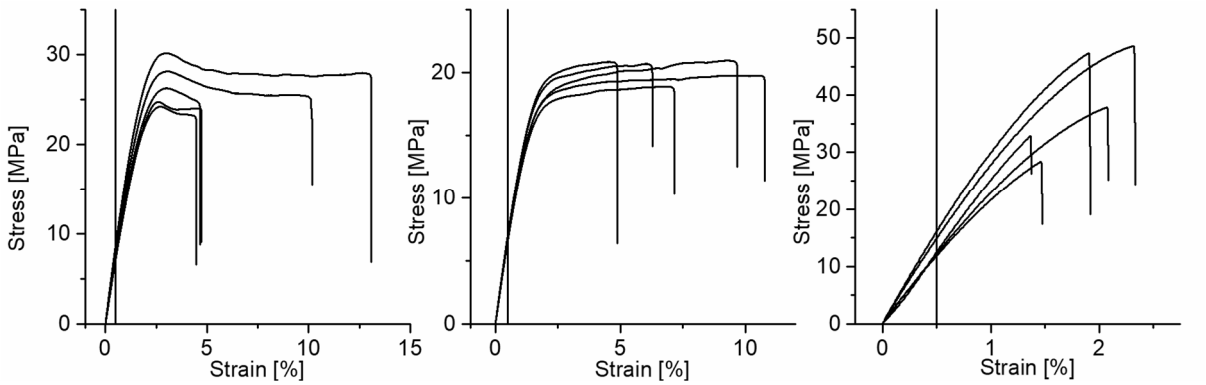

Figure 20: Exemplary stress-strain curves from tensile tests. Left: Tough material with yield point. Middle: Tough material without yield point. Right: Brittle material (n = 5). Line represents the 0.5 % strain to visualize the linear region the secant modulus was determined from.

"maximum tensile stress sustained by the test specimen during a tensile test" (DIN, 2012). With this definition, the tensile strength can equal the tensile stress at break as well as the tensile stress at yield, which represent two clearly different points on the stress-strain curve. Figure 20 shows three possible stress-strain curves from a tensile test of oral films, which visually demonstrate that the maximum tensile stress can be attained at different points of the stress-strain curve. They reveal that by providing the single measurement value, a clear distinction between the deformation behavior is not possible. For the handling of the long ODF, it makes an important difference whether the maximum stress applicable to the film causes rupture or deforms it irreversibly. Therefore, the yield stress as the tensile stress at the point where the plastic deformation starts was chosen as alternative value, which gives more important information to the handling of the film. A breakage of the film is not that relevant if the film was already strongly deformed in advance. The tensile strain at break was rejected due to high statistical scattering that can be seen in Figure 20 and is also described in literature (Grellmann, 2007). Furthermore, the first part of the stress-strain diagram is the more meaningful one for the mentioned purpose. The changes in the front part of the curves are a good indicator for the deformation behavior of the film.

Figure 21 presents the results of the tensile tests for two different test specimens and two different cutting methods performed for all nine oral films. The secant moduli and the yield stresses were compared as test parameters. F-tests were performed to analyze the differences in the variances between the investigated samples. Two shapes of specimens (rectangle and dumbbell, Figure 19) were compared to each other as well as two cutting methods for specimen preparation (knife and cutting plotter). The mean values were not compared since it is obvious that the mean value differs when changing the specimen. Moreover, it is unknown which mean

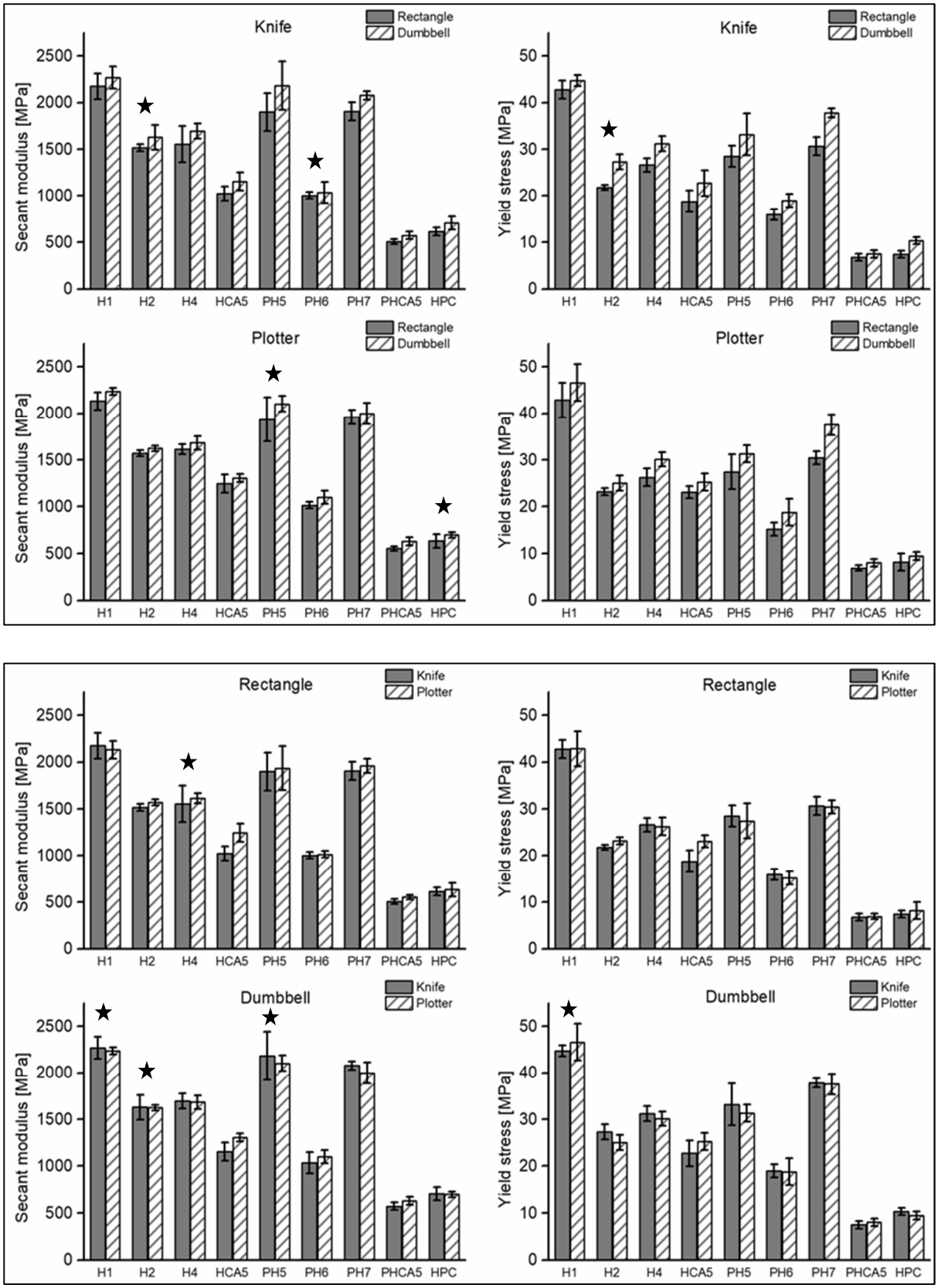

Figure 21: Results of the tensile tests: Comparison of the shapes of the test specimen (top) and the cutting methods (bottom). ★: Variances differ on a significance level of α = 0.05. Secant modulus (left) and yield stress (right) (mean ± sd, n = 5).

Table 6: Average of the standard deviations of all nine tested formulations for samples cut with either the knife or the plotter, in either the shape of the rectangle or the dumbbell. Raw data are shown in Figure 21. Left: secant modulus; right: yield stress.

Secant modulus [MPa]			**Yield stress [MPa]**		
	Rectangle	Dumbbell		Rectangle	Dumbbell
Knife	94.67	106.85	Knife	1.46	1.73
Plotter	79.55	57.99	Plotter	1.84	1.94

value is “correct”. Therefore, only the variances as measure of variation were compared since their values demonstrate the reproducibility of the test. The stars in the graphs indicate the films, which showed a significant difference in their variances for the compared specimen shape or cutting method. Additionally, the average of the standard deviations of all nine film formulations was calculated for samples prepared with either the knife or the plotter in either the shape of the rectangle or the dumbbell (Table 6). These values were used for further comparison of the tested options and to quantify the influence of the cutting method and specimen shape on the results.

The comparison between the two test specimens shows that the samples cut with the knife have three formulations with significantly different variances whereas the samples cut with the plotter only have two (Figure 21, top). In case of the samples cut with the knife, the variances that were significantly higher were from samples with the dumbbell shape. This is also recognizable in the averages of the standard deviations (Table 6). This emphasized the aforementioned assumption that the dumbbell shape is more challenging to cut by hand. The plotter was expected to be more favorable to use for the dumbbell specimens. When comparing the scattering of the data obtained from knife-cut and plotter-cut dumbbell samples, the data for the samples cut automatically with the plotter showed a generally lower average of the standard deviation values for the secant moduli. The yield stresses show little higher scattering for the plotter than for the knife. The significantly different variances for the comparison of the cutting methods are marked at the bottom part of Figure 21. Whereas four samples show significantly different variances for the dumbbell specimen, only one was found for the rectangular specimen. This shows that for the rectangular specimen the cutting method is not as relevant since it is easily cut with a knife due to its straight shape. For the dumbbell shaped specimen, the plotter is more favorable since it is better in cutting the more complicated shape of this specimen. This is only pronounced for the secant modulus, where there is a big difference between the averages of the standard deviations of the dumbbell specimens cut with

the knife or the plotter. For the yield stress the differences are less pronounced and rather preferring the knife as cutting method.

The results were expected to be more distinctive preferring one option. Since the secant modulus is measured at lower stresses a more sensitive method is more important for this value than for the yield stress that is measured at higher tensile stresses. Therefore, cutting with the plotter that showed less scattering for the secant moduli for both specimens is preferred for further works.

Overall, it is concluded that the cutting with the plotter is preferred over the cutting with the knife. Although the superiority of the plotter was not that pronounced in the test results as expected, it was more favorable because of less time-consuming cutting work and less touching of the film with the hands or gloves. The preferred use of a specimen with a dumbbell-shape compared to an easy rectangle could not be confirmed in this work. The dumbbell cut by hand did not show better results with less scattering than the easy to cut rectangle. The average standard deviations were higher for the dumbbell specimen than for the rectangular specimen cut with the knife for both the secant moduli and the yield stresses. For the use of a cutting plotter the differences were very small. The average standard deviation of the secant moduli was smaller for the dumbbell specimen whereas the average standard deviation of the yield stresses was smaller for the rectangle cut with the plotter. Since there was no clear superiority of the dumbbell-shaped specimen, the more complicated and time-consuming preparation of this test specimen was not found reasonable.

Looking at the mean values of the secant modulus and the yield stress, the dumbbell-shaped specimen showed the tendency to result in higher values than the rectangular-shaped one. This behavior was observed for both samples, cut with the knife and cut with the plotter (Figure 21, top). Since the rectangular specimen represents the shape of the real oral film, the difference between the mean values of the specimens is not of great relevance and does not mean that the dumbbell is a better specimen. The secant modulus was highest for the films without plasticizer. For the HPMC films glycerol and triethyl citrate showed similar reduction of the secant modulus and therefore the stiffness of the film. Triethyl citrate did not show a reduction of the secant modulus for the film with PVA and HPMC as matrix. It was assumed that the triethyl citrate is not a suitable plasticizer in combination with PVA. The citric acid reduced the secant modulus for both films the most, probably because of the high amount of plasticizer. HPC showed a very low secant modulus although no plasticizer was incorporated. A similar

trend was observed for the yield stress that is a measure for the tensile stress, which is necessary to deform the sample irreversibly.

For further investigations, the rectangular test specimen cut with the plotter was used in this work to best reflect the long film that will be used in the dosing device later on.

3.2.2.4 Characterization of drug-free films

The prepared long ODFs from Table 5 were characterized regarding their masses and thicknesses (refer to section 5.4.5 and 5.4.6), their mechanical properties (refer to section 5.4.11.2), their disintegration time (refer to section 5.4.7) and their water vapor sorption behavior (refer to section 5.4.8).

Figure 22 presents the mass and thickness values of the prepared long ODFs. HPMC and HPC films showed higher masses since they contained higher polymer contents than the films with PVA and HPMC as matrix. The clearly higher thickness of the H3 film might result from the observation that the film samples curled up before measuring. The curled edges might distort the thickness measurement of the micrometer screw with the attached plates by pretending a higher thickness than the actual film had. The other thicknesses showed similar values since they were all cast with a gap height of 500 µm on the pilot-scale coating bench. In comparison to the films prepared with the small-scale coating bench the mass and thickness values of the long films reached only around 50 % (Figure 13). The polymer mass was cast at a gap height of 500 µm for both manufacturing methods. The factor between the gap height and the WFT of the polymer mass after film casting was not transferable between the two coating benches due to the different processes. The pilot-scale coating bench produced thinner films at the same gap height of the knife, probably due to the liner moving beneath the knife and stretching the coating mass over the liner, yielding a thinner film.

The mechanical properties were evaluated by performing the tensile test for the prepared films. The data were collected by measuring the rectangular specimen that was cut with the cutting plotter. The secant modulus and the yield stress were evaluated as measurement values giving information about the deformation behavior of the produced long oral films. A low secant modulus indicates a low slope in the linear region of the stress-strain curve that means that the elastic deformation of the film occurs already at low applied stresses. The region of elastic deformation is rather spread over a longer range of strain. A low yield stress indicates that only little tensile stress is needed to reach the region of plastic deformation by overcoming the yield point. To ensure consistent dosing of the developed ODF, high secant moduli and yield stresses

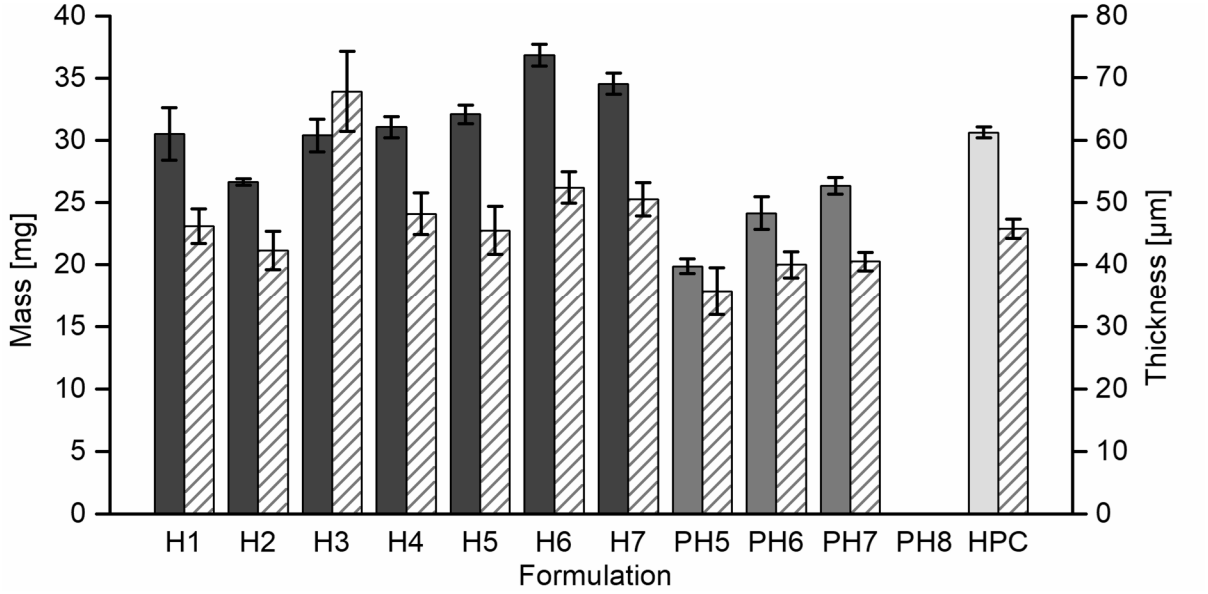

Figure 22: Masses and thicknesses of 6 cm² film pieces of the formulations from Table 5 that were cast to a film. PH8 was not measured. Filled columns: mass; dashed columns: thickness (mean ± CI, α = 0.05, n = 10).

are preferable for safe handling and minimum deformation. Therefore, extreme levels of deformation were used as exclusion criteria in this study.

The results of the tensile test are shown in Figure 23. The plasticizer added to the formulations to improve sticking of the film to the process liner also had an influence on the mechanical properties. The HPMC films, glycerol as plasticizer (H2 and H3) showed significantly lower values for both the secant modulus and the yield stress than the plasticizer-free film (H1). Three percent triethyl citrate (H4) also reduced the mechanical strength of the HPMC film. H5 with only 2 % triethyl citrate and the films with citric acid as plasticizer (H6 and H7) showed no clear differences to H1 for their secant moduli. The yield stresses of H5 to H7 were higher than the yield stress from the plasticizer free film. The deformation behavior at lower stresses presented by the secant modulus did not change because of the plasticizer addition. The yield stress as the stress where the plastic deformation starts was increased by the investigated amounts of plasticizer. Therefore, the mechanical strength of the film improved because it was able to resist to increased applied tensile stress but did not become too flexible to deform already at low tensile stresses. Increasing the plasticizer concentration would probably lead to reduced mechanical strength becoming clear in high elastic films. For the films based on PVA and HPMC, the results showed significant lower mechanical strengths for all films containing a plasticizer compared to the one without (PH5). The films with glycerol (PH6) and citric acid (PH8) showed much lower values than the triethyl citrate film (PH7). For the evaluation of the mechanical properties of oral films it is important to note that the films are neither too flexible,

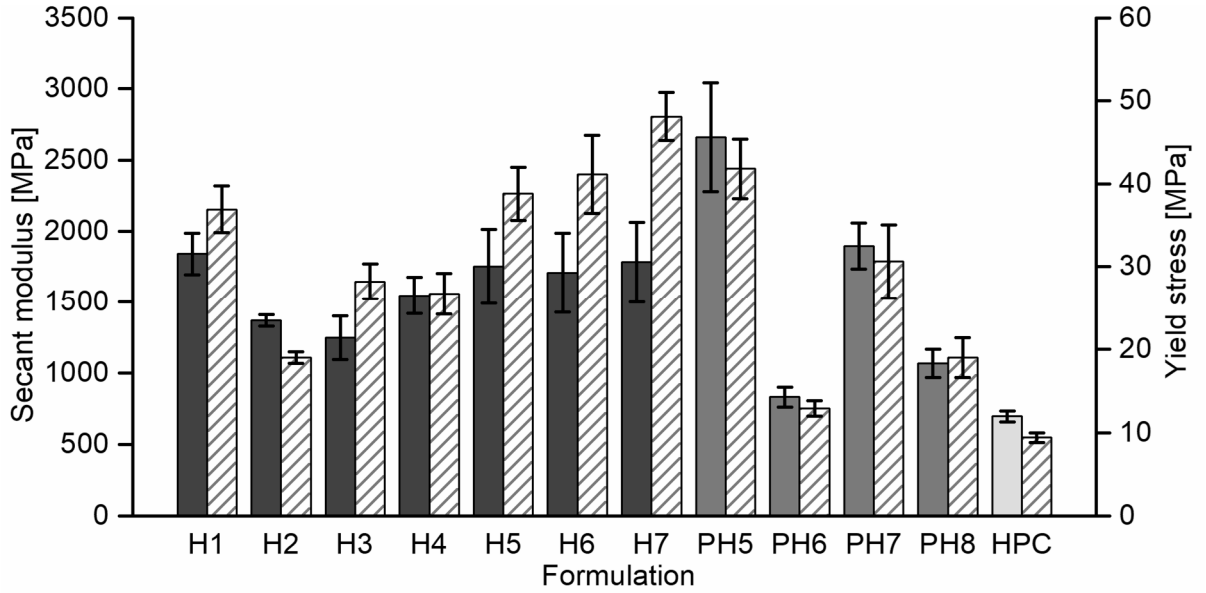

Figure 23: Mechanical properties of the drug-free films from Table 5. Filled columns: secant modulus; dashed columns: yield stress (mean ± sd, n = 5). Used by courtesy of the European Journal of Pharmaceutics and Biopharmaceutics, Elsevier (Niese and Quodbach, 2019).

presented by a low secant modulus nor too brittle, presented mainly by a stress-strain curve as shown in the right graph in Figure 20. The yield stress is a measure for the plastic deformation that shall not start at low stresses as well. Since the aim of the study was to find a formulation that would not deform easily the high values for the secant modulus and the yield stress were considered positive since the films revealed a good handling with low deformation and flexibility without breakage. Formulations H4, H5 and PH7 were discarded due to the reason that triethyl citrate revealed a very bitter taste that was not acceptable for an ODF. The ODF is supposed to dissolve rapidly in the mouth of the patient (Ph.Eur 9.3, 2018a). By this means, the dissolved molecules are presented directly to the taste buds in the oral cavity. An unpleasant taste negatively affects the compliance of the patient, especially if the film is intended for the use in children. The films with citric acid as an alternative plasticizer showed a pleasant taste and promising results but revealed incompatibilities with the model drug warfarin due to pH incompatibility (refer to section 3.2.4). Films HPC and PH6 showed unacceptable mechanical behavior since they exhibited very low secant moduli and yield stresses. The indicated easy deformation and therefore change of the film length was confirmed by manual handling of the films. Handling by a patient, who dispenses the film from the dosing device would not be safe since the dose of the delivered film piece would change depending on the length. These formulations were therefore excluded from the study. PH5 showed high values for the secant modulus and the yield stress since no plasticizer was added. However, this film was very stiff and it could not be coiled up reliably. This step is essential for the use in the dosing device and

hence, the film was excluded as well. H2 and H3 were the remaining formulations and H3 was preferred for further investigations because of the higher yield stress that promises better resistance to pulling force.

A severe problem with the mechanical testing that was observed during the course of this work was the extreme impact of the climatic conditions on the films. Especially the relative humidity of the measurement room showed a critical effect on the mechanical behavior of the film. It was noticed that films that were stored at defined relative humidities changed their mechanical behavior within minutes after taken from their storage place into the measurement room. During the measurements in a room without humidity control, changes in the test results for samples from the same batch were apparent. The fast water sorption kinetic can be recognized in the water vapor sorption measurement exemplarily shown for one thin film sample in Figure 24. The stepwise vapor sorption curve illustrates how fast the film sample absorbed the water. The steps representing the measured mass change of the sample virtually show the same sharp shape as the steps of the relative humidity controlled by the machine. In the zoomed picture section, it becomes clear that within minutes after the machine changed the relative humidity to the next higher level, the mass of the sample increased because of the absorbed water. The left vertical line in the zoomed picture section represents the start of the relative humidity

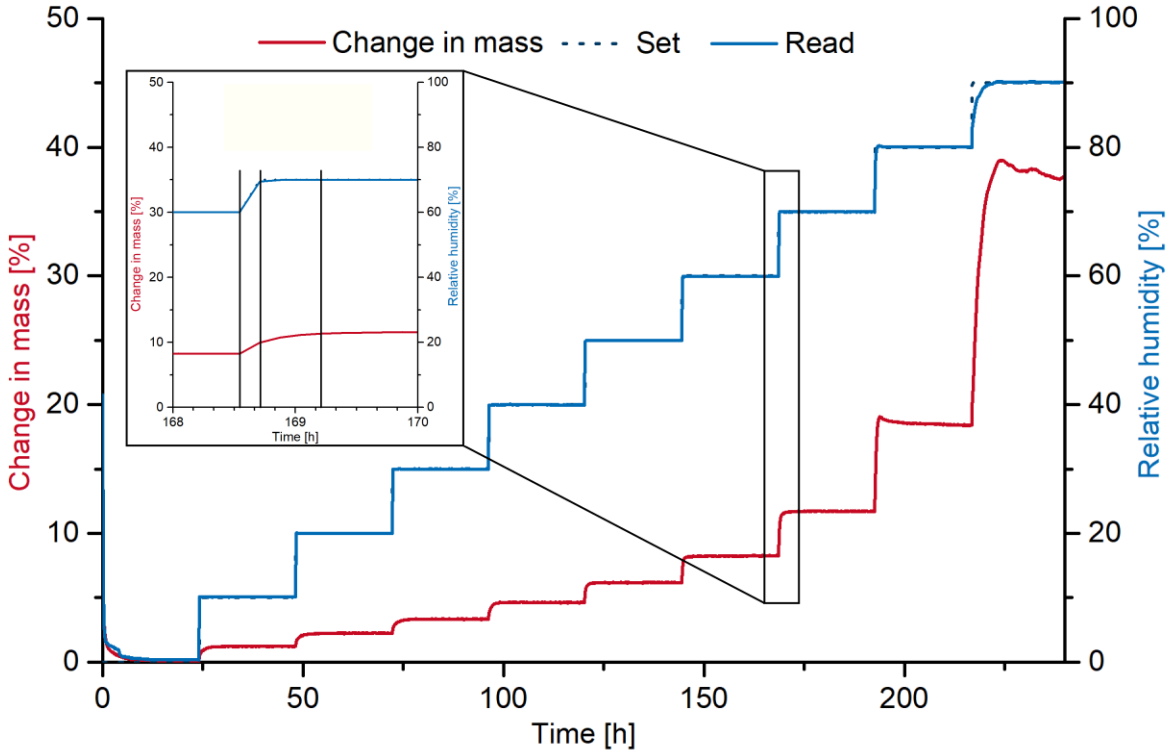

Figure 24: Exemplary dynamic vapor sorption curve of PH8. In blue the set (dashed line) and the read (solid line) relative humidity, increasing stepwise from 0 – 90 %. In red the measured change in mass of the film sample. The zoomed picture section shows the two-hour interval of the relative humidity step from 60 to 70 %.

change by the machine. The next relative humidity step is reached after ten minutes (middle vertical line). At this point, the film sample already absorbed about 50 % of the totally absorbed mass of water during this humidity increase. The final equilibrium of the change in mass is reached after 40 minutes (right vertical line). These data confirmed the aforementioned observation. Samples that were stored under controlled conditions and then brought into the measurement room changed their mechanical resilience within a short time period during the tensile test because of the absorbed water that also acts as plasticizer in the thin polymeric films. Since the humidity in the measuring room was not controlled this effect was not clearly noticed until the summer caused relative humidities of over 70 % in the 21 °C cold room. Therefore, it cannot be ruled out that some differences in the mechanical properties were rather due to changing climatic conditions in the room that were not noticed before than due to film properties. To minimize this impact factor and to be able to compare the data from mechanical tests, they should always be performed in climatic controlled rooms under defined conditions. The standards for example recommend 23 °C and 50 % relative humidity (ASTM, 2012; DIN, 2012). Looking at the water sorption isotherms (Figure 25) it is apparent that it makes a big difference to measure the samples at humidities that differ up to 30 % as it was possible in the measurement room. The higher water content at higher relative humidities acts as plasticizer in the films and leads to higher flexibilities, critically changing the test results (Karlsson and Singh, 1998).

There are further characteristics of ODFs that are important for their suitability and their evaluation besides the previously discussed mechanical properties. The results for the disintegration time, the water content and the water vapor sorption are shown in Table 7. The disintegration testing showed results of lower than 60 s for all the tested film samples. These results were all below the threshold value of 180 s given by the European Pharmacopoeia for ODTs (Ph.Eur 9.3, 2018b) that was applied since a specification for ODFs is still lacking from regulatory side (refer to section 3.1.6). The results of the disintegration time, the water content and the vapor sorption are linked to each other. The disintegration time of an ODF, which is required as low as possible is positively affected by higher water contents and higher hygroscopicity of the film sample. However, it is important to find a good compromise between high water sorption and low disintegration times since too high water content or sorption adversely affects the properties of the ODF such as mechanical properties. The mechanical integrity suffers due to the plasticizing effect of the incorporated water as already mentioned before. Furthermore, too much water in the film sample leads to stickiness and also microbial

Table 7: Film properties of the drug-free formulations from Table 5. Disintegration time (mean ± sd, n = 6), water content (mean ± sd, n = 3) and water vapor sorption at 70 % relative humidity (n = 1).

Formulation	Disintegration time [s]	Water content [%]	Vapor sorption [%]
H1	54 ± 12	7.4 ± 0.3	10.7
H2	32 ± 6	10.2 ± 2.3	16.9
H3	55 ± 4	4.7 ± 0.3	13.7
H4	46 ± 3	4.6 ± 0.2	7.7
H5	58 ± 2	3.5 ± 0.3	7.2
H6	54 ± 2	5.1 ± 0.2	11.3
H7	58 ± 5	4.9 ± 0.1	10.8
PH5	22 ± 5	6.8 ± 0.7	11.3
PH6	27 ± 4	8.1 ± 0.5	13.4
PH7	38 ± 3	6.1 ± 0.2	10.0
PH8	44 ± 4	3.8 ± 0.1	11.7
HPC	30 ± 4	6.1 ± 0.1	9.9

stability issues. The vapor sorption isotherms are presented in Figure 25 for the most promising drug-free formulations. It is obvious that glycerol as plasticizer showed the highest impact on the water absorption (blue curves). The films with citric acid as plasticizer were comparable to the non-plasticized film samples. The higher hydroscopic behavior of glycerol favored the water sorption of the films in comparison to the other formulations. Due to these findings, the citric acid would be the more favorable plasticizer for the film formulation development. Unfortunately, the acidic character of the substance made it incompatible with the model drug warfarin (refer to section 3.2.4.1). Therefore, it can be concluded that for APIs not being sensitive to the acidic character of the citric acid, this plasticizer is a promising alternative for the use in oral films.

For the films with caffeine as model drug, used for the validation of the optical probe in the next chapter (refer to section 3.2.3), citric acid revealed beneficial properties since it helped to prevent recrystallization of the caffeine in the oral film, which was stated in literature (Garsuch, 2009). The citric acid probably formed caffeine citrate with the model drug, which is better soluble than the free caffeine base. Therefore, the recrystallization was prevented and the ODFs stayed transparent over the investigated storage period. Additionally, it improves the taste after disintegration in the mouth, which is of great relevance for ODFs. The saliva production increases as well because of the citric acid, which favors the disintegration time because of more available liquid in the oral cavity.

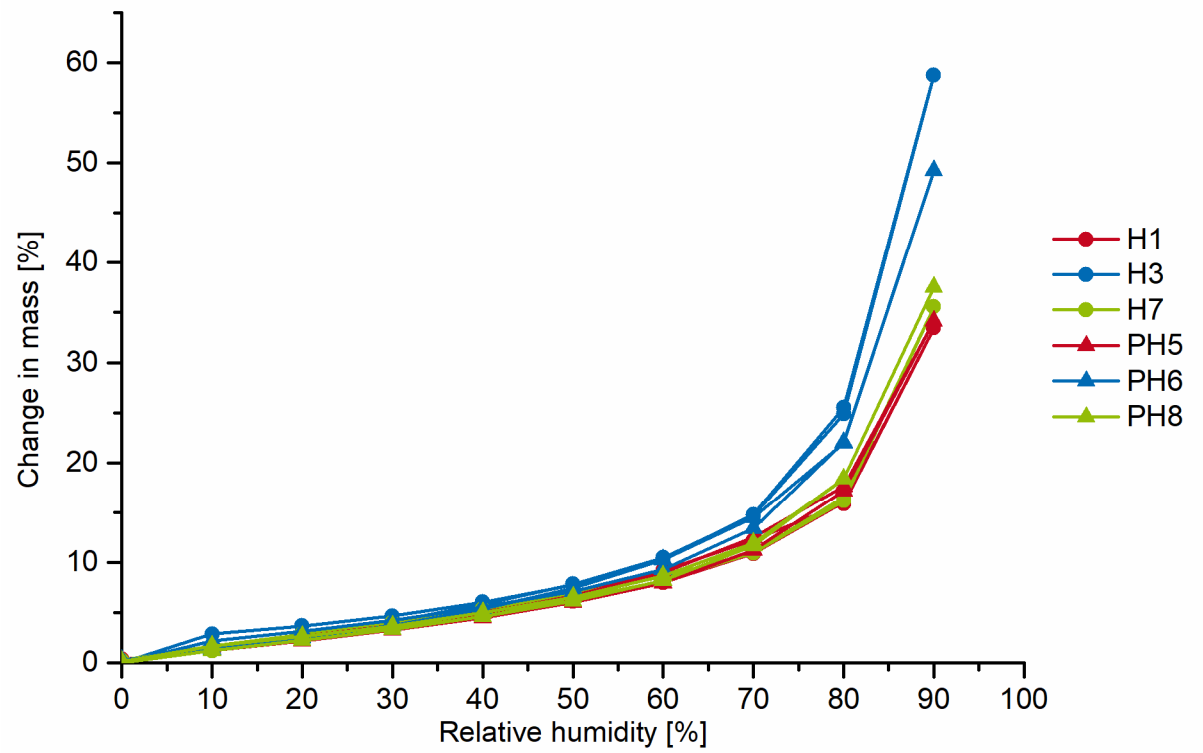

Figure 25: Water vapor sorption isotherms of the drug-free film formulations at 25 °C. Red: without plasticizer; blue: with glycerol as plasticizer; green: citric acid as plasticizer (n = 1).

Due to the incompatibility of citric acid and warfarin, the drug-free formulation H3 was the first choice for the incorporation of the API. H3 showed acceptable mechanical properties as well as disintegration time and water content. Since the vapor sorption was rather high due to the hygroscopic effect of glycerol, the stability tests of the ODF have to be performed at different relative humidities to ensure that the stability is not affected (refer to section 3.2.4.3).

3.2.3 Process control - in-line wet film thickness determination

3.2.3.1 Problems of current situation and objectives

The wet film thickness is a key parameter for the manufacturing of an ODF since it has a major influence on the properties of the dry film as e.g. disintegration time, mechanical properties, dissolution, handling and the mouth feel. However, especially when incorporating an API, the drug content and hence the dose of a film is defined over the thickness of the wet coating mass during film manufacturing (Borges et al., 2015; Dixit and Puthli, 2009; Krampe, 2015; Susarla et al., 2013). To clarify different terms from literature they are defined as follows and used throughout the present work accordingly. The “wet film thickness” means the same as the “coating thickness” and describes the practical film thickness that is obtained during the film manufacturing process behind the knife. It is the height of the formed wet film on the process liner. In contrast, there is the “theoretical wet film thickness” that describes the distance of the coating knife to the process liner. This thickness is referred to as “gap height” in this work. In practice, the WFT is usually less than the theoretical one due to shearing effects on the film forming mass (Erichsen, 2016; Visser et al., 2017a). The “dry film thickness” refers to the thickness of the dried film after manufacturing.

The adjustment of the API content during the formulation development of an oral film is not described in most published works covering this topic. General recommendations are lacking but there are many trial and error approaches. The gap height was adjusted individually for every new polymer formulation to meet the target content (Garsuch, 2009). Another way was the attempt to develop a formula that was used to calculate the gap height necessary to reach a target content. The area of the film and the gap height were used to calculate the theoretical volume of the film mass and the drug content was calculated in regard of this volume (refer to section 5.3.2.2). The formula was extended with the trial to use a factor to compensate the difference between the WFT and the gap height or with a surplus of API added to the film forming mass to compensate the same (Krampe, 2015; Lindert, 2016; Preis et al., 2012; Wörtz, 2015). There are different parameters that affect the WFT during the coating process. The viscosity of the film forming mass affects the thickness because of different shear behaviors (Krampe, 2015; Thabet and Breitkreutz, 2018), whereas the process liner has also an influence on the spreading behavior of the coating mass (refer to section 3.1.4) (Thabet et al., 2018c). Due to these dependencies of the WFT, it is not reasonable to define a factor for the gap height only once. It is therefore common procedure to calculate the gap height or the drug content of the film forming mass, produce the film and then test whether the target amount was met.

Iterations of this procedure were performed until the measured content matches the target value. The disadvantage of a trial and error approach like this, are the high costs of resources, time and money. The WFT has to be controlled during the production process because of its relevance for the adjustment of the drug content as well as the impact it may show on the release profile of poorly water-soluble drugs incorporated into oral films (Dave et al., 2013). For the continuously working pilot-scale film manufacturing process, an in-line method to control and measure the WFT is very valuable to reduce trial-and-error-based film formulation development. Furthermore, problems during the production may be observed already during the process, which enables an intervention into the process to improve the results and to avoid shortfall batches.

3.2.3.2 Operating principle of the optical system

To improve the current state-of-the-art, comprising of trial and error approaches, an in-line measurement tool for the WFT was implemented into the film manufacturing process on the continuously working pilot-scale coating bench (refer to section 5.3.4). For a non-destructive and contactless measurement, a sensor with an optical probe head operating with a chromatic

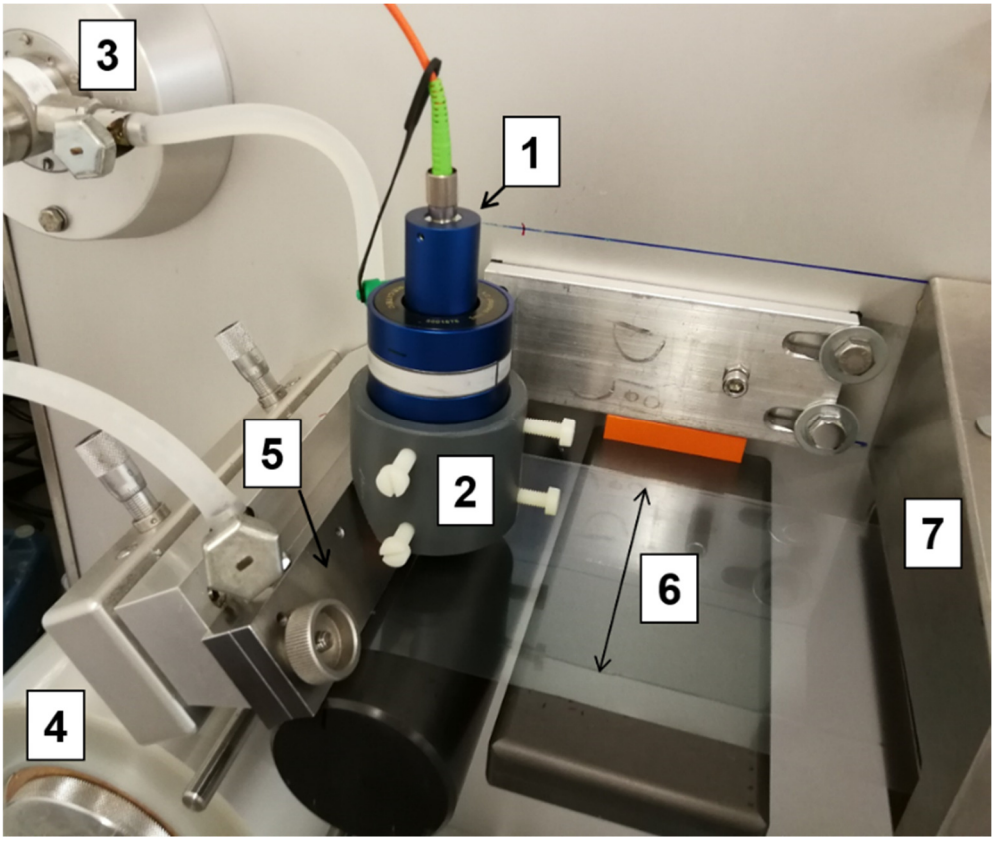

Figure 26: Assembly of the optical probe at the pilot-scale coating bench showing the probe head (1), probe head mount (2), pump (3), process liner (4), coating knife (5), coated film on liner (6) and the drying oven (7). Used by courtesy of the International Journal of Pharmaceutics, Elsevier (Niese and Quodbach, 2018).

confocal measuring principle was chosen, which is applicable for transparent and non-transparent materials (refer to section 5.3.4.2, CHRocodile S, Precitec). Figure 26 shows the assembly of the optical probe mounted on the pilot-scale coating bench. A probe head mount was developed and built to install the optical probe on the pilot-scale coating bench. A fixed and solid mounting was important since moving of the optical probe head would disturb the highly accurate measurements of the film thickness. The developed mount is fixed to the housing of the coating bench and can be relocated for cleaning purposes of the coating bench and for the correct positioning of the measuring point.

The operating principle of the optical probe is shown in Figure 27. A distance measurement to measure the distance between a material surface and the optical probe and a thickness measurement to measure the thickness of a transparent material are possible. The light coming from a white-light source is focused by the optical probe head separately for the different wavelengths. The wavelength that is in the focal plane of the measured object is reflected from the material surface and is detected in the optical probe head. The received spectrum shows the wavelength of the reflected light as a peak. The distance between the probe head and the material surface corresponds to the wavelength of the peak (Figure 27, left). For the measurement of the thickness of a transparent material, two peaks representing the position of the two interfaces of the material show up in the spectrum. The difference between these peaks

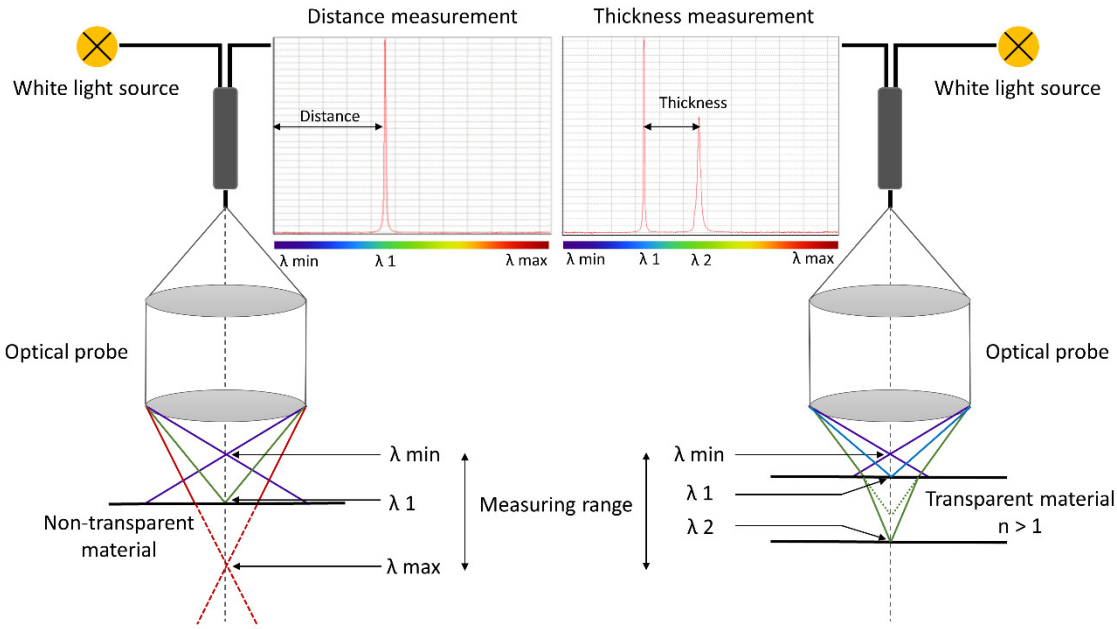

Figure 27: Measuring principle of the chromatic confocal optical probe. Left: distance measurement; Right: thickness measurement. Schematic drawing according to and with kind permission of Precitec (2018). Used by courtesy of the International Journal of Pharmaceutics, Elsevier (Niese and Quodbach, 2018).

represents the optical thickness of the measured material (Figure 27, right). The physical thickness can be calculated by using the optical properties and the refractive index of the material. Optical and physical thickness of a material differ because of the differing light refraction in a materials that is optical denser than air (Precitec, 2018).

3.2.3.3 Validation of the new in-line process control method

3.2.3.3.1 General considerations

A method validation according to the International Council for Harmonisation (ICH) guideline Q2 (ICH, 2005) for the new in-line WFT measurement was performed as described in section 5.3.4.3. The chromatic confocal optical probe was used as process analytical technology tool. Typical validation characteristics as listed in the guideline were assessed concerning their applicability regarding the new in-line method to determine the WFT.

3.2.3.3.2 Specificity

A validation characteristic that was not applicable for the in-line WFT measurement method was the specificity since the measurement was not meant to identify or to determine the amount of the API in the oral film. The probe is not meant to be specific for only one composition since a widespread use in the film manufacturing process of oral films is targeted at. Different kinds of coating masses and process parameters shall be usable, which is further investigated and discussed in a comprehensive analysis of the robustness of the method in section 3.2.3.3.8.

3.2.3.3.3 Linearity

A range covering commonly used WFTs for ODFs was investigated for linearity. A linear relation was observed for thicknesses of 100 – 350 µm of the wet coating mass. The regression line pictured in Figure 28 on the left shows the measured content plotted against the WFT. A y-intercept close to zero and a slope that allows a clear distinction of different WFTs were obtained. A good coefficient of determination was presented as well, which is important if WFTs between the ones investigated are produced. On the right side of Figure 28 the regression line of the plot of the measured content against the target content is presented. It was shown that the relation between the WFT that was set to reach a target content and the measured content was not only linear ($R^2 = 0.9990$) but also it was obvious that the target content was precisely met for the films produced.

Furthermore, the dried film mass and film thickness were related to the WFT. The results are shown in Figure 29. A good correlation for the mass and the WFT can be seen ($R^2 = 0.9978$). The dry film thickness did not correlate that well with the WFT. The trend was comparable but

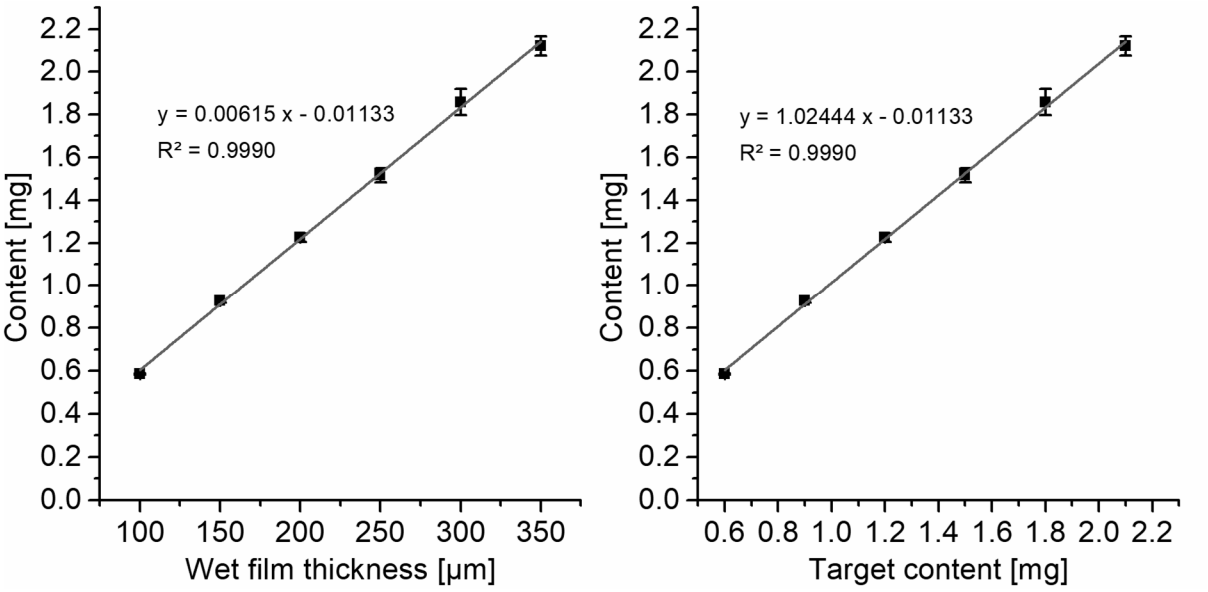

Figure 28: Linearity - Regression lines of the content plotted against the wet film thickness (left) and the target content (right) (mean ± sd, n = 6). Used by courtesy of the International Journal of Pharmaceutics, Elsevier (Niese and Quodbach, 2018).

the coefficient of determination only was $R^2 = 0.9593$ and the data showed high scattering for the measured dry film thicknesses. This can be traced back to the measuring method since a modified micrometer screw was used for the performed measurements. This modification did not seem suitable for such thin films. The films with higher thicknesses revealed less scattering (300 and 350 µm). The plates attached to the measuring points of the micrometer screw were able to move slightly, which might affect the measurement in the low µm-ranges.

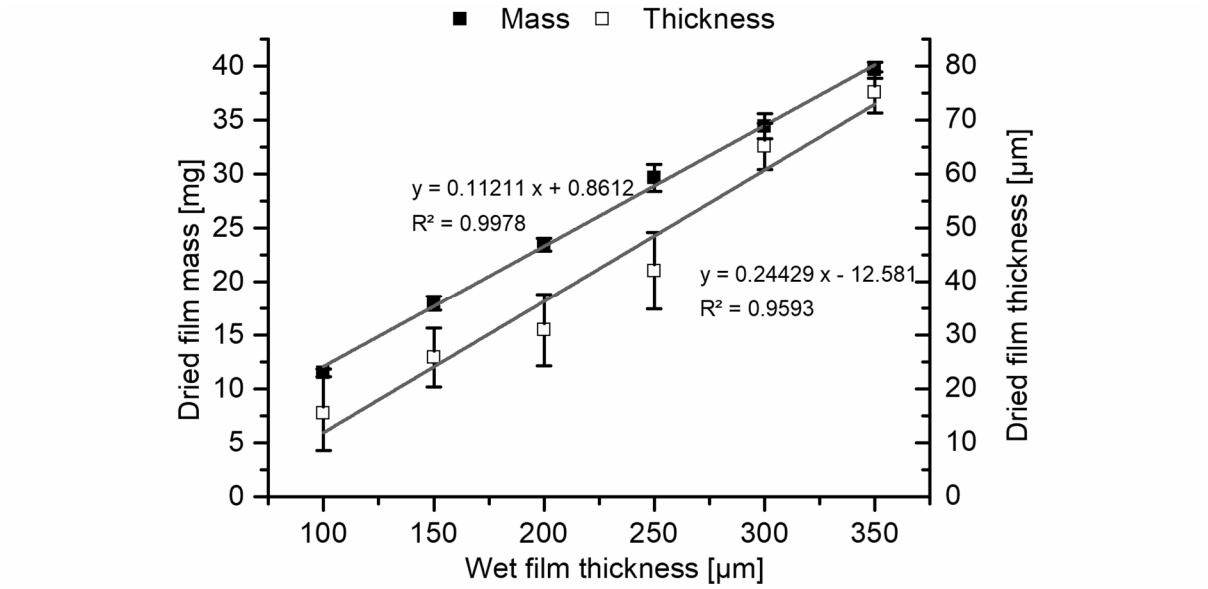

Figure 29: Linearity - Regression lines of the relation between the mass and the thickness of the dried film to the wet film thickness (mean ± sd, n = 6).
Used by courtesy of the International Journal of Pharmaceutics, Elsevier (Niese and Quodbach, 2018).

3.2.3.3.4 Range

Acceptable results were shown for the linearity, the accuracy and the precision of the in-line film thickness measurement with the optical probe. The range of the method was established by presenting these positive results. The investigations were performed for the model API caffeine in one concentration in the polymer solution but in case of the linearity, six different measured WFTs of 100 – 350 µm were evaluated resulting in six different contents per area of the film piece. The gap height of 500 µm commonly used in the trial and error approaches corresponds to a measured WTF of approximately 250 µm, depending on the polymer mass and the release liner. In case of the accuracy and the repeatability, three WFTs were assessed. The results were further considered as valid for other thicknesses within the range covered by these results.

3.2.3.3.5 Accuracy

The investigation of the accuracy for the new in-line WFT measurement was performed within the established range of linearity. Three WFTs of 150, 250 and 350 µm were evaluated for this purpose. Acceptable results for the average contents of the three produced films for every WFT were defined as in the range of 95 – 105 % of the label claim. With these limits it would be possible to reach adequate acceptance values (AV) according to the European Pharmacopoeia (Ph.Eur 9.1, 2017) if acceptable standard deviations were obtained. The results were calculated as percentage of the target value according to the set WFT (label claim in this case, calculated according to Equation 3, refer to section 5.3.2.2). No reference standard was used for the calculation of the results since the investigated thickness measurement method is not meant to determine a content. The outcomes of the accuracy investigation for the prepared films are shown in Table 8. It is noteworthy that the mean value of the three films per examined WFT was slightly higher than the limit specified as acceptable for all three investigated WFTs. The variation within one thickness was very low and the relative deviation from the target value was similar for all three WFTs. This indicated that the film manufacturing process was consistent, but some effect was responsible for the exceeding results. After repeating the experiment and finding the same outcome, a closer examination of the process was conducted. The homogeneity of the film thickness over the width of the manufactured film was investigated (refer to section 5.3.4.3.4) and the outcome is presented in Table 9. The assumption of surface effects affecting the results was confirmed. It was shown that the coating mass contracted during the process, which became clear observing the data from the content determined over the width of the film. The caffeine content in the center of the film exceeded

Table 8: Accuracy - Comparison of the obtained caffeine content to the target content for three different wet film thicknesses (n = 3).

	150 µm	250 µm	350 µm
Mean value [%]	106.4	106.3	105.2
Standard deviation [%]	0.8	0.7	0.7
Coefficient of variation [%]	0.72	0.69	0.66

Table 9: Accuracy - Film thickness homogeneity over the width of the film (n = 3).

	Left edge	Middle	Right edge
Mean value [%]	90.9	108.1	90.5
Standard deviation [%]	4.1	0.4	2.4
Coefficient of variation [%]	4.52	0.34	2.68

the 100 % whereas the content at the edges of the film was lower. The samples that were investigated for the accuracy determination were taken from the middle of the films and therefore from the region being overdosed because of the contracted coating mass. This effect is clearly unwanted, but it was difficult to avoid on the pilot-scale coating bench since the width of the produced film is limited due to the size of the liner and the size of the coating bench. The edge effect was substantial for the manufactured film with a width of around 10 cm. However, for broader films, which are produced on production sized machines the effect might be negligible since edges are normally discarded and do not show a large relative part of the whole film. Furthermore, larger manufacturing lines can be equipped with several probes to monitor edge effects. It was concluded that the accuracy values that were higher than acceptable were not because of the new WFT measurement method but due to general process effects. The application of the optical probe on the pilot-scale coating bench still contributes to a better process understanding and a better formulation development. Control of the process is possible since changes of the WFT are immediately recognized and a reaction on the changes is possible. Since the deviation for the average value from the target value was reproducible, it is possible to calibrate the WFT measurement for the use on the pilot-scale coating bench.

3.2.3.3.6 Precision

The investigation of the precision for the new in-line WFT measurement was performed within the established range of linearity and the coefficient of variation (CV) as a result of the measurements of three films was defined as acceptable for values lower than 2 %. For the determination of the intra-day precision, also called repeatability, three films for every WFT were prepared and evaluated at the same day. The coefficients of variation for 150 µm resulted

in 0.72 %, for 250 µm in 0.69 % and for 350 µm WFT the result was 0.66 %. The intermediate precision, which is also called inter-day precision, was determined at three different days that were spread over a time interval of one month. The WFT of 250 µm was investigated. The outcome was a CV of 0.47 % for all samples. For the three single days, values of 0.69 %, 0.76 % and 0.36 % were obtained. All results for the precision examination were in the defined limits. The low values for the CV indicate that the investigated method works reliable since the results were hardly changing over time. For the pharmaceutical production and development, this is an important criterion for a process analytical technology to ensure proper working.

3.2.3.3.7 Detection and Quantitation limit

Detection and quantitation limit, which are important validation characteristics for the determination of an API content or impurities were not investigated for the evaluated method. The limits for the WFT are rather given by the handling of the film. Casting a film with a small WFT results in a thin dry film, which is very fragile. Unacceptable handling results due to easy breakage of the film. Therefore, the lowest covered WFT in this study was 100 µm yielding a dry film thickness of around 15 µm (Figure 29).

3.2.3.3.8 Robustness

The ICH guideline Q2 (2005) defines the robustness of a method as the "capacity to remain unaffected by small, but deliberate variations on methods parameters". The robustness was an important validation characteristic to evaluate in this study, to prove the reliable applicability of the new in-line WFT measurement method under different conditions. In this course, different parameters for the film manufacturing process regarding the coating bench or the polymer mass were evaluated and their influence on the thickness measurement was monitored.

Liner speed

To investigate the influence of the liner speed on the WFT measurement all other settings of the coating bench were kept constant except of the adjustable speed setting. A slower liner velocity (5 cm/min) than the basic setting (12.5 cm/min) and a faster velocity (19.8 cm/min) were investigated. It was observed that the results for the films produced with the slower liner speed showed good results with a content of 102.1 ± 2.4 %, whereas the faster liner speed produced films with a content of just 86.2 ± 3.0 %. This indicated a difference between the WFT at the point where the optical probe measured and at the point where the film finally dried. Different possible explanations were taken into consideration. It might be the case that

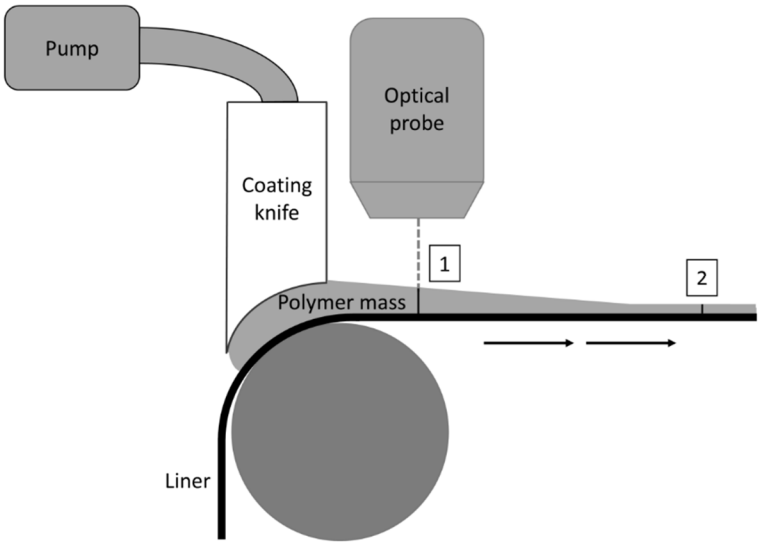

Figure 30: Robustness - Influence of the liner speed on the measured film thickness. 1: Thickness measured by the optical probe. 2: Corresponding thickness after spreading and movement of the mass by the fast-moving liner. Measured film thickness at point 1 would be always higher than on point 2.
Used by courtesy of the International Journal of Pharmaceutics, Elsevier (Niese and Quodbach, 2018).

the polymer mass did not have enough time to fully spread before the measuring point at faster liner speeds and, therefore, continued to spread after the thickness was measured resulting in a lower WFT until the film dried. Another explanation might be the option that the polymer mass formed a slope behind the knife while being delivered on the liner because it was pulled away by the faster moving process liner. The measuring point would measure a higher WFT if it was located before the slope ended (Figure 30, 1) and not the lower thickness after it decreased due to the movement of the liner (Figure 30, 2). This measurement error would result in too low contents of the prepared films. Therefore, it was concluded that the process should not be run too fast. If a higher speed is necessary, the position of the optical probe has to be adapted. Additional trials would be required to find the optimal position for the probe head.

Polymer matrix

A polymer mass with another matrix former than the basic solution containing HPMC was investigated to examine the effect of different matrices on the in-line thickness measurement. The mass with PVA and HPMC as film formers (refer to Table 27 and section 5.3.4.3.6) was used for this comparison. The polymer mass was slightly opaque instead of the clear and transparent appearance the HPMC solution showed. The film prepared from the PVA and HPMC mass showed a content of 103.3 ± 1.8 %, which was less than the content of the HPMC film prepared under the same settings (106.3 ± 0.7 %). A less pronounced edge effect yielding in less retraction of the polymer mass after the measuring point could be the reason for the

better result of the PVA and HPMC coating mass. Likewise, the polymer solution with PVA and HPMC showed a lower viscosity (1.26 ± 0.02 Pa*s) than the pure HPMC solution (1.49 ± 0.02 Pa*s), which might lead to less inner friction and therefore, less retraction and better flowing of the film forming polymer mass.

Colorant

The red coloring agent E 124 was added to the polymer solution. No effect of the colorant was apparent in the resulting content of the film (106.0 ± 1.3 %) compared to the content of the basic film without colorant (106.3 ± 0.7 %). The colorant dissolves and forms a red transparent solution. Due to its small amount in the entire batch, it did not have an apparent influence on wetting properties.

Viscosity

The dynamic viscosity of the coating mass is a key parameter for the film coating process as already described in literature (Krampe, 2015; Thabet and Breitkreutz, 2018) and previous sections of this work. Therefore, its impact on the film production using the in-line thickness measurement was investigated. For this examination, the film preparation applying the in-line measurement (refer to section 5.3.4.2) and the film preparation as it was done before using the formula to calculate the gap height (refer to section 5.3.2.2) were compared. Five polymer solutions with HPMC as matrix in varying amounts were included in this investigation (refer to Table 27 and section 5.3.4.3.6). The polymer content ranged from 11 – 19 % resulting in dynamic viscosities of 0.5 – 4.5 Pa*s. The previously already reported problem of not reaching the desired content for oral films by using the gap height as wet film thickness in the calculation of the content (Krampe, 2015; Lindert, 2016; Preis et al., 2012; Wörtz, 2015) was confirmed by the results shown in Figure 31. The film preparation with calculating the gap height was not able to attain a content of 100 %. The caffeine content for these films varied with increasing polymer content between almost 90 % and as little as 36 %. The deviation of the measured content to the target content of the film became higher with increasing viscosities of the polymer solutions. The higher inner friction of a viscous solution might reduce the flowing ability so that a reduced amount of coating mass enters the liner through the coating knife. The liner though was moving at the same velocity. This led to a thinner film and therefore a lower API content of the dried film sample. Looking at these results the need of a surplus was obvious as it was stated in the aforementioned literature. The disadvantage of a surplus is that it has to be determined again for every new formulation since it depends on the viscosity and other film forming properties of the mass and the process liner. This trial and error approach can be

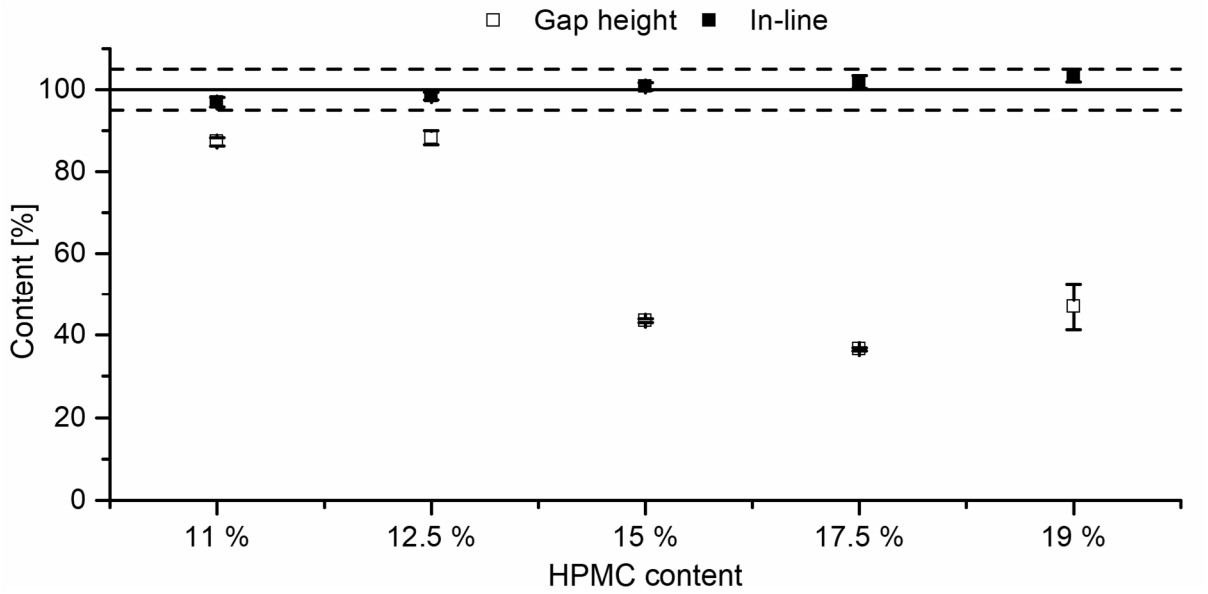

Figure 31: Robustness - Dependency of the caffeine content of the dried film on the polymer content of the polymer solution. Dotted lines show acceptable limits for the caffeine content of the film (mean ± sd, n = 6). Used by courtesy of the International Journal of Pharmaceutics, Elsevier (Niese and Quodbach, 2018).

replaced by using the optical probe for the in-line WFT measurement. Using the measuring probe, adjustments of the film manufacturing process settings were possible to reach the desired WFT. The pump flow, the liner speed or the gap height were the parameters that were adapted at the coating bench. The films prepared using the in-line measurement of the WFT showed caffeine contents close to 100 % (Figure 31), for all different polymer contents in the polymer solutions. A slight increasing trend of the results within the range of an acceptable content was noticed. A potential explanation might be that the viscosity can also have a slight impact on the in-line method as well. In case of higher viscosities, spreading of the film after the WFT measurement point would be reduced and rather low retraction of the film would be promoted. This would lead to an increased content for higher viscosities. For lower viscosities, the film might keep spreading after the WFT measurement yielding to lower contents.

Suspension

The polymer masses measured with the optical probe until this point were all fully dissolved solutions with a mostly transparent appearance. To prove the correct working of the in-line method for non-transparent polymer masses as well, an insoluble filler, microcrystalline cellulose (MCC) was added to the HPMC solution to form a non-transparent suspension (refer to Table 27 and section 5.3.4.3.6). Because of the non-transparent appearance of the polymer mass, the distance measurement principle was used in this part of the study (refer to section 3.2.3.2). The MCC particles, which were dispersed in the polymer solution showed a particle

size distribution with x1 = 3.6 ± 0.0 µm, x50 = 20.4 ± 0.1 µm and x99 = 105.8 ± 1.8 µm in the polymer mass. It was measured to ensure that no problems might occur during the film manufacturing process due to blocking the coating knife and the gap between knife and liner. Three homogenous films were prepared with the MCC suspension showing caffeine contents of 104.4 ± 0.6 % and a CV of only 0.53 %. This result was lower than the caffeine content of the compared pure HPMC films (106.3 ± 0.7 %). The MCC probably showed an effect on the surface properties of the coating mass resulting in less retraction. The particles of the MCC did neither negatively affect the measuring of the optical probe by its non-transparent appearance nor did the MCC change the caffeine content.

3.2.3.4 Conclusion

It can be concluded that the development of an in-line method for the measurement of the WFT during the film manufacturing on the pilot-scale coating bench was successful and the method was validated to prove the applicability for the intended purpose. The implementation of the chromatic confocal optical probe offers a new approach for the process control of the film manufacturing process. Trial and error approaches can be avoided and therefore, resources, time and money can be saved. The possible real-time control of the WFT during the film manufacturing process ensures the quality of the product since changes in the WFT and therefore the API content can be observed right away, and the process can be adjusted to prevent shortfall batches. The validation of the method proved good results under different conditions, such as changing process settings or properties of the polymer mass.

3.2.4 Orodispersible warfarin films

3.2.4.1 Formulation development of ODFs containing warfarin sodium

Warfarin was chosen as model drug since the flexible and individualized dosing was the primary focus of this work. The vitamin K antagonist with anticoagulant activity is known for a narrow therapeutic index as well as high inter- and intra-individual variations in the drug response (Ma and Lu, 2011; Reynolds et al., 2007). The range of a required and safe dose of warfarin varies widely among individuals because of a high risk of toxicity and the variability between different patients (Aithal et al., 1999; Reynolds et al., 2007). Warfarin exhibits genetic variations for enzymes affecting the drug action as well as the metabolism leading to a higher risk of side effects or to problems in the starting phase of a warfarin therapy (Aithal et al., 1999; Ma and Lu, 2011). Most important side effect is the risk of bleeding complications as a consequence of overdosing the API. Overdosing is possible because of too high given API doses as well as because of decreasing the API metabolism by inhibiting the degrading enzymes. The risk of bleeding is dependent on the INR and increases drastically for an INR greater than 5 (Aktories, 2005), underlining the importance of regular INR monitoring. Furthermore, there were observations reported that the warfarin requirements vary in people with different ethnical background as well as in different ages, especially in children (Biss et al., 2012; Shastry, 2006; Yu et al., 1996). With these background information, there clearly is a special need for individualized therapy with warfarin. Especially an urgent need for an child appropriate dosage form for warfarin was stated by the Paediatric Committee of the European Medicines Agency in their “Inventory of paedeatric therapeutic need” (PDCO, 2013). The currently available dosage forms for a warfarin therapy are limited to tablets that have to be split in case of a required flexible dose regime. An injection is the only true flexible dosage form available but not applicable for a daily drug treatment. The British National Formulary for children further describes a “Specials” formulation for a liquid dosage form for warfarin. This oral suspension contains 1 mg/ml warfarin sodium and can be flexibly dosed (Paediatric Formulary Committee, 2014) but is not available outside the United Kingdom. Therefore, the aim of this work was to develop an ODF containing warfarin for the use in children as well as adults. The film should be flexibly dispensed with the dosing device developed in course of this work to enable individualized therapy with warfarin in people of different age groups. The target dose of the warfarin film was 0.5 mg/cm² and attained by adding 2 % warfarin to the polymer mass and casting the mass with a wet film thickness of 250 µm.

Table 10: Formulations with warfarin. Percentages referred to total weight (w/w). Viscosity measured at 4 s^{-1} (mean ± sd, n = 3).

Formulation	Warfarin [%]	Polymer [%] (ratio)		Plasticizer [%]		Viscosity [Pa*s]
W1	2	HPMC	15	Glycerol	2	1.74 ± 0.02
W2	2	PVA:HPMC (2:3)	15	Citric acid	2	---
W3	2	PVA:HPMC (2:3)	15	---		2.64 ± 0.02
W4	2	PVA:HPMC (6:7)	13	---		1.46 ± 0.01
W5	2	PVA:HPMC (2:3)	13	PEG 300	3	1.49 ± 0.03
W6	2	PVA:HPMC (2:3)	13	PEG 300	1	1.33 ± 0.04

Table 10 lists the formulations that were tested for the incorporation of warfarin into the film forming mass. Formulation W1 is close to the drug-free formulation H3 with additional 2 % warfarin. This formulation was chosen due to the suitability to cast an acceptable long drug-free oral film on the pilot-scale coating bench with this coating mass (refer to section 3.2.2). The first trial to incorporate warfarin into the drug-free formulation H3 revealed a polymer solution with a viscosity of 3.24 ± 0.07 Pa*s. The manufacturing of this formulation on the continuously working coating bench was possible. However, due to the higher viscosity compared to the drug-free formulation H3 (2.68 ± 0.01 Pa*s) it was necessary to waste a larger amount of the polymer mass to ensure a consistent process with a consistent and smooth film as outcome. The polymer content was therefore reduced to 15 % of HPMC to minimize the toxic waste containing warfarin. The final HPMC formulation with warfarin showed a viscosity of 1.74 ± 0.02 Pa*s and was easily processible on the continuously working coating bench.

Since the drug-free film formulation PH8 formed a suitable drug-free film (refer to section 3.2.2), a formulation with PVA and HPMC in combination as polymer matrix was tried to be found as well for the incorporation of warfarin. Formulation PH8 contained citric acid as plasticizing agent. Incorporating warfarin into formulation PH8 formed a white suspension (W2) instead of the slight opaque appearance of the drug-free solution. The acidic plasticizer led to the precipitation of the API warfarin as free acid since the solubility of warfarin is pH dependent. Figure 32 a shows the structural formula of warfarin and the keto-enol tautomerism that presents the acidic hydrogen between the two electron-withdrawing carbonyl groups. In section b the ionization of warfarin is shown. Whereas the polymer solution W1 showed a pH of 9, the polymer mass with 2 % citric acid revealed a pH of 2.5. In the acidic pH the warfarin is mainly protonated because of a pk_a of warfarin of 5.0 (Cairns, 2012). The protonated warfarin is practically insoluble and therefore precipitates in the acidic polymer solution. The deprotonated warfarin, present in the API warfarin sodium, is very soluble and therefore no

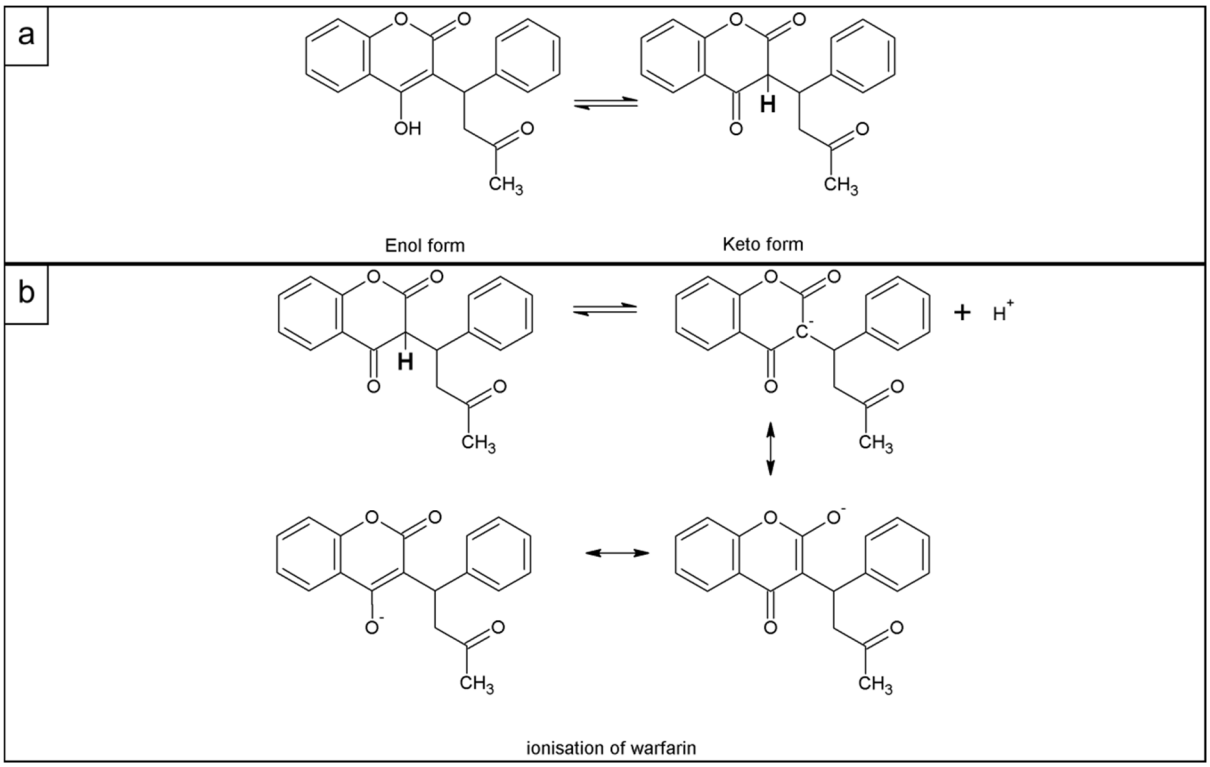

Figure 32: Structural formula of warfarin. a: Keto-enol tautomerism of warfarin, presenting the acidic hydrogen (bold). b: ionisation of warfarin, starting from the keto form with the acidic hydrogen (bold).

problems were observed in the other polymer solutions with higher pH values (Ph.Eur 9.0, 2017c). Therefore, two different formulations with PVA and HPMC as polymer matrix were tested without plasticizer to incorporate warfarin (W3 and W4). Formulation W3 contained the same polymer matrix as W2 but without citric acid. The film from W3 was brittle and easily broke when coiling it up. The mechanical properties revealed a high secant modulus that conformed the low flexibility of the film. The yield stress was not much higher than for the plasticized films (Figure 33). The low flexibility combined with the yield stress being in the medium range might explain the behavior of the film that it did not deform but broke after applying a stress on it. This was visible in the stress-strain diagram obtained from the tensile test where the curve showed a usual shape of a brittle material without a yield point as transition period between the elastic and plastic deformation area. The film broke already in the ascending front part of the curve. Therefore, in this case the yield stress was the same as the tensile stress at break. The elongation at break was very small (1.34 ± 0.22 %) underlining the low flexibility.

The formulation W3 was changed to W4 by changing the ratio of the two polymers in advantage of the PVA to increase the elastic amount of the polymer matrix. Further, the polymer content was lowered from 15 % to 13 % to reduce the viscosity due to the reason

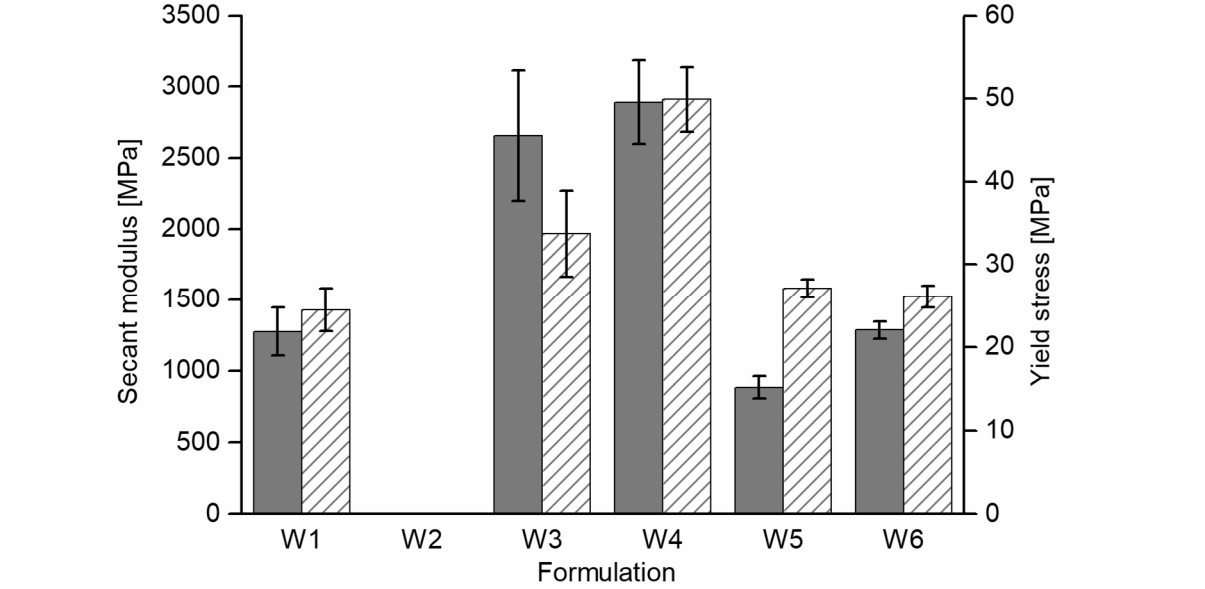

Figure 33: Mechanical properties of the warfarin films from Table 10. Filled columns: secant modulus; dashed columns: yield stress (mean ± sd, n = 5). W2 was not measured since no film was manufactured.

mentioned above. The film manufactured from formulation W4 showed a comparable secant modulus to W3 but a higher yield stress that also revealed a higher elongation at break (2.20 ± 0.45 %). The shape of the stress-strain diagram was comparable with the shape of the diagram of the film prepared from W3. No area of plastic deformation was reached. The higher yield stress implied that the film would withstand higher stress input before breaking.

Even though the films without a plasticizer did not show problematic deformation behavior, they showed a very brittle behavior that was not optimal for further handling. Therefore, a plasticizer was added again to the formulation. The already tested plasticizers were all excluded due to the mechanical properties of the film (PH6), the bitter taste (PH7) and the incompatibility with the API warfarin (PH8, W2). However, the PVA and HPMC combination was chosen to be used as film matrix for a warfarin film and therefore, the low molecular polyethylene glycol (PEG 300) was incorporated as alternative plasticizer in the formulation (Panchal et al., 2012; Patel et al., 2010). A content of 3 % PEG 300 revealed a film that was very elastic showing a low secant modulus (W5). Although the yield stress was in the same range as for formulation W1 the low secant modulus represents the flexible manner of the film and the easy deformation. Therefore, the PEG 300 content was lowered to 1 % (W6). Formulation W6 produced an acceptable and smooth film with acceptable mechanical properties comparable to W1.

Table 11: Properties of the ODFs W1 and W6 containing warfarin. Disintegration time (mean ± sd, n = 6), water content (mean ± sd, n = 3) and water vapor sorption at 70 % relative humidity (n = 1). Mechanical properties (mean ± sd, n = 5).

Formulation	Disintegration time [s]	Water content [%]	Vapor sorption [%]
W1	23 ± 2	5.9 ± 0.1	14.4
W6	16 ± 2	5.8 ± 0.1	12.2
	Secant modulus [MPa]	**Yield stress [MPa]**	
W1	1276 ± 169	24.5 ± 2.6	
W6	1287 ± 60	26.1 ± 1.3	

Formulations W1 and W6 were chosen to be further examined. The film properties are summarized in Table 11. The water content of both film samples showed no major differences. The water vapor sorption though, was higher for W1 than for W6. Especially for relative humidities higher than 60 % the difference between the two film samples became more pronounced (Figure 34). Although the water sorption was lower for W6 the disintegration time showed lower results for this formulation. The reason might be that the W6 formulation contained less polymer matrix than W1 that needed to disintegrate.

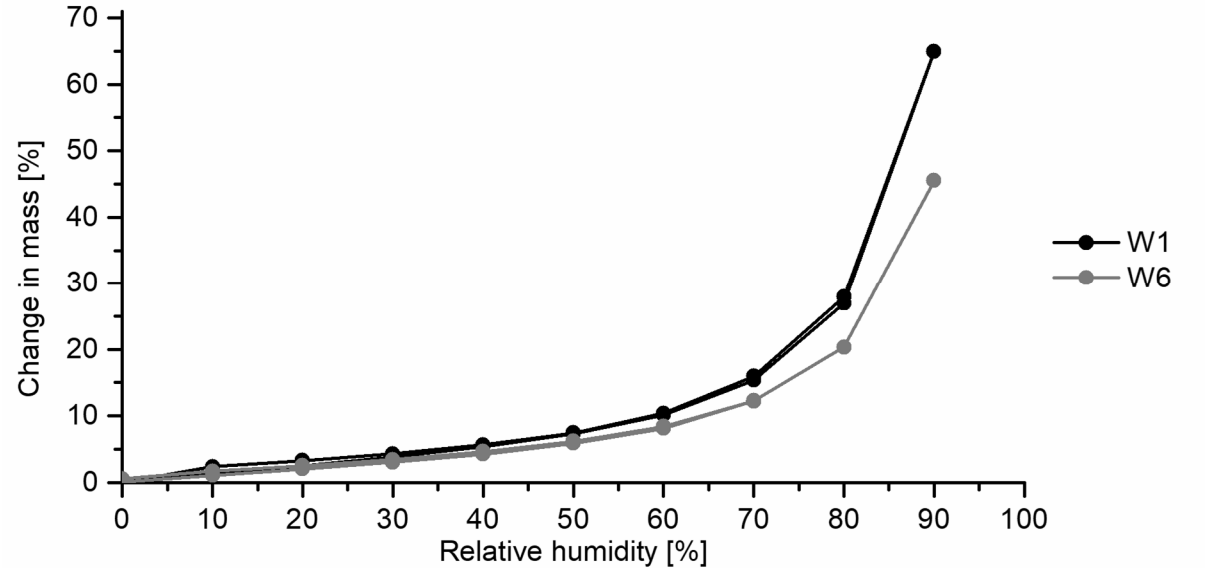

Figure 34: Water vapor sorption isotherms of the warfarin ODFs W1 and W6 for relative humidities of 0 – 90 - 0 % at 25 °C (n = 1).

3.2.4.2 Content uniformity of long warfarin ODFs

A very critical parameter in drug manufacturing is the content uniformity of the dosage form. For oral films, the content uniformity is even more relevant due to the usually low doses of a single dosing unit. To achieve content uniformity the API needs to be homogenously distributed in the entire manufactured film to ensure a homogenous drug content throughout all single films (Jansen and Horstmann, 2014). An even distribution was assured by blending the polymer solution thoroughly. Another claim for the prepared films is not only the evenly distributed API but also the right amount of API. The content of an oral film produced with the solvent casting technique is dependent on the casting height of the polymer mass. In section 3.2.3, a process control tool was introduced and validated to measure the WFT of the cast film during the production process as an in-line tool. The control of the WFT using the in-line measurement ensured an even thickness of the polymer mass throughout the casting process. This reduced scattering of the content over the length of the manufactured film. Furthermore, the WFT measurement was essential for the right adjustment of the process settings (gap height, pump volume, liner speed) to obtain the WFT necessary for the intended content of the film. Preliminary tests and the comparison of the in-line measurement tool with the trial and error method (refer to section 3.2.3.3.8) demonstrated that depending on the viscosity of a polymer mass, deviations up to 64 % below the label claim were possible without measuring the WFT during the process. Therefore, the control of the WFT with the developed in-line method considerably improved the film manufacturing process on the continuously working pilot-scale coating bench. All films that were prepared with 2 % warfarin as API were cast with a WFT of 250 µm to achieve the target content of 2.5 mg / 5 cm² film sample. Achieving content uniformity as specified in the European Pharmacopoeia Monograph 2.9.40 (Ph.Eur 9.1, 2017) was feasible for all long ODFs manufactured with the in-line WFT measurement. Film W1 showed an AV of 5.97 and formulation W6 an AV of 2.75 both laying far beneath the threshold of 15 given by the European Pharmacopoeia. The low AV values indicated acceptable results for the mean content as well as the scattering of the investigated samples that were collected from the whole length of the manufactured long films. This means that it was feasible to produce homogenous oral films with a length of at least 7.5 m over a process time of at least 60 min.

3.2.4.3 Stability testing of unpacked warfarin ODFs

ODFs W1 and W6 were successfully produced with sufficient mechanical properties, good disintegration times and an acceptable content uniformity. They were further evaluated and

tested regarding their stability over three months. The films were tested without packaging to mimic the worst-case scenario of storage of an unpacked film. W1, the warfarin ODF containing HPMC as polymer matrix was tested at two different climatic conditions. The temperature was kept constant at 21 °C for both conditions. Two different relative humidities were investigated to evaluate whether there is a difference in storing the ODF under standard storage conditions according to ICH guideline Q1A (ICH, 2003) at 60 % relative humidity or at 40 % relative humidity. To evaluate the drug and film stability over storage of twelve weeks, the warfarin content and the mechanical properties of the ODF were measured every four weeks according to section 5.4.10.1 and 5.4.11.2. Figure 35 (top) displays the performance of the warfarin content during the stability testing. The content of the W1 ODF showed no significant changes over twelve weeks of storage for the controlled conditions of 40 % relative humidity ($p = 0.6255$) as well as for the standard storage conditions of 60 % relative humidity ($p = 0.5139$). The AV value of the samples stored at standard conditions slightly increased due to rising standard deviations. But yet, with the highest AV of 10.1 the film was still below the threshold of the European Pharmacopoeia. The performance of the mechanical properties is shown in the bottom part of Figure 35. The fluctuations of the secant modulus and the yield stress were higher than of the contents. It might be traced back to the sensitivity of ODFs to ambient conditions during the measurements as already discussed in section 3.2.2.4. Slight changes in the surrounding relative humidity of the measurement room changes the water content of the tested film (Figure 34). This leads to changes in the measured mechanical properties due to the plasticizing effect of the incorporated water (Boateng et al., 2009; Hoffmann et al., 2011; Karlsson and Singh, 1998). Since the humidity in the room with the measurement equipment for the tensile test was not controlled, the assumption cannot be excluded that changes in the mechanical properties originated from the changing conditions rather than from the storage impact. The secant modulus measured for the W1 ODF over twelve weeks showed no significant changes during the storage time for both conditions ($p(40\ \%) = 0.5786$ and $p(60\ \%) = 0.5009$). The yield stress significantly increased at 40 % relative humidity ($p = 0.0005$), which is not seen as disadvantage since the film would resist higher tensile stresses before starting to irreversibly deform. At standard conditions no significant change was observed for the yield stress ($p = 0.1330$). The influence of the storage conditions was not much pronounced, but a trend was visible. Both the secant modulus and the yield stress showed a tendency to lower values for the samples stored at 60 % relative humidity (Figure 35, right) explainable with the higher relative humidity the films were stored at, which offered more water that might be absorbed by the thin polymeric films.

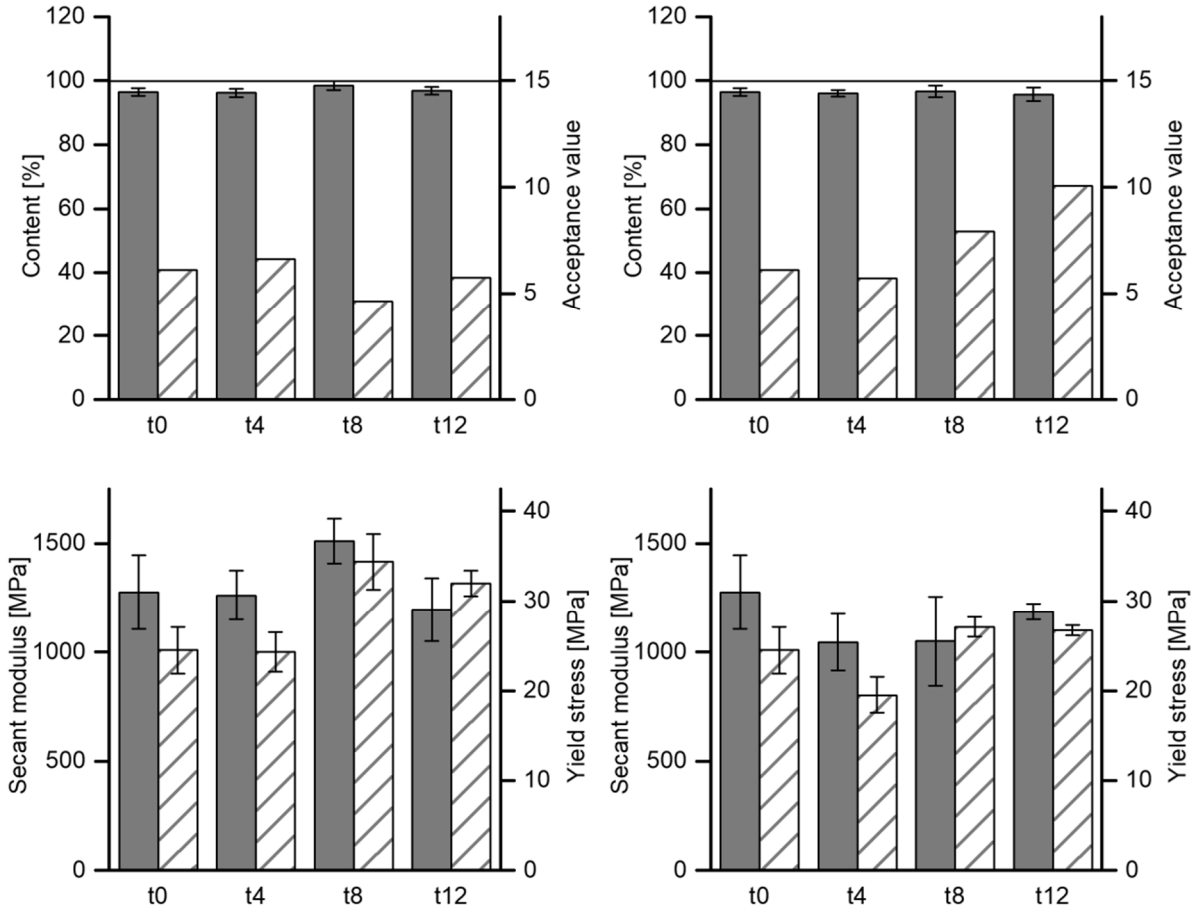

Figure 35: Stability testing of warfarin sodium HPMC film (W1) over twelve weeks. Left: 40 % relative humidity; right: 60 % relative humidity. Top: API content relative to target value (filled columns) and acceptance value in accordance with Ph.Eur. 2.9.40 (dashed columns). The line represents content = 100 % and acceptance value threshold = 15 (mean ± CI, α = 0.05, n = 10). Bottom: Mechanical properties. Filled columns: secant modulus; dashed columns: yield stress (mean ± sd, n = 5). Used by courtesy of the European Journal of Pharmaceutics and Biopharmaceutics, Elsevier (Niese and Quodbach, 2019).

The ODF W6 with a polymer matrix formed from PVA and HPMC was only stored at 60 % relative humidity as the more challenging condition since formulation W1 showed no advantage of the storage at 40 % relative humidity. The results are presented in Figure 36 with the mechanical properties on the left side and the content on the right side. The values from the measuring point after four weeks of storage were unexpected. The mechanical properties decreased extremely whereas the content did not noticeably change. Due to unusually hot summer weather, the relative humidity in the measuring room that was tempered to 21 °C increased to over 70 %. This extremely affected the measurement of the mechanical properties of the thin polymer films. In the short time when the films were taken from the controlled storage environment until they were measured at the texture analyzer, they absorbed enough water to change their mechanical resilience and to exhibit low values for the measured mechanical properties. The fast water uptake kinetics of the thin films were shown in the

measurements of the water vapor sorption (Figure 24). Because of this, the following measurements were performed in a room with controlled climatic conditions (21 °C and 45 % relative humidity). Although the values from the beginning of the stability test were not as low as the four-week values they differed significantly from the results at the end of the test after twelve weeks (secant modulus $p = 0.0022$; yield stress $p = 0.0007$). This cannot unequivocally be related to the storage and the stability of the film since the climatic conditions between the first and the last measuring point differed. The same limitation has to be considered when comparing the results from the ODF W1 with W6. The starting results for both films were comparable as well as the secant moduli for the results after eight and twelve weeks of storage. The yield stress for the W6 ODF was lower after storage. This implied that this film lost part of its mechanical resilience since it withstood less tensile stress before reaching the region of plastic deformation or breaking. This behavior would not be suitable for the use in the device and must be tested with the device prototype for applicability (refer to section 3.3.5). The content of the film using PVA and HPMC as polymer matrix slightly seam to increase over storage time ($p = 0.0098$). Yet, the AV is far below the threshold of the European Pharmacopoeia for all measuring points. The highest AV of 5.1 is still within the limits of the European Pharmacopoeia. The samples for the content determination were collected from the whole length of the film, and, therefore a low AV showed homogenous distribution of the API and a uniform WFT for the whole production process.

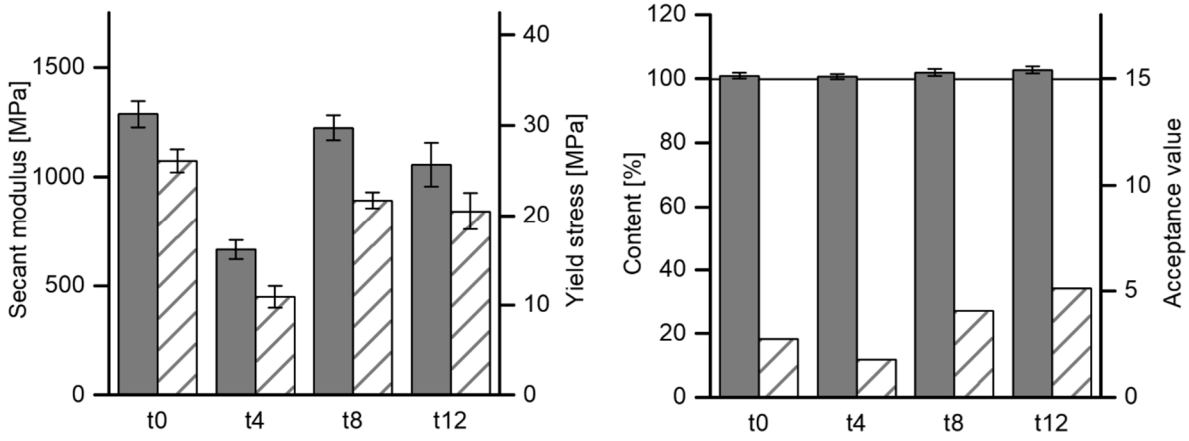

Figure 36: Stability testing of warfarin sodium PVA and HPMC film (W6) over twelve weeks stored at 60 % relative humidity.
Left: Mechanical properties. Filled columns: secant modulus; dashed columns: yield stress (mean ± sd, n = 5). Climatic conditions of measurement room: t0+t4: uncontrolled; t8+t12: 21 °C / 45 % relative humidity.
Right: API content relative to target value (filled columns) and acceptance value in accordance with Ph.Eur. 2.9.40 (dashed columns). The line represents content = 100 % and acceptance value threshold = 15 (mean ± CI, α = 0.05, n = 10).
Used by courtesy of the International Journal of Pharmaceutics, Elsevier (Niese et al., 2019).

3.2.4.4 Packaging

Although the stability testing for the unpacked films did not show significant complications during storage over twelve weeks regarding the API content and the mechanical properties of the films (refer to section 3.2.4.3), it was decided to pack the long film with aluminum foil before using it in the device. This additional effort should improve the stability of the drug component in the dosing device especially in regard of changing climatic conditions that have shown an impact on the mechanical properties.

The packaging is supposed to be air- and watertight and lightproof to minimize possible moisture-, oxygen- or light-induced instabilities of the film or the API. Sealed aluminum packages were selected, which were prepared in the desired length with a rotary sealer. It is important that the sealed aluminum packages are possible to reopen in the device to release the ODF while dosing. Therefore, a special lamination is required for the aluminum. Two different aluminum foils coated with polyethylene in one case and a special lamination in the other case were used (refer to Table 23 and section 5.1). The special lamination called “Rayopeel” was described in the patent US 3879492 and developed to form peelable seals after heat-sealing (Bontinick, 1972; Greenland, 1997). In this work, the two aluminum foil strips were placed on top of each other, touching with the laminated side. First, one long side and one small side of the package were sealed using a rotary sealing device (refer to section 5.6.1 and Figure 37, top). Then the film was placed between the strips and the other long side was sealed as well. The package was coiled up and the second small side was sealed after winding, so no air was entrapped in the package.

The packaging was tested in a stability test over 30 days (refer to section 5.6.2), since this is the time range the device can be used with one long film by the patient. Formulations W1 and W6 were tested in heat-sealed aluminum packages for the use in the device (Figure 37, bottom). To mimic the use of the packed film in the device over the time of 30 days the packages were cut open at one small side after coiling it up. This imitates the situation in the device where the aluminum package is always open at one small side since the film has to be dispensed there (Figure 46). At every time point samples were cut from the long film after unpacking, to measure the mechanical properties. The API content was not investigated under these conditions since no significant changes were shown for the stability testing with unpacked films. Therefore, the more controlled conditions in the aluminum packaging should not impair the behavior of the drug content.

Figure 37: Packaging of the long ODF (transparent) in aluminum packages (top) and samples for the packed stability testing with 3D-printed reels and clips (bottom).

The results of the stability testing of the packed ODFs are shown in Figure 38 for formulation W1 on the left and W6 on the right. It is obvious that the data from the tensile test after three days of storage widely vary from all the other measurement points. The reason for these results were the extreme climatic conditions in the measurement room. Since the humidity could not be controlled in the usual measurement room, the relative humidity increased up to over 70 % due to the hot and humid summer weather at measurement time point t3 (refer to Figure 36). This increase in humidity had an influence on the mechanical properties of the ODFs since the films absorbed water that acted as plasticizer (Karlsson and Singh, 1998). The exact conditions of time point t0 were not recorded and therefore it was not possible to gain meaningful findings from the first two time points. However, the learning from these results was important

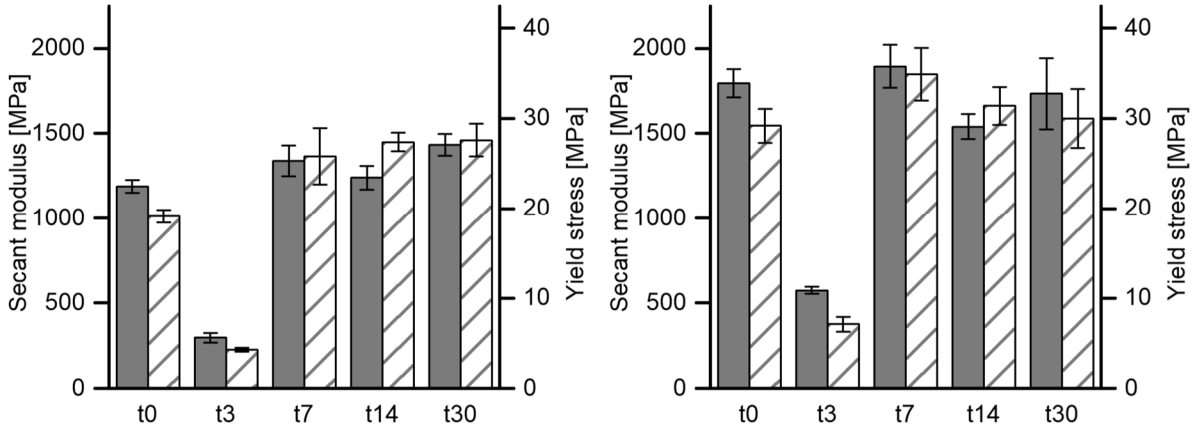

Figure 38: Stability testing of packed ODF W1 (left) and W6 (right) over 30 days at 60 % relative humidity and 21 °C. Filled columns: secant modulus; dashed columns: yield stress (mean ± sd, n = 5).
Climatic conditions of measurement room: t0+t3: uncontrolled; t7-t30: 21 °C / 45 % relative humidity.

and made clear that the mechanical testing of thin films is massively influenced from surrounding conditions during the measurement. Although the films were stored at controlled conditions, the time when the films were taken from the storage place into the measurement room was obviously long enough to absorb water that changed the mechanical behavior. To avoid such uncertain climatic conditions for the following measurement time points, they (t7, t14 and t30) were measured in a different room that enabled a control of the climatic conditions. In this room, the temperature was set to 21 °C and the relative humidity to 45 %. Only controlled conditions like this enable to compare the data of the tensile tests. The low humidity in this measurement room led to higher mechanical properties than for the t0 data. Therefore, less water was absorbed and less plasticizing effect became possible. Comparing the results of the mechanical testing for the three time points under controlled conditions no significant changes for the secant modulus ($p = 0.0911$) and the yield stress ($p = 0.2693$) for film W1 as well as for W6 ($p = 0.2240$ and $p = 0.0511$) between t7 and t30 were observed. Therefore, it was concluded that the storage of the oral film in aluminum packages as it happens in the device does not negatively affect the mechanical properties, which represent the most critical parameter for the handling of the film. A direct comparison of the results from the stability test of the packed ODFs to the unpacked ODFs is not meaningful because of the uncontrolled climatic conditions of the unpacked stability tests.

3.2.5 Summary

This section covered the formulation development of long ODFs containing the API warfarin. The 2 cm wide films were produced on the continuously working pilot-scale coating bench, as a long film was necessary for the use in the dosing device to enable flexible dosing of the warfarin film for the individualized therapy with this API. Because of differences in the process, the transfer from the small-scale process to the pilot-scale process cannot be easily performed and the small-scale coating bench was not further used in this part of the work.

The formulation development was mainly performed without an incorporated API because of the high toxicity of warfarin. The drug-free films were evaluated regarding their mechanical properties as most important parameter for the handling of the films in the dosing device. Since the mechanical testing was of high importance for the development, the test methods were evaluated and the tensile test as most suitable test was critically investigated regarding the influence of the shape of the test specimen and the preparation method of the same. It was discovered that the often-used dumbbell shaped test specimen did not show an advantage over

the easy to prepare rectangular test specimen, which is recommended by the standard (DIN, 2003). The use of a cutting plotter simplified and improved the test specimen preparation and was therefore used for further sample preparation in this work. The pronounced dependency of the mechanical behavior of polymeric films upon the climatic conditions was realized during the hot and humid weather. Measurements of the mechanical properties require controlled climatic conditions for both, the temperature and the humidity in the measurement surrounding.

An in-line tool for the measurement of the WFT was introduced and validated for the production process of oral films on the pilot-scale coating bench. The aim was to enable optimal dosing of the oral films over the whole length of the long film. Therefore, a real time determination of the WFT as the most important parameter of the content adjustment was an important step towards improvement of the continuously working film manufacturing process on the pilot-scale coating bench. The in-line WFT measurement with the chromatic confocal optical probe is not limited to the pilot-scale coating bench but could also be included into production processes. The method was found to be linear in the range of 100 – 350 µm and to be robust against different changes of the polymer mass as well as the process.

It can also be concluded that it was possible to develop two long ODFs containing warfarin that showed acceptable content uniformity over the whole length of the film and were therefore suitable for the use in a dosing device to enable flexible dosing of the API. The stability was demonstrated unpacked as well as packed in heat-sealed aluminum packages to mimic the use in the device. Both, the content of the API as well as the mechanical properties of the ODF did not significantly change over the storage of twelve weeks for the unpacked films.

3.3 Development of a new dosing device for orodispersible films

Parts of this section have already been published in a peer-reviewed journal. The content was linguistically adapted, and data sets were partly extended.

- Niese, S., Breitkreutz, J. and Quodbach, J., 2019. *Development of a dosing device for individualized dosing of orodispersible warfarin films.* Int J Pharm. 561, 314-323. DOI: 10.1016/j.ijpharm.2019.03.019.

3.3.1 Introduction and objectives

The main focus of this work was the development of a dosing system enabling flexible dosing of oral films. The dosing system was supposed to consist of a dosing device and an orodispersible film that may be flexible dispensed by the device. Formulation development of the long ODFs was already described in the previous sections of this work. This chapter deals with the development of the dosing device. It shall open individualized therapeutic concepts to the easy to administer solid dosage form ODF with its advantages for patients of all age groups. As shown in the overview of the patent situation in the introduction of this work (refer to section 1.2.1), there were already several ideas about dosing devices for film shaped dosage forms. None of them have reached the pharmaceutical market. Therefore, such a device was developed, and criteria were chosen that are important for a successful implementation to the individualized therapy with oral film strips. The missing possibility of flexible dosing for ODFs was already addressed in the review paper of Wening and Breitkreutz (2011) where a patent for an electronic tape dispenser was mentioned (Allen et al., 1985). The disadvantage of this patented device are the high costs due to the electronic power unit. This was taken as motivation to develop a prototype of a dosing device without electronic parts. The prototyping should be performed by 3D-printing using a commercial fused filament fabrication 3D-printer to reduce development costs and time. Furthermore, the 3D-printed device shall be tested for correct working according to the specifications given by the European Pharmacopoeia.

3.3.2 Requirements on the dosing device

The development of the dosing device followed partly the basic principle of the “Design control guidance for medical device manufacturers” as pictured in the “waterfall model” (Figure 39) to illustrate the design control influence on the design process (FDA, 1997). In the beginning,

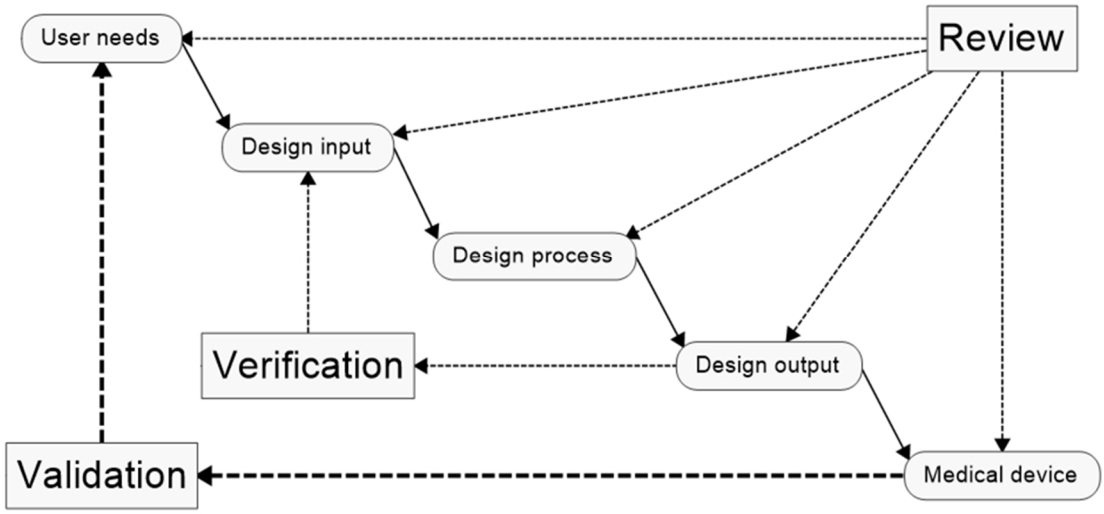

Figure 39: "Waterfall model" according to the FDA, illustrating the waterfall-like design process of a medical device with its control elements throughout the process. Solid arrows visualize the design process; dashed arrows visualize the control elements (FDA, 1997).

the potential users of the dosing device were identified and with that, the user needs. Possible user groups are patients, caregivers and medical staff. The user shall be able to flexibly dose the ODF with the dosing device him- or herself, without an individualizing manufacturing step in a pharmacy or the industry as it is proposed for the personalization of an oral warfarin film by ink-jet printing (Vuddanda et al., 2018). Therefore, the design requirements have to be determined to meet the needs of the user. The design requirements influence the design input of the design process, which then leads to a design output. The design output has to be verified to make sure the output meets the design input. This feedback path is necessary throughout the whole design process. In the end, the final product needs to be validated to show conformity with the user needs defined in the beginning of the design process. All steps shall be captured in reviews, which are documented in the design history file. In this work, no patient data were available and used to define the design requirements. Furthermore, the performance of the developed prototype of the dosing device was examined only to test the conformity to the European Pharmacopoeia regarding the dosing of the ODFs. No functionality tests were performed with potential users of the dosing device. Therefore, the development might rather be described as a suitability study in this case.

The most important points to consider were an adequate operating of the system, the stability of the dosage form and the safety of the patient during the use of the device. The operating aim for the device was that an inserted ODF can be dispensed from the device in flexible doses without electronic power. The flexible dosing shall be performed by cutting various lengths of the film. Therefore, the device needs a cutting unit and an opening where the film can exit the

device. The long ODF that will be cut in pieces needs to be coiled up on a stock roll placed in the device. Additionally, the stock roll might be replaceable to reduce costs. A dosing unit is required to enable precise dosing of the ODF that allows flexible dosing within the specifications of the European Pharmacopoeia. The length according to the desired dose shall be adjusted by this unit and the movement of the film piece to the outside of the device shall be coordinated. The stability of the dosage form is most critical regarding moisture in the environmental air. Therefore, the device shall be closed towards the surroundings as much as possible. When the device is not used, a closure cap shall be placed in front of the opening where the film is dispensed. To improve the stability conditions for the ODF, the film can be seal-packed in protective material or the climatic conditions can be controlled in the interior of the device by desiccants. To ensure the safe handling by the patient without accidental risks of injuries the cutting unit shall be shielded from the outside. Furthermore, the packaging waste of the ODF shall be collected in the device to avoid accidental intake of the material together with the ODF by the patient. The handling of the device shall be kept as easy as possible to ensure successful handling for all patient groups. In the following sections of this work, the design process based on the defined requirements will be discussed.

3.3.3 Design process of the dosing device

3.3.3.1 General considerations

The developed dosing device consists of the outer housing, which comprises the different operating units described in the following sections. The inner composition of the device and the used materials mainly affect the size and the shape of the housing. Since the prototype of the device was meant to be 3D-printed, a limitation towards the size of the device was given.

Table 12: Color code for the 3D-CAD models and the 3D-printed models of the developed dosing device.

Model part	Color	Position in the device
Stock roll	white	back right
Dosing roll	orange	back left
Dosing scale	orange	in upper part
Dose indicator	blue	in upper part
Waste roll	blue	front left and right
Turning knob	blue	in upper part / on waste roll
Knife fitting	white	front left
Housing	green	

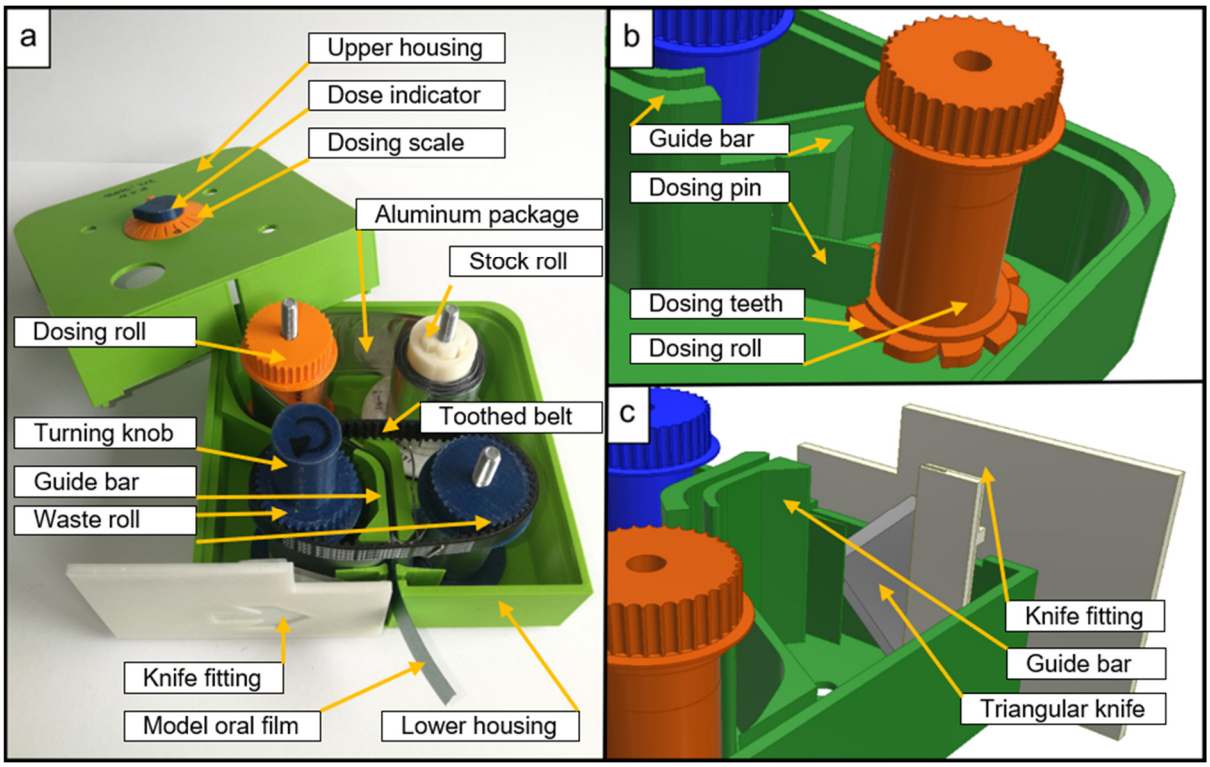

Figure 40: Overview of the final prototype of the developed device with a base area of 13x13 cm and a height of 7 cm. a: full top view of the printed device; b: close-up view of the dosing unit (3D-CAD model); c: close-up view of the cutting unit (3D-CAD model).
Used by courtesy of the International Journal of Pharmaceutics, Elsevier (Niese et al., 2019).

Materials and parts that could not be produced with the 3D-printer showed fixed sizes that the device had to be adapted to e.g. the utilized toothed belts. The following pictures show 3D-CAD models designed with the software Inventor® Professional 2016 or the pictures taken from the 3D-printed models. A color code was used for the different parts of the dosing device for 3D-CAD models as well as the 3D-printed models (Table 12). For better presentation, a green ribbon as model ODF was placed in some of the models. The real ODF would not be visible on a picture due to its transparent appearance. Not all pictured models are fully functional. Some intermediate stages of the model were further improved before the full functionality was inserted into the model design. A labeled overview of the final prototype of the developed device is pictured in Figure 40. It is meant to assist with the terminology used in the following description of the development towards this final prototype of the dosing device.

Two different models were designed for the dosing device differing in the storing of the ODF. Figure 41 shows the model with a slot for a desiccant cartridge (Figure 41 b) to control the moisture conditions in the device. In this model, there is no need for the ODF to be packed. The ODF is coiled up with the process liner on the white stock roll in the back of the device

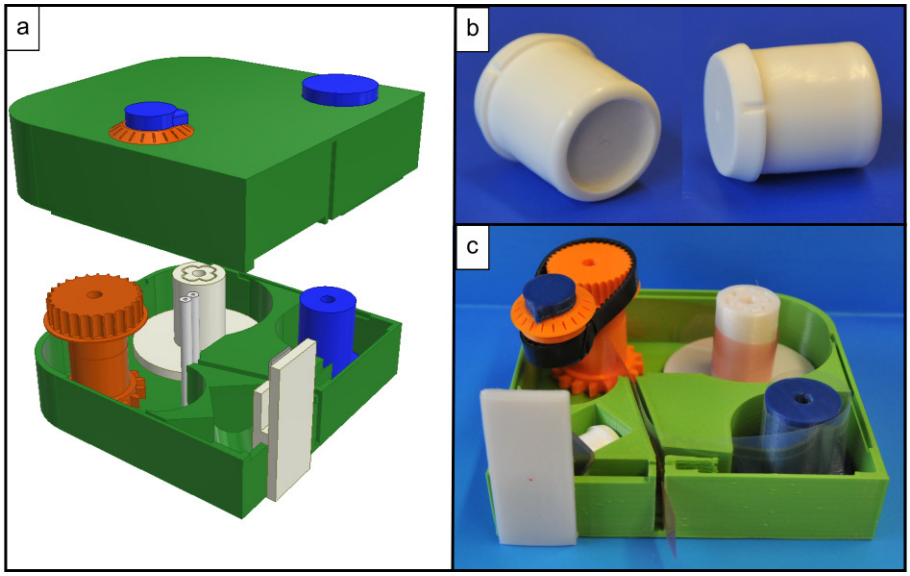

Figure 41: 3D-CAD model of the dosing device draft with a slot for a desiccant cartridge for storing the ODF without packaging (a). Desiccant cartridge that can be incorporated to control the moisture in the device (b). 3D-printed version with incorporated desiccant cartridge and transparent red drug-free ODF (c).

after cutting to the defined width. The ODF with the liner moves around the orange dosing roll and then through the two thin white rolls (only depicted in Figure 41 a) to the front part of the device. The two white rolls seal the back part where the main ODF is stored from the front part that has access to the outside of the device. In the front part, a desiccant cartridge reduces the moisture in the device since the beginning of the film is presented to the outside conditions through the opening slot after separation from the liner that is coiled up in the device. The second model was an option where the ODF is packed in a sealed aluminum package to ensure stability of the ODF (Figure 46).

Packaging of the ODF in tight aluminum packages was preferred during the model development and therefore, the model using the desiccant cartridge was not further refined. From this point on, only the development of the dosing device for a packed ODF will be described in following sections divided into the main operating principles. For the correct and safe operation of the dosing device, four main units were of interest. The supply unit stocking the coiled up ODF. The dosing unit to enable flexible and accurate dosing of the ODF. The packaging waste unit that separates the aluminum package from the ODF and keeps the waste inside of the device and at the end the cutting unit to partition the dose from the long ODF during dispensing.

3.3.3.2 Operating principle I: Supply unit

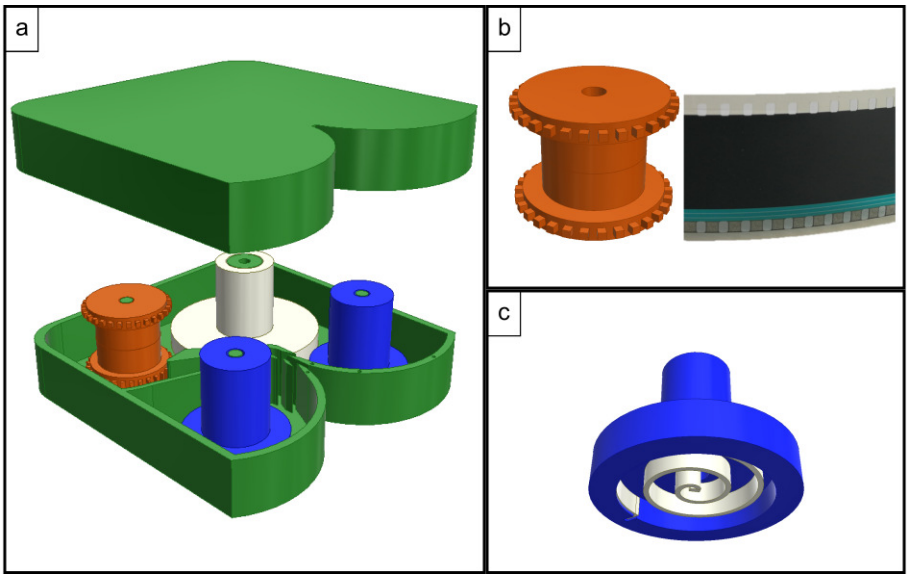

Figure 42: 3D-CAD model of a dosing device draft using a dosing roll with notches to convey an ODF with a packaging perforated like a photographic film (a and b). 3D-CAD model of the waste roll with a spiral spring responsible for the motion in the device (c).

The supply unit consists of the white stock roll in the back right of the device. Starting with a pivoted roll as shown in Figure 42 a, it became obvious that the roll was moving uncontrollable. A control element was necessary since the roll unwound more of the stocked film than needed by the dosing unit. The uncontrolled unwinding happened because of the tension the film was exposed to because of coiling it up on the stock roll. A piece of felt was attached to the bottom

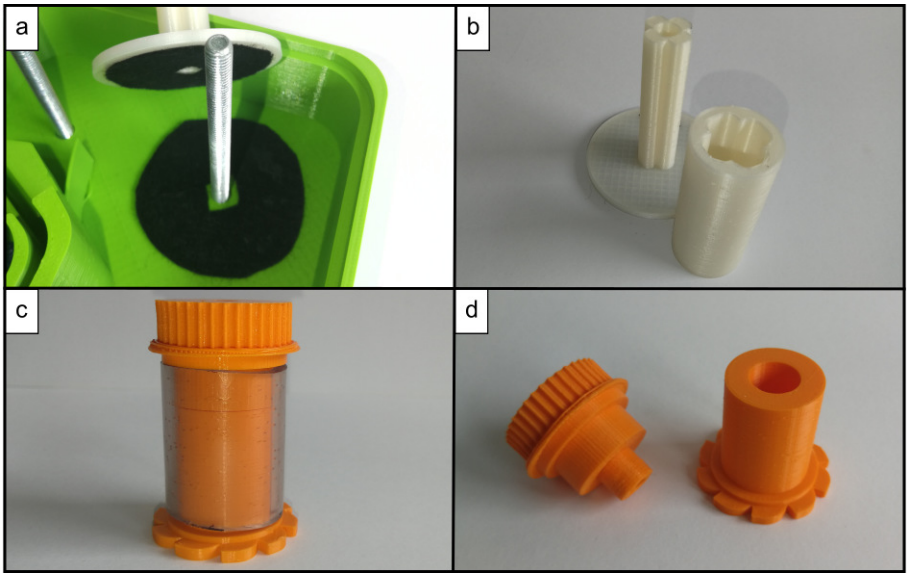

Figure 43: 3D-printed parts of the final prototype of the developed dosing device. Stock roll and corresponding place of the lower part of the device with attached felt pieces to increase friction (a). Both parts of the stock roll allowing reuse of the device by refilling it with a new ODF coiled up on the exchangeable part of the stock roll (b). Dosing roll assembled with the plastic tube (c) and the two printed parts of the dosing roll (d). Used by courtesy of the International Journal of Pharmaceutics, Elsevier (Niese et al., 2019).

of the stock roll and the associated place in the lower housing of the device to increase friction between these parts and to prevent uncontrolled unwinding of the stock roll (Figure 43 a). The unwinding was then only controlled by the pulling through the dosing unit. Furthermore, a reuse option was implemented by designing the stock roll in two parts (Figure 43 b). The lower part is still pivoted on the lower housing of the device, but the pin presents a cross-shaped axle. The replaceable part shows the cross shape as a recess and can be placed on the pin of the lower part. No rotation of the replaceable part on the lower part is possible because of the cross-shaped conjunction. When the film on the replaceable part is empty, it can be substituted by a new replaceable part with a full film again.

3.3.3.3 Operating principle II: Dosing unit

For the exact dosing of the ODF, a mechanism was necessary that does not allow a lot of uncontrolled movement of the rolls. Uncontrolled moves would cause incorrect dosing which is not acceptable for the use in a therapeutic concept with highly potent drugs, such as warfarin showing a very small therapeutic window. The aim was to develop a device that delivers uniform doses according to the specifications given by the European Pharmacopoeia. A dosing element was necessary to control the length of the film, which is delivered to the patient using the device. Therefore, the dosing roll was incorporated into the device between the stock roll and the waste unit. The dosing roll is responsible for the exact forward motion of the ODF. The first approach was to use a dosing roll with notches to convey the packed ODF through the device (Figure 42 a and b), a principle known from photo cameras with a photographic film. By turning the orange dosing roll, it delivers the length of the ODF that corresponds to the rotary motion. An operating unit is necessary to move the delivered length forward towards the opening in the front of the device. This is done by the packaging waste unit with the two blue rolls in the front of the device (Figure 46). In the first approach spiral springs were inserted in the bottom of the blue waste rolls (Figure 42 c). For this purpose, the waste roll bottom had to be hollow. This was printed using a water-soluble support structure as shown in Figure 44 c. The support structure was printed with a white PVA filament together with the rest of the object that was printed with the blue polylactic acid (PLA) filament. After the printing process, the object was put into water until the PVA dissolved completely. The middle end of the spring was fixed to a pin in the housing of the device and the outer end was fixed to the waste roll. When loading the device with a new packed ODF, one end of the two packaging foils is attached to each of the two waste rolls after the spring is stretched by turning the waste roll. As soon as the dosing roll releases a piece of the film, the waste rolls coil up the released length

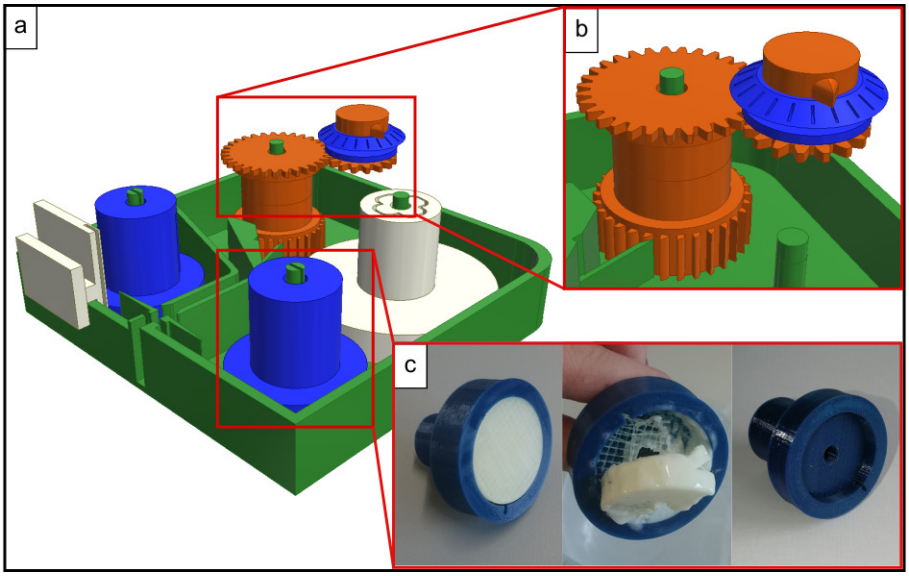

Figure 44: 3D-CAD model of a dosing device draft using gear wheels to dose the packed ODF and spiral springs for motion of the packaging (a and b). 3D-printed waste roll (blue) with a water-soluble PVA support structure (white) before, after partly dissolution in water and after complete dissolution (c).

of the packaging foils because of the spring tension. Doing so, the aluminum package is further opened and the ODF released and moved forward trough the opening. The problem of this first approach was that this spring mechanism did not work with consistent power since the force that is applied by the springs differs between the moments when they are initially coiled up and when the stretching decreases. The power decreases and the packaging foils are not coiled up properly resulting in reduced ODF delivery. Furthermore, using notches on the dosing roll demanded for the corresponding holes in the aluminum package. A special punching device would have been necessary to realize the proper preparation of the aluminum package.

Therefore, the dosing mechanism was reviewed. In the next approach gear wheels were considered to turn the dosing roll (Figure 44 a and b). Since no notches were attached to the dosing roll anymore, a different mechanism was necessary to move the packed ODF when turning the dosing roll. The dosing roll was covered with a plastic tube to increase adhesion of the aluminum package to the dosing roll (Figure 43 c). Because of the adhesion, the packed ODF is transported forward, when a user turns the dosing roll by the gear wheel mechanism from the outside of the device. The problem is that also for this approach the springs in the waste rolls are necessary to coil up the packaging foil on the waste roll and to deliver the ODF out to the opening in the front of the device.

In order to avoid the use of springs as motion producer, a third approach was developed. In this model, toothed belts (refer to Table 25 and section 5.1) were used as drive system to transfer

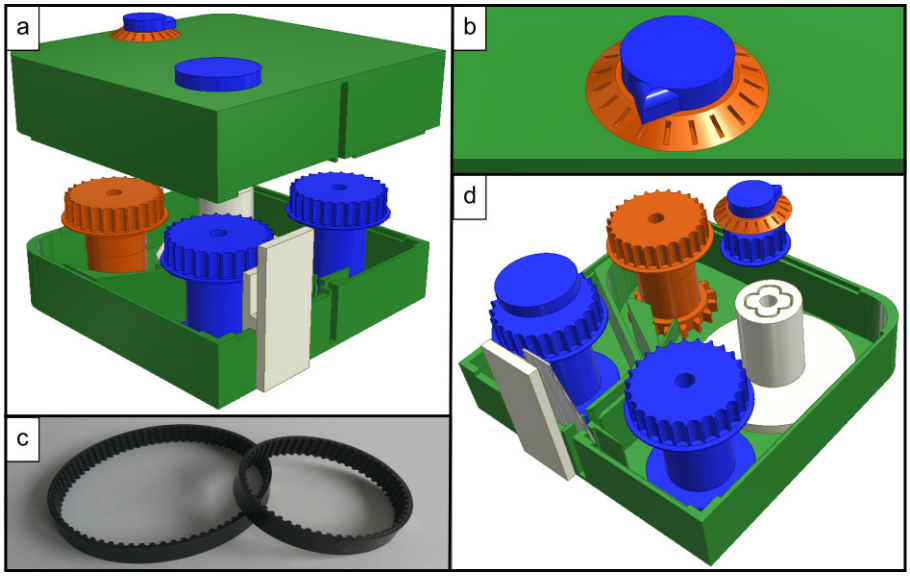

Figure 45: 3D-CAD model of a dosing device draft using toothed belts for dosing of the ODF and coiling up the packaging waste in one step (a and d). 3D-CAD model of the dosing scale with dose indicator on the outside of the device (b). Toothed belts used in the device (c).
Used by courtesy of the International Journal of Pharmaceutics, Elsevier (Niese et al., 2019).

the movement of the dosing roll to the waste rolls in one step (Figure 45). Toothed belt disks were attached to the top of the dosing roll and to the top of both waste rolls. Furthermore, the dose indicator that reaches outward of the device to be seen by the user got a toothed belt disk on the bottom. The smaller toothed belt connects the dosing indicator and the dosing roll. The larger toothed belt connects the two waste rolls (Figure 49). The packed ODF is inserted in the device as explained for the first approach. It is now important that the foils are attached to the waste rolls in the right direction. Both rolls need to turn the same direction to coil up the packaging waste to enable the connection by the toothed belt. Therefore, the foils are attached to the waste rolls as pictured in Figure 46 b. Another important addition in this third approach is the turning knob on the left waste roll. To deliver a dose of the ODF the user turns on the knob and moves one waste roll by doing so. The second waste roll moves as well because of the connecting toothed belt. The packaging foils are coiled up at both sides, releasing the ODF from between them. Since the aluminum package adheres to the plastic tube on the dosing roll, the movement of the packed film turns it passively. This movement in turn is transferred to the dose indicator by the second toothed belt. The user can watch the turning dosing indicator on the outside of the device. At the beginning of the dosing process, the dosing scale needs to be rotated that the dosing indicator points to the zero position (Figure 45 b). During the dosing process, the user can monitor the delivered dose by looking at the indicator and the scale and stop turning the knob when the desired dose is reached. Before the next dosing step, the scale needs to be returned to zero to start over again. The rotation of the dosing scale is only possible

in the opposite direction than the dosing indicator turns to avoid a rotation of the scale by the indicator during dispensing the ODF. To achieve a step-wise dosing that can be read off at the dosing scale, teeth were attached to the bottom of the dosing roll (Figure 40 b). The pin attached to the housing reaches in the gap between two teeth. When the dosing roll is moved, it can only turn in the direction where the pin can slide over the rounded side of the teeth (counterclockwise). The other direction is prevented since the teeth show straight sides that interlock with the pin. This mechanism enables a step-wise dosing of the ODF and an additional assurance for the patient that the device is dispensing correctly. The patient can listen to the click sound that results from the pin sliding over the teeth of the dosing roll. Especially for patients with visual impairment this is an additional assistance for safe usage of the device. By varying the size and number of the teeth, the dosing steps can be changed. The length of the dispensed ODF is equivalent to the arc of the circle that the dosing roll is turned. The arc is dependent on the central angle of the rotary motion of the dosing roll. The number of teeth attached to the dosing roll is dependent on the angle necessary to rotate the dosing roll by the desired length. In the final prototype of the developed device 10 mm of the 2 cm wide ODF is dispensed per step resulting in an ODF piece of 2 cm² per dosing step. According to Equation 1, the dispensing of this 10 mm film piece with a given radius of the dosing roll of 15.9 mm needs the dosing roll to be turned by an angle of 36.04°. Equation 2 then results in a number of teeth of 9.99. Therefore, the dosing roll for the final prototype was produced with 10 teeth at the bottom.

Equation 1: Calculation of parameters for step-wise dosing of the long ODF by the developed dosing device. Arc: arc of the circle, is equivalent to length of dispensed ODF. r: radius of the dosing roll including the plastic tube at the point the packed ODF moves around it. α: central angle of the rotary motion of the dosing roll.

$$arc\ [mm] = \frac{\pi * r * \alpha}{180°}$$

Equation 2: Calculation of parameters for step-wise dosing of the long ODF by the developed dosing device.

$$central\ angle\ \alpha\ [°] = \frac{360°}{number\ of\ teeth}$$

The advantage of the toothed belts used as drive system is that they were not dependent on electricity but were only moved by the user with the knob on the outside of the device. They showed no uncontrolled movement and worked robust. Because of the satisfying performance, this approach was used for the final prototype of the developed dosing device.

3.3.3.4 Operating principle III: Packaging waste unit

The packaging waste unit in the front of the device has an important responsibility for the correct working of the dosing device. It is the drive mechanism for the dosing process moving the toothed belts forward as already explained in the preceding section. By turning the knob on the left waste roll, the packaging foils are coiled up and the dosing mechanism is activated. For the separation of the aluminum package into the original two foils it is major important that the heat-sealed seam is easy to reopen without destroying the foils and without too much power needed. Therefore, an aluminum foil with a special lamination was used for packaging of the long oral film (refer to section 3.2.4.4). The sealed aluminum package is separated into the two original sides behind the guide bar in the housing of the device (Figure 46 b). By moving one roll, the other is moved as well because of the connecting toothed belt. As consequence, one foil moves to the right and one to the left before the ODF leaves the device through the opening in the housing. The packaging foil is coiled up in the housing of the device to avoid an accidental intake of the packaging material together with the ODF by the patient. An intake and swallowing of the packaging foil can cause major health issues and needs to be avoided.

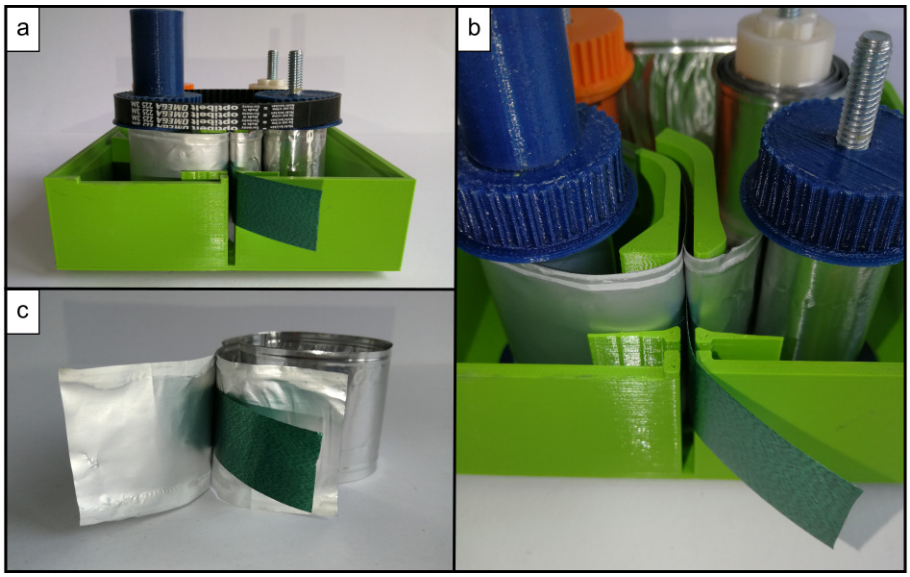

Figure 46: 3D-printed model of the dosing device picturing the waste unit with the rolls coiling up the packaging in the inside of the device (a and closer look b). Packed model ODF in the aluminum package (4.5 cm wide) (c). Partly without toothed belts for better overview.
Used by courtesy of the International Journal of Pharmaceutics, Elsevier (Niese et al., 2019).

3.3.3.5 Operating principle IV: Cutting unit

The cutting unit, located in the front of the device before the opening where the ODF leaves the device, cuts the desired length off the long ODF. An accurate cutting is important to guarantee dosing accuracy of the API from the long ODF (Jansen and Horstmann, 2014).

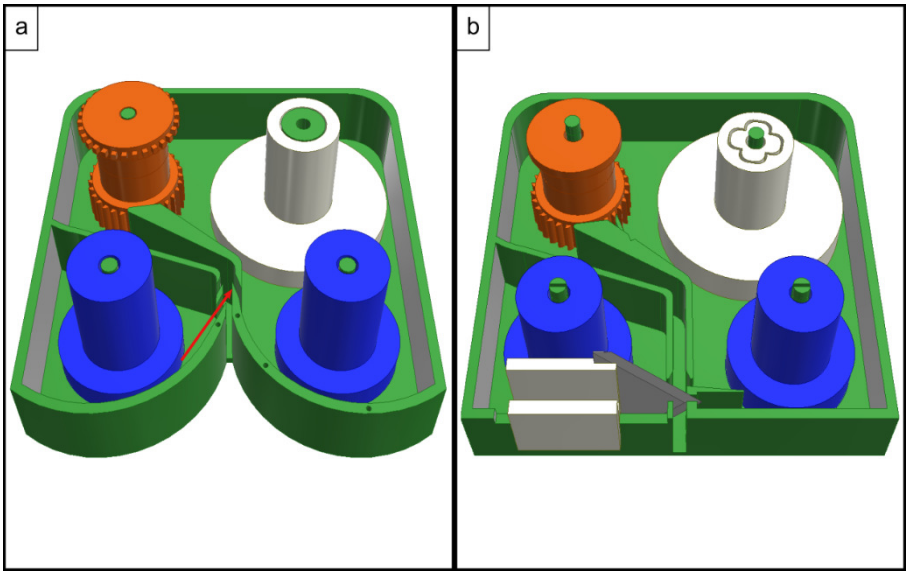

Figure 47: 3D-CAD model of two drafts for the dosing device, differing in the front part for the cutting unit. Curved front that would not enable a proper use of the knife (not pictured) as depicted with the red arrow (a) and straightened front for correct function of the knife to cut the ODF before leaving the device (b).

Figure 47 a shows the first approach for the front part of the device with a curved shape. The housing was initially developed with a curved shape in the front to reduce the way the ODF moves unpacked after the packaging foil is separated and moved to the waste rolls. The problem with this shape was that the cutting blade was not able to cut the ODF since the tip of the knife would hit the guide bar right behind the ODF. The triangular blade could not move far enough to cut the whole width of the ODF. Therefore, the shape of the device was changed to a straight shape as shown in Figure 47 b. In this approach, the knife can slide from left to right reaching the ODF in the middle and cutting the whole width of the film. The guide bar was extended to decrease the way the film is unpacked.

A triangular blade was used that is attached to the white fitting, positioning the knife between the top and bottom part of the housing of the device. The fitting connects the blade that is located in the housing with the patient at the outside of the housing. To move the knife for cutting off a piece of ODF the patient just moves the fitting. The tip of the blade punctures the ODF at first contact and enables a smooth and easy cutting of the ODF. A blade in this shape and with the correct dimensions was not commercially available. Therefore, it was designed with the 3D-CAD software, and manufactured from a stainless-steel sheet by cutting and sharpening it manually.

For safety reasons, the fitting of the blade was enlarged as shown in Figure 40 c. The blade fitting now shields the blade as a cover to prevent accidents by touching the blade. Furthermore,

the cover ensures the correct positioning of the film during dispensing and cutting. The front part of the cover pushes the film to the right side after leaving the device and stretches it to enable easy and precise cutting with the blade that can penetrate the film at an angle of 90 °. After using the device, the cover closes up the opening of the device to ensure stability of the film as much as possible and to prevent anything from inserting the device.

3.3.4 Manufacturing of the dosing device

Parallel to the design process, intermediate stages of the dosing device were 3D-printed (refer to section 5.5). The utilized 3D-printing technique was the fused filament fabrication technique, which is ranked among additive manufacturing technologies. A three-dimensional model is built up layer by layer with a molten polymer strand (Gardan, 2015; Upcraft and Fletcher, 2003). 3D- printing was chosen as rapid prototyping technology in this work since it is successfully used for the manufacturing of prototypes and enables to reduce time and costs during product development. It provides the possibility to validate functionality of a created model and helps the engineer in the conceptualization step. Therefore, production time is reduced because of product cycle development since the prototype might be checked at early development stages and modifications might be incorporated in the design process (Ashley, 1991; Gardan, 2015; Upcraft and Fletcher, 2003). The main advantage of 3D-printing as rapid prototyping technology in this work was the independency of the service of skilled model-makers. Changes to the model were easily and promptly performable to promote the development of the prototype for the dosing device.

The final prototype of the developed dosing device was fully designed in an animated 3D-CAD model for further processing (Figure 48 a). The animation of the model enabled a first performance check of the developed device. It would be obvious in the model if parts would not fit together or if a motion would not be possible as intended. The 3D-CAD models were processed as shown in Figure 66 and 3D-printed with commercial PLA filaments in different

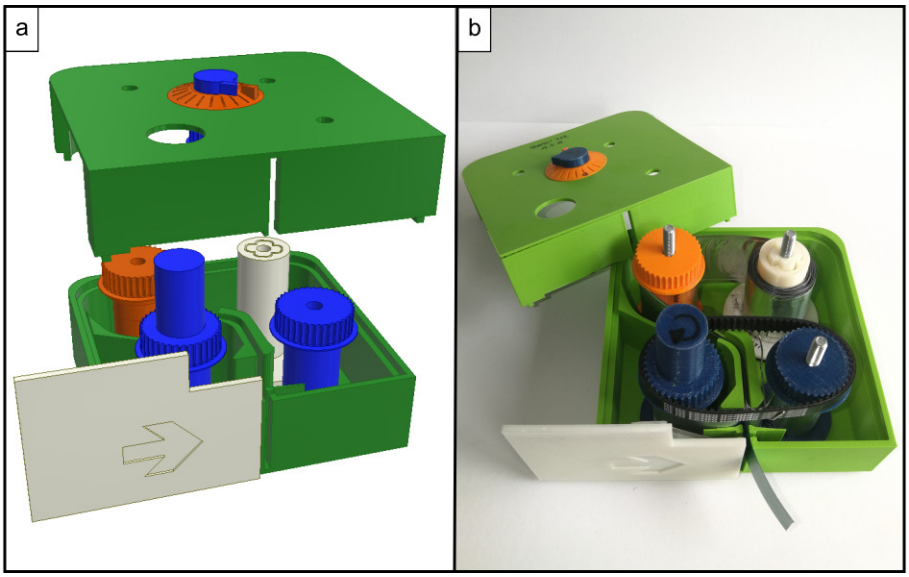

Figure 48: 3D-CAD model (a) and 3D-printed model (b) of the final prototype of the developed dosing device. The model ODF packed in the aluminum package was inserted in the 3D-printed model. Used by courtesy of the International Journal of Pharmaceutics, Elsevier (Niese et al., 2019).

colors for better presentation purposes (Table 12). Different print settings were tested and the best working settings for small, middle-sized and big parts were used for manufacturing of the device components (refer to Table 28 and section 5.5.1). Since in this work no pharmaceutical ingredient was processed during 3D-printing, the focus was to receive a working prototype of the dosing device. Most critical was the fitting of the printed parts since they had to be assembled to the complete dosing device. Furthermore, it was important that the printed parts fitted the elements that were commercially acquired e.g. the toothed belts, which had to fit the printed toothed belt disks or the packaging foil for the ODF that limited the height of the device. The 3D-printer used to produce the final prototype only had one print head, which made it impossible to print soluble support structures. Therefore, supports were avoided by involving this problem in the design process. The parts were designed to present no large overhangs. If unavoidable, the models were divided into two or more parts that were printed up-side down to avoid overhangs. The parts were glued together after printing. The dosing roll was printed in two individual pieces to attach the plastic tube cover by slipping it over (Figure 43 c and d).

The fully 3D-printed prototype of the dosing device is presented in Figure 49. The sides were left open for better demonstration of the working principle of the device. The size of the final prototype resulted in a base area of 13x13 cm and a height of 7 cm. Smaller dimensions would be desirable for the patient using it. However, the acquired packaging foils showed a defined width that made it impossible to reduce the size of the device significantly. Therefore, the ODF width was adjusted to the packaging foils and the device was designed to fit the foils as well.

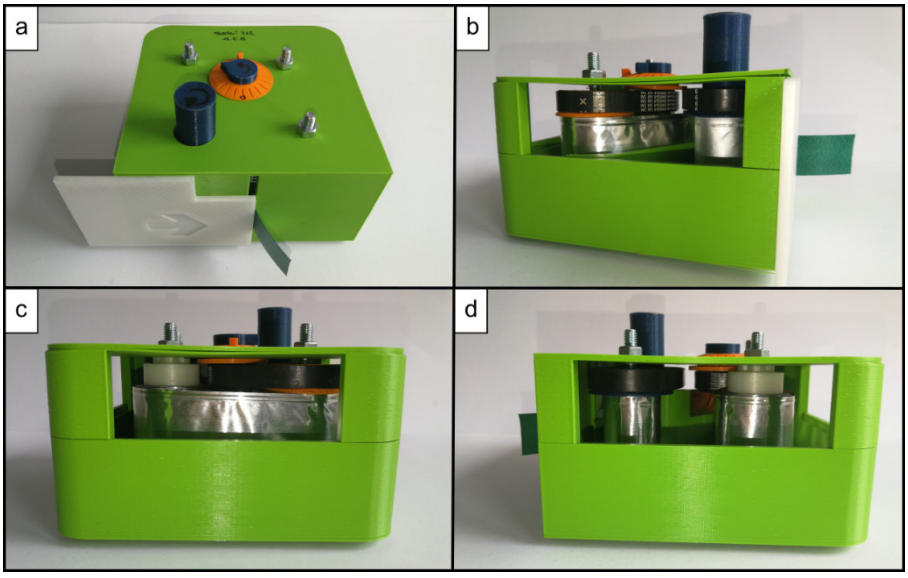

Figure 49: 3D-printed model of the final prototype of the developed dosing device from all sides. Used by courtesy of the International Journal of Pharmaceutics, Elsevier (Niese et al., 2019).

3.3.5 Application of the dosing system

3.3.5.1 General considerations

The newly developed and 3D-printed prototype of a dosing device for flexible dosing of ODFs, as shown in Figure 49 was applied to test proper working in accordance to the specifications of the Ph.Eur. First, a commercially produced green ribbon with a fixed width of 2 cm, which is the same size as for the ODFs, was used as a model film to test the dosing device prototype. The influences of the ODF manufacturing process regarding mass and content homogeneity were excluded by this approach. Since the ribbon did not contain any API, only the test for the uniformity of mass (refer to section 3.3.5.3) was performed. The warfarin ODFs W1 and W6 were tested for their use in the device as well. Three different tests according to the Ph.Eur. were assessed (refer to sections 3.3.5.3 - 3.3.5.5). The tests on the uniformity regarding the content of the samples are not intended for their application to dose from multidose containers. Nevertheless, the tests were performed since the uniformity of mass was not regarded as sufficient for the evaluation of the applicability and functionality of the developed dosing system.

3.3.5.2 Preparation of the test samples

Exemplarily, samples with lengths of 1, 2 and 5 cm (corresponding to 1, 2 and 5 steps of the dosing knob) were cut with the prototype to mimic the intended use for individual dosing (refer to section 5.6.3). Cutting of the films revealed slight differences between W1 and W6. The ODF W6 with PVA and HPMC as polymer matrix showed slight splintering during the cutting that might be because of a more brittle behavior of this film compared to W1. The variations showed up in the test results as higher scattering for the ODF W6 and can probably be traced back to a shortage of plasticizer for this formulation.

3.3.5.3 Uniformity of mass of delivered doses from multidose container (Ph.Eur.2.9.27)

The European Pharmacopoeia contains a monograph for testing the use of a multidose container (Ph.Eur 9.0, 2017b). In this test, the mass variation is checked as parameter, which is why there is no control of the delivered content of the dosage form. The review of the mass uniformity is only meaningful if a correlation between the mass and the content of a dosage form is expected. Then, the mass might be able to show a tendency of the correct dosing but cannot completely replace the content determination.

This test was first performed for the green ribbon as model film. To ensure the suitability of the green ribbon for the evaluation of the dosing process with the device prototype, the ribbon

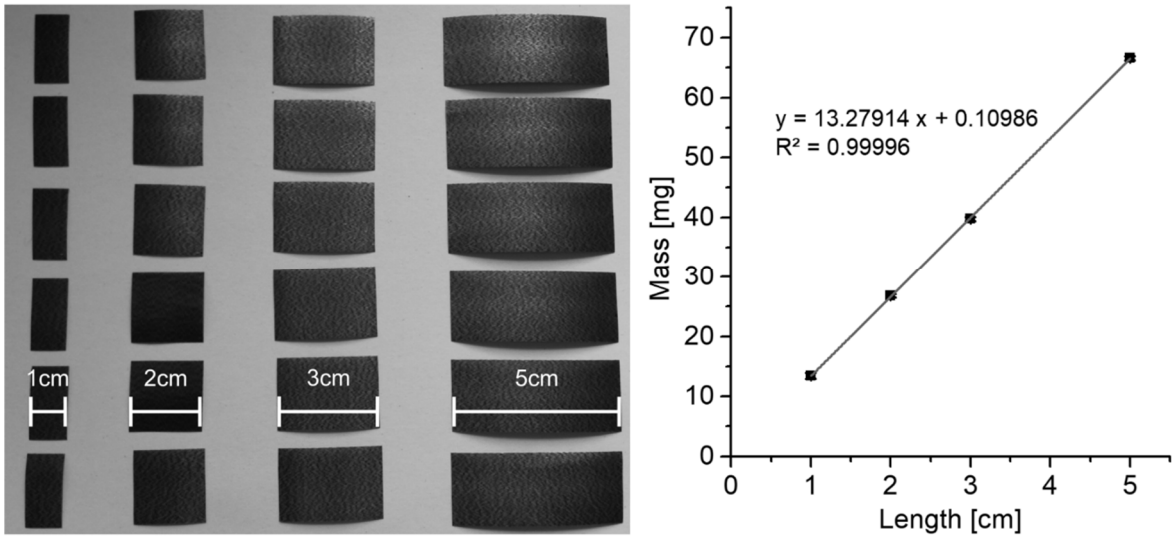

Figure 50: Pieces of the ribbon as model film cut with a knife for calibration purposes (left). Regression line of the mass of the green ribbon plotted against the length cut with the knife (mean ± sd, n = 6) (right).

was cut in different long pieces with a knife. This was done to make sure that the ribbon was uniformly produced regarding the mass over the length of the ribbon. Precise cutting with a knife should exclude the variations in mass due to the cutting step when using the device. Therefore, it was expected to examine the mass variation of the ribbon cut with the device without other impacts. Pieces of 1, 2, 3 and 5 cm were cut (Figure 50, left) and weighed for the calibration purpose. The data were plotted, and the regression line is depicted in Figure 50 on the right. It was obvious that the correlation between the mass and the cut length of the ribbon was linear and that the scattering of the mass was extremely low. Therefore, it was concluded that the use of the ribbon as model film was feasible to predict the correct working of the dosing device.

Ph.Eur. 2.9.27 was performed as described in section 5.6.4 with each 20 test pieces of 1, 2, and 5 cm. The results are shown in Table 13 and Figure 51 and present that the developed prototype met the specifications of the European Pharmacopoeia for this test for all three tested lengths. The scattering of the data points, shown on the right was higher for the shorter pieces since the absolute cutting and weighing errors became more pronounced for smaller pieces when calculated as a percentage, as it was done for the percentage of mass with regard to the mean value. Nevertheless, all samples of the 2 and 5 cm pieces were within the first threshold of ± 10 % of the mean value and a maximum of 2 samples of the 1 cm pieces were between the first and the second threshold of ± 20 %. These results complied with the specifications of the European Pharmacopoeia with regard to the precision of the dosing by the device. The bottom

Table 13: Masses delivered from multidose container (Ph.Eur. 2.9.27) for the green ribbon as model film. Top: measured mass of the samples. Bottom: percentage of the mass of the samples referred to the mass received by the calibration curve.

Dosed length	Mass [mg]
1 cm	13.68 ± 0.81
2 cm	26.86 ± 0.96
5 cm	67.02 ± 1.39
	(mean ± sd, n = 20)

Dosed length	Mass referred to the calibration [%]
1 cm	102.2
2 cm	100.7
5 cm	100.8

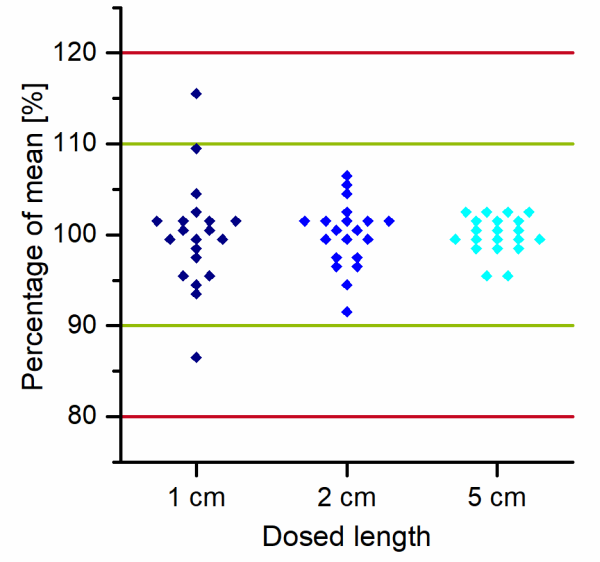

Figure 51: Masses delivered from multidose container (Ph.Eur. 2.9.27) for the green ribbon as model film. Raw data, n = 20. Green and red lines representing the thresholds of the specifications. Used by courtesy of the International Journal of Pharmaceutics, Elsevier (Niese et al., 2019).

of Table 13 shows further that the dosing is also accurate. The 2 and 5 cm pieces met the calibration curve well, whereas slightly longer pieces were dispensed for the 1 cm samples. In this case, the absolute cutting error might be the reason as well, since it would have a higher impact on smaller pieces than on larger ones.

Since the test with the green ribbon demonstrated correct working of the prototype of the dosing device the test was also performed with the warfarin ODFs W1 and W6. Table 14 and Figure 52 show the results of the ODF W1 with HPMC as polymer matrix. All three test lengths of the ODF W1, dispensed with the 3D-printed prototype met the specifications. It showed a similar trend than the green ribbon. Only the 1 cm pieces revealed samples between the first and second threshold. All other samples laid within the first threshold. The mean masses of the samples showed a linear trend ($R^2 = 0.99998$) pretending a correct working of the dosing process for W1. Nevertheless, the mean values of the mass cannot make a prediction about the accuracy of the dosing process and the scattering is more informative for the precision.

The results for W6 with PVA and HPMC as polymer matrix are shown in Table 15 and Figure 53. It was obvious that the specifications were not met for the 1 cm film pieces for this ODF. One sample exceeded the second threshold and seven samples laid between the first and second threshold. It was noteworthy that the samples deviated evenly in both directions from the mean

Table 14: Masses delivered from multidose container (Ph.Eur. 2.9.27) for the warfarin ODF W1. Measured mass of the samples.

Dosed length	Mass [mg]
1 cm	10.16 ± 0.58
2 cm	19.98 ± 0.81
5 cm	50.13 ± 1.52
	(mean ± sd, n = 20)

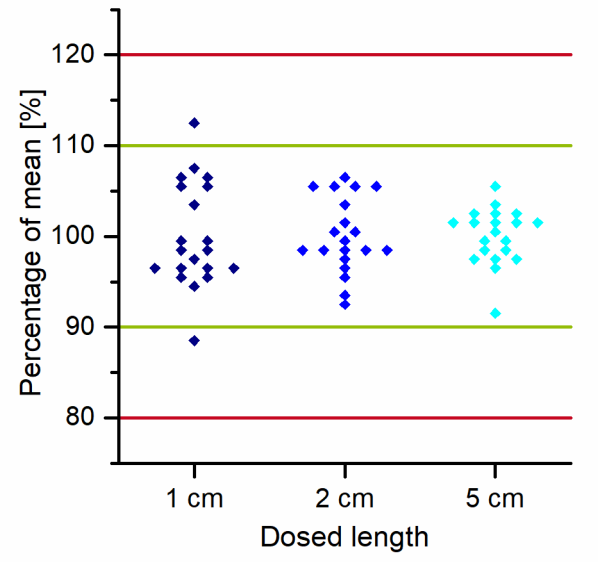

Figure 52: Masses delivered from multidose container (Ph.Eur. 2.9.27) for the warfarin ODF W1. Raw data, n = 20. Lines representing the thresholds of the specifications. Used by courtesy of the International Journal of Pharmaceutics, Elsevier (Niese et al., 2019).

value. Since only the masses were examined in this test, it was not possible to make a statement about the accuracy of the dispensed doses. However, also the mean values of the mass of ODF W6 showed a linear correlation ($R^2 = 0.99999$) pretending a correct working of the dosing device. In this case the precision is showing issues that are clearly present in the scattering of

Table 15: Masses delivered from multidose container (Ph.Eur. 2.9.27) for the warfarin ODF W6. Measured mass of the samples.

Dosed length	Mass [mg]
1 cm	8.50 ± 0.99
2 cm	17.25 ± 1.03
5 cm	43.08 ± 0.99
	(mean ± sd, n = 20)

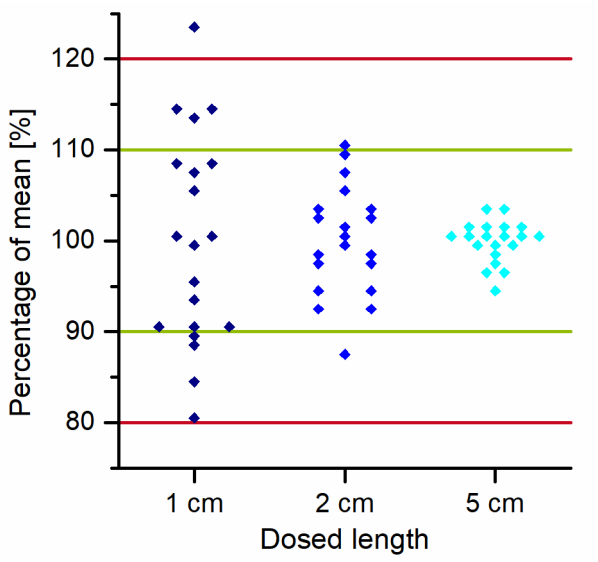

Figure 53: Masses delivered from multidose container (Ph.Eur. 2.9.27) for the warfarin ODF W6. Raw data, n = 20. Lines representing the thresholds of the specifications. Used by courtesy of the International Journal of Pharmaceutics, Elsevier (Niese et al., 2019).

the masses tracing back to the brittle film behavior during the cutting process. Although the mechanical properties of the warfarin film W1 and W6 show similar results in Figure 33, the ODFs act differently during the cutting process with the dosing device. This might be traced back to the different climatic conditions during the measurement of the mechanical properties and the cutting with the device.

For all three tested films, it was obvious that dosing gets more challenging for short film strips. The data showed that the scattering becomes higher for the shorter samples. The reason was that the absolute cutting error of the dosing device as well as the absolute weighing error of the balance had a higher impact on the short pieces than on the longer pieces since the test specification are expressed in relative figures (Jansen and Horstmann, 2014). A limitation of Ph.Eur. 2.9.27 is that only the uniformity of masses is tested. This allows no statement about the accuracy of the dosing process with the device regarding the correct dose. Therefore, the tests about the uniformity of the content were performed hereafter although they are not explicitly stated for the application in case of multidose containers by the European Pharmacopoeia.

3.3.5.4 Uniformity of content of single-dose preparations (Ph.Eur.2.9.6)

The test 2.9.6 of the European Pharmacopoeia is clearly stated for single-dose preparations only (Ph.Eur 9.0, 2017a). However, since a content uniformity testing for multidose preparations is lacking by the official bodies, Ph.Eur. 2.9.6 was performed for the dosing device as alternative test. The approach of this test is similar to Ph.Eur. 2.9.27 since in both cases only the precision of the tested data is evaluated. Evaluation of the accuracy is missing because simply the deviation from the mean value is calculated and considered with regard to defined thresholds. A difference is that Ph.Eur. 2.9.6 consists of a two-stage evaluation for the case that one content lays between the first and the second threshold. This second step was not carried out in this work as it was not regarded as acceptable for the cutting process with the device to produce too many pieces varying widely from the specifications.

Ph.Eur. 2.9.6 was performed as described in section 5.6.5 with 10 test pieces of each 1, 2, and 5 cm. It was applied only for the ODFs since no content could be determined from the green ribbon as model film. The results are shown in Table 16 and Figure 54 for the ODF W1. All samples tested met the specifications of the first threshold of ± 15 % of the mean value. The difference in the scattering of the measured values was not that pronounced for the three tested lengths as it was for Ph.Eur. 2.9.27. Only the 5 cm pieces scattered less around the mean value.

Table 16: Content uniformity (Ph.Eur. 2.9.6) of the warfarin ODF W1. Measured API content of the samples.

Dosed length	API content [mg]
1 cm	1.06 ± 0.04
2 cm	2.12 ± 0.09
5 cm	5.40 ± 0.14
	(mean ± sd, n = 10)

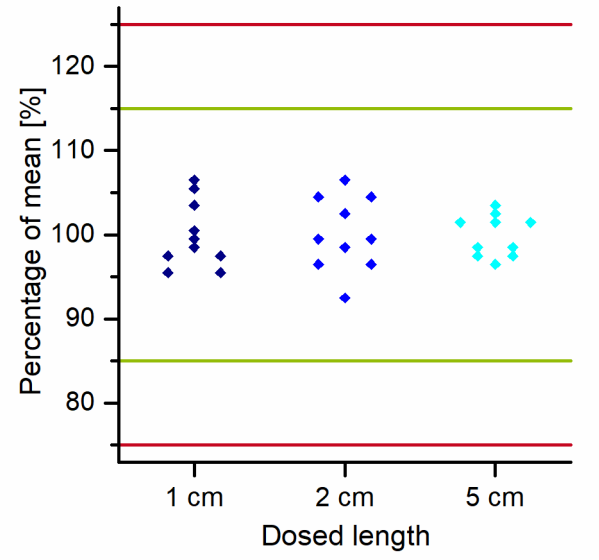

Figure 54: Content uniformity (Ph.Eur. 2.9.6) of the warfarin ODF W1. Raw data, n = 10. Lines representing the thresholds of the specifications.

As well as shown for the mass of the different long dispensed pieces, a linear correlation was observed for the content of the 1, 2 and 5 cm ODF pieces ($R^2 = 0.99996$). This demonstrates that the 3D-printed prototype of the dosing device performed uniform dosing steps for all tested lengths regarding the dispensed doses. A prediction about the accuracy is likewise not possible since the contents are not referred to a label claim that was meant to meet. Table 17 and Figure 55 show the results from testing the ODF W6. The film strip samples for 2 and 5 cm length

Table 17: Content uniformity (Ph.Eur. 2.9.6) of the warfarin ODF W6. Measured API content of the samples.

Dosed length	API content [mg]
1 cm	1.05 ± 0.11
2 cm	2.22 ± 0.05
5 cm	5.50 ± 0.15
	(mean ± sd, n = 10)

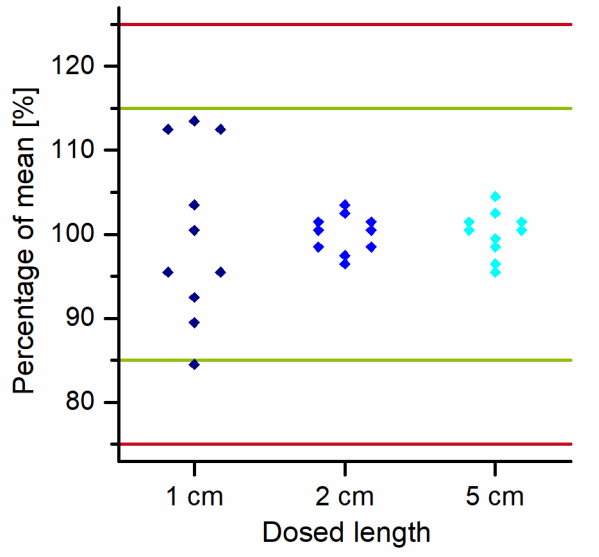

Figure 55: Content uniformity (Ph.Eur. 2.9.6) of the warfarin ODF W6. Raw data, n = 10. Lines representing the thresholds of the specifications.

complied with the specifications of the first threshold and showed both low scattering around the mean value. The 1 cm specimen scattered more around the mean value, which led to one sample that only just fell out of the first threshold. Therefore, the second step of the testing would be necessary. Since the first threshold of ± 15 % was thought to be quite broadly formulated, the result was not found to be acceptable and the second step of the testing procedure was not performed. The results in Table 17 show that the test specifications were much more difficult to meet for the shorter pieces than for the long ones. The absolute standard deviation of the 1 cm pieces was less than for the 5 cm pieces but in the relative application on the right in Figure 55, the differences are the other way around. The linearity of the contents was given for W6 as well ($R^2 = 0.99984$), which has to be considered with the same caution as for W1.

3.3.5.5 Uniformity of dosage units (Ph.Eur.2.9.40)

Ph.Eur. 2.9.40 is the only test that compares the measured contents with the declared content ("label claim") of the dosage form and does not only refer it to the mean value of the measured contents. Therefore, the informative value of this test is much higher than for Ph.Eur. 2.9.6. The mean value of the measured contents referred to the label claim of the dosage form as well as the standard deviation are included in the study to calculate the acceptance value (Ph.Eur 9.1, 2017). However, this test is also only meant for the testing of single-dose preparations. In the present case a multidose preparation and the use of a multidose container were investigated. Since flexible doses were dispensed by the device, no fixed label claim was available. To compare the calculated AVs from the samples delivered by the device with single-dose preparations, the label claim was defined as the assumed content of the delivered film piece with the respective length (refer to section 5.6.3).

The test was performed for both ODFs containing warfarin as API with 10 test pieces of each 1, 2, and 5 cm (refer to section 5.6.6). The results are presented in Table 18 showing the AV as well as the mean contents. The ODF W1 complied with the specifications again for all three examined lengths showing AVs < 15. The mean contents all exceed 100 % relative to the label claim. In absolute values the excess amounted for 0.03 mg (1 cm), 0.06 mg (2 cm) and 0.25 mg (5 cm). These values support the statement that the evaluation of relative figures makes it more difficult for small pieces with low doses to comply with the specifications than it is for larger pieces. The ODF W6 met the specification for the 2 and 5 cm film strips, but not for the 1 cm film strip because of a high standard deviation. The AV exceeded 15 although the mean API content was lower than for the other two samples. The results matched the preceding tests since

Table 18: Results of the Ph.Eur. 2.9.40 test for the warfarin ODFs. Acceptance value (n = 10), API content (% of label claim) (mean ± sd, n = 10) and CV of the API content (n = 10).

Film	Dosed length	Acceptance value		API content [%]	CV [%]
W1	1 cm	11.30	✓	103.1 ± 4.1	4.0
	2 cm	12.04	✓	102.9 ± 4.4	4.3
	5 cm	10.19	✓	105.0 ± 2.8	2.7
W6	1 cm	26.54	✗	102.5 ± 10.6	10.3
	2 cm	11.87	✓	107.9 ± 2.3	2.1
	5 cm	12.69	✓	107.2 ± 2.9	2.7

again, only the 1 cm piece of the ODF W6 failed the correct dosing with the device in accordance to the specifications.

As well as the other performed tests for uniformity by the European Pharmacopoeia, the calculation of the AV showed some critical points to consider. The AV might be an informative value to orientate during process control for a finished product. However, for a formulation development it should be well considered what mean value would still be acceptable although the standard deviation is small. The AV would allow large deviations from 100 % if only the standard deviation was small enough. On the other hand, the discrimination of low-dosed samples was apparent for this test as well. Hermes (2012) addressed the same problem for the testing of low-dosed solid dosage forms like orodispersible mini-tablets. He showed the strong dependency of the CV of the API content in a tablet from the API content and the tablet mass. For low-dosed mini-tablets, the acceptable absolute standard deviations were extremely small since both the API content and the tablet mass were very low. In the case of the presented dosing device, the deviations for the API content rather originated from the cutting step than from the ODF itself. The absolute cutting error should be comparable for the different long film pieces. Therefore, the relative cutting error has a higher impact on the shorter film samples (Jansen and Horstmann, 2014). Hence, it is more difficult to comply with the test specifications, which are expressed in relative figures as well.

3.3.6 Summary

After evaluating the requirements on a dosing device regarding correct working and patient safety, a prototype of the dosing device for flexible dosing of oral films was developed and successfully produced with a commercial 3D-printer. No electricity is necessary to power the device. Two ODFs that were formulated and produced with regard to the use in the developed device were tested for their correct dosing. To implement the dosing system into individualized warfarin therapy the correct dosing of the ODFs by the device was of high importance. The general function of the dosing device was demonstrated by dosing different lengths of a model film consisting of a green ribbon and performing the test for delivering doses from a multidose container according to the European Pharmacopoeia. The test was successfully passed and demonstrated general functionality of the device prototype. The dosing of the packed ODFs showed that the ODF with HPMC as polymer matrix met the specifications for all tests of the European Pharmacopoeia for all three different tested lengths (Table 19, W1). The ODF with PVA and HPMC as polymer matrix showed problems for the shortest pieces with 1 cm length. The scattering of the samples was too high to comply with the thresholds (Table 19 W6). This was rather a problem of the film formulation than of the dosing device since the ODF with PVA and HPMC revealed easy breakage during the cutting (refer to section 3.3.5.2).

The developed dosing device in combination with the ODFs containing warfarin enabled flexible dosing of this API. The ODF is an easily applicable dosage form that is showing advantaged for the use in geriatric as well as pediatric patients. The individualized antithrombotic therapy can be made possible for patients of different age groups with different needs of warfarin doses with the dosing device. For more flexibility of the dosing, the device

Table 19: Results of the tests for the dose delivery from the device prototype according to the Ph.Eur. ✓: data within the specifications; test passed. ✗: data not within the specifications; test failed. 2.9.40: acceptance values shown.

Film	Dosed length	2.9.27	2.9.6	2.9.40	
W1	1 cm	✓	✓	11.30	✓
	2 cm	✓	✓	12.04	✓
	5 cm	✓	✓	10.19	✓
W6	1 cm	✗	✗	26.54	✗
	2 cm	✓	✓	11.87	✓
	5 cm	✓	✓	12.69	✓

might be further refined e.g. by changing the number of teeth at the bottom of the dosing roll. For example, a dosing roll with more teeth for smaller pieces per step could be inserted in a device for a child. Another possibility to increase flexibility of the dosing by the device would be to change the API amount incorporated in the long ODF, either by increasing the API fraction added to the polymer mass or by increasing the coating thickness of the film during production process. Higher API contents per area of the dried ODF would result from that. Then the device could be used for a child with an oral film with lower API loading and for an adult with a film with higher drug loading. The gap of a missing possibility for flexible dosing of an oral film that was mentioned by Wening and Breitkreutz (2011) was closed by developing and manufacturing a functional dosing system in this work. The dosing system comprises the 3D-printed dosing device prototype and the developed ODF with the Formulation W1. This dosing system met the specifications of the European Pharmacopoeia for all three tests performed regarding the correct dosing. Contemporaneously with the present thesis, a patent was published by Blomenkemper et al. (2017), presenting similar thoughtful ideas on a dispenser for an API-loaded strip that also might contribute to the improvement of individualization of the therapy with oral films. This patent application from the pharmaceutical industry underlines the relevance of the topic of this thesis. Nevertheless, no application data of the presented dosing device are demonstrated in the patent.

4. Summary

This work focused on the development of a novel dosing system for the individualized therapy with oral films. A long oral film containing warfarin as model API for individualized therapy was developed as well as a dosing device to flexibly dispense the oral film. The long oral film together with the dosing device represents the dosing system.

First, small-scale solvent casting was elaborated to conduct a systematical formulation development approach for oral films. The small-scale coating bench allowed for the formulation screening in small batches of 50 -100 g to reduce material consumption and manufacturing time. Different formulations were prepared and characterized regarding the viscosity of the polymer solution as a key parameter for the solvent casting manufacturing process, the mechanical properties and the disintegration time of the dried film as essential parameters for the correct application of the oral film. The interactions of the process liners and the polymer solutions were investigated for this manufacturing method. It can be concluded that the selection of a suitable process liner for casting an oral film can be assisted by contact angle measurements and the determination of the SFE of the liner and the SFT of the solution.

For the most promising formulations from the small-scale trials, the film formulation development was pursued for the manufacturing process on the continuously working pilot-scale coating bench. This coating bench was used to obtain a long oral film of several meters applicable in the dosing device. First, drug-free formulations were tested for their suitability as films for the dosing device to reduce toxic waste with the API warfarin. Especially the mechanical properties of the prepared films were investigated since they represent important markers for the handling of the film in the device by a patient. The tensile test was preferred instead of the puncture test since it better represents the stresses the film is exposed to in the device and by the patient. A critical investigation of the tensile test for oral films showed that a rectangular test specimen was preferred over the often-used dumbbell-shaped specimen since no advantages of the dumbbell could be identified and the rectangle presented easier preparation and handling. The cutting of the specimens was performed with a cutting plotter instead of a knife to receive more accurate test specimens and to reduce preparation time and effort. The most promising formulations for long oral drug-free films were identified and used for the incorporation of the model drug warfarin.

Two different warfarin ODFs based on HPMC and a mixture of PVA and HPMC as polymer matrix were successfully produced on the pilot-scale coating bench in a continuous manufacturing mode. These films were characterized with special regard on the content uniformity of the warfarin throughout the long film and the stability over three months. The mechanical properties as well as the warfarin content did not reveal problems during storage of the samples. The content uniformity was successfully achieved for the long oral films (AV of HPMC film = 5.97 and PVA/HPMC film = 2.75) due to the new in-line tool implemented in the continuous solvent casting process.

The new in-line tool is a chromatic confocal optical measurement system that was applied for the first time into the film casting process to measure the wet film thickness during the solvent casting process before the film has been dried. The wet film thickness mainly determines the uniformity of dose in an oral film revealing the importance of controlling this parameter during the production process. The manufacturing process of long oral films was therefore significantly improved by this measuring tool since the thickness of the produced film was measured in real-time and monitoring as well as manual interventions became possible to reduce shortfall batches and inconsistent film products. Deviations from the targeted wet film thickness of up to 60 % were avoided and trial-and-error-based approaches can be reduced by implementation of the in-line tool.

The long oral film was developed for the usage in a dosing device for individualized therapy with oral films. Therefore, a dosing device was developed using a 3D-CAD software. The virtually designed 3D-models were then produced with a fused filament fabrication 3D-printer to obtain a prototype. The 3D-printed prototype was stepwise tested regarding its functionality and further refined. The final prototype of the dosing device was fully functional without electricity. It was tested with a ribbon as model film and both long warfarin ODFs packed in aluminum packages regarding the tests of the European Pharmacopoeia for correct doses. Three different lengths of the films (1, 2 and 5 cm corresponding to 1, 2 and 5 mg warfarin) were dispensed to mimic the flexible dosing. The model film successfully passed the test for uniformity of mass of delivered doses from multidose containers (Ph.Eur. 2.9.27) and demonstrated correct working of the dosing device. The warfarin films were tested for Ph.Eur. 2.9.27 as well and furthermore for the more challenging tests for uniformity of content of single-dose preparations (Ph.Eur. 2.9.6) and uniformity of dosage units (Ph.Eur. 2.9.40). The HPMC film successfully passed all tests for all three dispensed film lengths. The acceptance values of ten delivered film samples were all lower than the accepted limit of 15

(1 cm: AV = 11.30, 2 cm: AV = 12.04, 5 cm: AV = 10.19). The PVA and HPMC film passed all tests for the longer dispensed pieces but revealed high scattering for the shortest dispensed film piece due to brittle film properties (1 cm: AV = 26.54, 2 cm: AV = 11.87, 5 cm: AV = 12.69).

In conclusion, a dosing system that enables individualized therapy with oral films was successfully developed and tested according to the specifications given by the European Pharmacopoeia. The system passed the test for dose delivery of multidose containers as well as further tests with more challenging claims. The dosing system allows individual dosing of oral films, a dosage form suitable for all age groups, and therefore provides a promising option for personalized medicine.

5. Experimental Part

Parts of this section have already been published in peer-reviewed journals. The content was linguistically adapted and partly extended.

- Niese, S. and Quodbach, J., 2018. *Application of a chromatic confocal measurement system as new approach for in-line wet film thickness determination in continuous oral film manufacturing processes*. Int J Pharm. 551, 203-211.
  DOI: 10.1016/j.ijpharm.2018.09.028.

- Niese, S. and Quodbach, J., 2019. *Formulation development of a continuously manufactured orodispersible film containing warfarin sodium for individualized dosing.* Eur J Pharm Biopharm. 136, 93-101.
  DOI: 10.1016/j.ejpb.2019.01.011.

- Niese, S., Breitkreutz, J. and Quodbach, J., 2019. *Development of a dosing device for individualized dosing of orodispersible warfarin films.* Int J Pharm. 561, 314-323.
  DOI: 10.1016/j.ijpharm.2019.03.019.

5.1 Materials

Table 20: Substances used as model drugs

Substance	Batch	Source of supply
caffeine anhydrous	17082128	Siegfried Chemikalien, Zofingen, Switzerland
warfarin sodium	01011016	Farmak, Olomouc, Czech Republic

Table 21: Substances used for film preparation

Substance	Name/grade	Source of supply
citric acid	for analysis	Panreac, Castellar del Vallès, Spain
food coloring (red)	E 124	Caesar & Loretz, Hilden, Germany
glycerol 85 %	Ph. Eur. 6	Caesar & Loretz, Hilden, Germany
hydroxypropyl cellulose (HPC)	Klucel™ ELF Klucel™ EXF Klucel™ JXF Klucel™ LF	Ashland, Schaffhausen, Switzerland
hydroxypropyl methylcellulose, hypromellose (HPMC)	Pharmacoat® 606	Shin-Etsu, Tokyo, Japan
maltotriose polysaccharide polymer	Pullulan	Hayashibara, Okayama, Japan
polyethylene glycol (PEG)	PEG 300	Clariant, Frankfurt, Germany
polyvinyl alcohol (PVA)	PVA 26-88	Merck, Darmstadt, Germany
sodium carboxymethyl cellulose (CMC)	Walocel® C30 PA 09	Dow Wolff Cellulosics, Bomlitz, Germany
triethyl citrate	Citrofol®Al	Jungbunzlauer, Basel, Switzerland

Table 22: Process liners used for film preparation

Material	Designation	Source of supply
Mediflex® XM AMWL (45/105)	Liner 1	Amcor Flexibles, Ghent, Belgium
Scotchpak® 1022	Liner 2	3M, Neuss, Germany
Trespaphan® NNA 40.0	Liner 3	Hoechst Trespaphan, Neunkirchen, Germany
Silphan® S75M	Liner 4	Siliconature, Godega di Sant'Urbano, Italy
PPQ7667	Liner 5	Huhtamaki, Espoo, Finland

Table 23: Sealing foils used for film packaging

Material	Designation	Source of supply
ALU + PE	PE-foil	in-house
PET 12 TRAITE IMP + ALU 9/000 + 50 Å Rayopeel	RP-foil	Amcor Flexibles, Ghent, Belgium

Table 24: Materials used for 3D-printing

Material	Name/batch	Source of supply
blue PLA filament	ProFill™ PLA Night Blue	3D-printerstore.ch, Weinfelden, Switzerland
green PLA filament	013107	Prodim, Helmond, Netherlands
orange PLA filament	w1140-19	Prodim, Helmond, Netherlands
white PLA filament	013104	Prodim, Helmond, Netherlands
PVA filament	ProFill™ PVA	3D-printerstore.ch, Weinfelden, Switzerland

Table 25: Toothed belts used in the final prototype of the developed dosing device

Material	Type	Profile	Pitch	Width	Effective length	Number of teeth	Source of supply
Neoprene	HTD	3M	3 mm	9 mm	225 mm	75	Mädler, Stuttgart, Germany
Neoprene	HTD	3M	3 mm	9 mm	168 mm	56	Mädler, Stuttgart, Germany

Table 26: Substances used for analytical methods

Substance	Name/grade	Source of supply
acetic acid	Ph.Eur	VWR, Fontenay-sus-Bois, France
diiodomethane	ReagentPlus®	Sigma Aldrich, Munich, Germany
distilled water		freshly produced before usage
methanol	HPLC grade	Riedel-de Häen™, Seelze, Germany

5.2 Data, graphing and analysis methods

Arithmetic calculations were performed with Microsoft® Excel® 2013 (Microsoft Corporation, Redmond, USA) and Origin®Pro 9.0.0G (OriginLab Corporation, Northampton, USA). Origin®Pro 9.0.0G was further used for graphic representation of the data.

Statistical evaluation of the data was performed with Microsoft® Excel® 2013 (Microsoft Corporation, Redmond, USA) and the data analysis Add-in (Analysis ToolPak, Microsoft Corporation, Redmond, USA). F-tests and t-tests were performed for a significance level of $\alpha = 0.05$. Depending on the result of the F-test, the p-value was determined by either using the t-test for assuming equal or unequal variances.

Chemical structures were drawn with the freeware version of the software ACD/ChemSketch 12.01 (Advanced Chemistry Development, Toronto, Canada).

5.3 Film manufacturing methods

5.3.1 General concept

As film manufacturing method, the solvent casting technique was used in this work. The general manufacturing steps are depicted in Figure 56 and comprise the preparation of the polymer mass, which is further cast on a process liner to form a film. The dried film is then cut into the desired shape and size and removed from the process liner.

Figure 56: Film manufacturing steps.

5.3.2 Polymer mass

5.3.2.1 Preparation of the polymer mass

Drug-free solutions were prepared by dissolving the plasticizer in the adequate amount of cold water. The weighed polymer (except PVA) was added to the stirring solution. The mixture was stirred on a magnetic stirrer until the polymer was fully dissolved and no air bubbles were visible anymore.

Drug-free solutions containing PVA as film forming polymer were prepared differently because of the slow dissolution of the polymer flakes in cold water. The PVA was added to the

adequate amount of cold water while stirring and the mixture was heated up to 90 °C until the polymer was fully dissolved. Plasticizers were added to the polymer solution after cooling down. Evaporated water was added in the end to the cold solution.

Drug-free solutions with PVA and HPMC in combination as film forming matrix were prepared by dispersing the HPMC in the warm PVA solution and cooling down the mixture while stirring. Plasticizers were added to the polymer solution after cooling down and complete dissolution of the polymers. Evaporated water was added in the end to the cold solution.

The polymer solutions containing an API were prepared as follows. For HPMC solutions, the water was heated up to 80 °C before the polymer was added while stirring. The polymer dispersed and did not form a solution until cooling down. This preparation method was chosen to reduce preparation time. Plasticizers and the API were added to the cold polymer solution and evaporated water was added in the end. The solutions with PVA and HPMC as matrix were prepared as described for the drug-free solutions. The API and the plasticizers were added in the end to the cold solution before the evaporated water was refilled.

HPMC polymer suspensions containing MCC as insoluble filler were prepared as described for the solutions and MCC was dispersed in the fully dissolved polymer solution on a magnetic stirrer.

Batch sizes of 100 g for small-scale film manufacturing and 500 – 1000 g for pilot-scale film manufacturing were prepared.

5.3.2.2 Calculation of the API proportion

The API proportion of the polymer mass was calculated according to Equation 3 (Krampe, 2015):

Equation 3: Calculation of the API fraction in the polymer mass. API dose: targeted API amount per film sample; film size: area of the film piece; coating thickness: gap height or wet film thickness.

$$API\ fraction\ [\%] = \frac{API\ dose\ [mg] * 1000}{film\ size\ [cm^2] * coating\ thickness\ [\mu m]}$$

The film size and the applied coating thickness were used to calculate the volume of the wet film sample. The API fraction of the polymer mass as percentage is received by dividing the desired API dose for the single film sample by the volume of the wet polymer mass for this film sample.

5.3.3 Small-scale orodispersible film manufacturing

The bubble free polymer solution was cast on the process liner (Mediflex® XM AMWL 45/105, Amcor Flexibles, Ghent, Belgium, if not stated otherwise) that was fixed by vacuum on the film applicator (Coatmaster 510, Erichsen, Hemer, Germany). The solution was poured into the working area of the coating knife (Multicator 411, Erichsen, Hemer, Germany) and cast with a velocity of 6 mm/s and a gap height of 500 µm that was adjusted with the micrometer screw of the knife (Figure 57). The heating plate of the film applicator was adjusted to 40 °C.

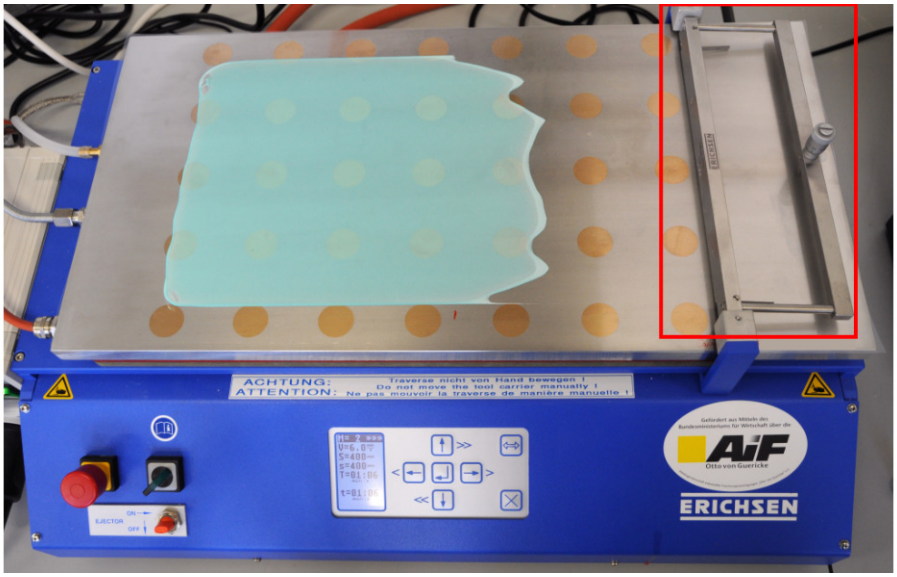

Figure 57: Coating knife marked in the red box (Multicator 411) and film applicator (Coatmaster 510).

5.3.4 Pilot-scale orodispersible film manufacturing

5.3.4.1 Film manufacturing

Continuous film manufacturing was performed with a pilot-scale coating bench (Figure 58, MBCD TGM-K-1.4, Optimags, Dr. Zimmermann, Karlsruhe, Germany). The pump delivered the film forming mass through the coating knife and the mass was cast on the non-siliconized side of the process liner (Silphan S75M, Siliconature, Godega di Sant'Urbano, Italy). For drug-free formulations, the gap height was set to 500 µm whereas for preparations containing API the WFT was adjusted to exactly 250 µm as mentioned in section 5.3.4.2 by changes of the pump flow and the gap height using the optical probe for in-line WFT measurements. The liner with the applied coating mass moved through the 80 cm long drying tunnel with a speed of 12.5 cm/min. The drying tunnel consisted of two independently adjustable heating plates of

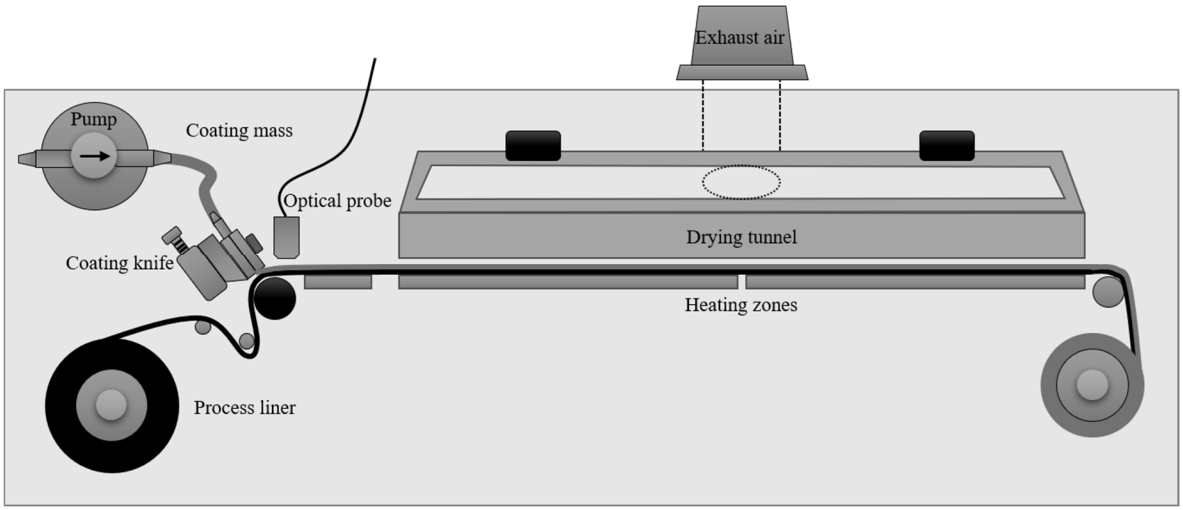

Figure 58: Schematic view of the pilot-scale coating bench for continuous oral film manufacturing equipped with the optical probe for wet film thickness measurement.
Used by courtesy of the International Journal of Pharmaceutics, Elsevier (Niese and Quodbach, 2018).

equal size. Temperature of the heating plates was set between 90 °C for the first heating plate and 110 °C for the second heating plate. These process settings resulted in a drying time of 6.4 min for the produced films. The liner holding the dried ODF was coiled up at the end for further processing.

5.3.4.2 In-line wet film thickness measurement

The continuous film manufacturing process was controlled by a sensor equipped with an optical probe (CHRocodile S, Precitec, Gaggenau-Bad Rotenfels, Germany) with a measuring range of 3 mm and a chromatic confocal measuring principle. The probe was used for in-line determination of the WFT during the film manufacturing process. Measurements were conducted using a scan rate of 2000 Hz. The probe was positioned after the coating knife of the continuous coating bench to measure the thickness of the wet coating mass (Figure 58). Two different measuring modes were selectable to control the WFT during the process (refer to Figure 27 and section 3.2.3.2).

For transparent materials the thickness mode of the probe software (CHRocodileExplorer 0.98.0.0) was used where the probe measured the optical thickness of both, the transparent film and the transparent process liner. To calculate the optical thickness for the corresponding target WFT (T_{opt}), the optical thickness of the liner (T_{opt}(Liner)) was measured first and summed up with the quotient of the WFT and the refractive index (n, refer to section 5.4.2) of the polymer solution (Equation 4):

Equation 4: Equation to calculate the optical thickness for the corresponding target WFT of the film.

$$T_{opt} = T_{opt}(Liner) + \frac{WFT}{n}$$

The in-line WFT of the non-transparent materials was measured using the distance mode since the light was not able to measure through the material (refer to Figure 27, right and section 3.2.3.2). In this case, first the distance from the probe to the process liner (D_0) was measured. Then the required physical thickness of the wet coating mass (WFT) was subtracted from this value. The result was the target value for the distance (D_{target}) to be measured between the probe and the surface of the cast coating mass during film production (Figure 59).

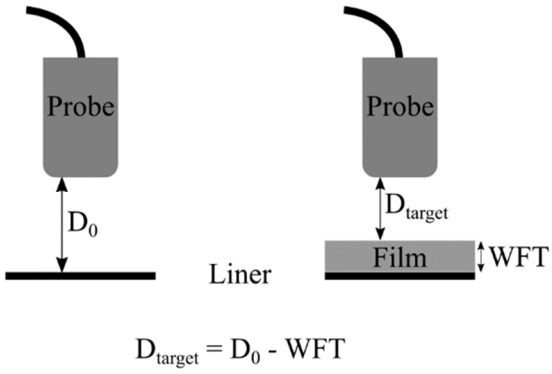

Figure 59: Wet film thickness measurement of non-transparent material using the distance mode. Determination of the distance values.

5.3.4.3 Method validation of the in-line thickness measurement

5.3.4.3.1 General considerations

ICH guideline Q2 served as reference for the validation of the new in-line film thickness measurement (ICH, 2005). All mentioned validation characteristics were taken into consideration and assessed concerning their applicability to the evaluated method. The specificity that is described as an unequivocal assessment of the substance under investigation (ICH, 2005) was not applicable for this study. The used optical probe is expected to be widely applicable for the ODF film manufacturing process and is not supposed to be specific to one substance. This was thoroughly investigated in the robustness section. The detection and quantitation limit were not applicable as well, since they are depending on the film manufacturing process.

The basic polymer formulation for the films produced during validation contained 15 % of HPMC, 3 % citric acid, 1 % caffeine and 81 % demineralized water. This formulation was used for all films in section 5.3.4.3 unless stated otherwise.

The caffeine content was determined for every film as mentioned in section 5.4.10.2. The WFT was set to 250 µm if not stated otherwise, resulting in a caffeine target content of 1.5 mg/6 cm² for the basic polymer formulation.

5.3.4.3.2 Linearity

Over a range of 100 µm to 350 µm in steps of 50 µm, the linearity between the set WFT and the measured caffeine content of the produced film was determined. The optical probe was used to adjust the desired WFT. Films with constant length (187.5 cm) were produced by keeping the thickness constant for 15 min for every set WFT. The measured caffeine content of the dry film was plotted against the set WFT and a linear fit was performed to determine linearity. The resulting coefficient of determination, the y-intercept and the slope of the regression line were evaluated.

5.3.4.3.3 Range

The range of the present method is derived from an adequate level of linearity ($R^2 > 0.99$), accuracy (mean = 95 – 105 %) and precision (CV < 2 %).

5.3.4.3.4 Accuracy

The accuracy of the measurement was determined for three WFTs within range of linearity (150, 250 and 350 µm). Three films of 1 m length were independently produced for each thickness. For evaluation of the accuracy, the measured caffeine content was compared to the target content of the set WFT. Mean value and standard deviation were calculated from the three films of each thickness.

The film thickness homogeneity over the width of the film was determined by taking samples of the dried film at three different points spread over the film width. The samples were cut in the size of 0.5*6 cm from the position where the WFT was measured by the probe (in the middle of the film) and 0.5 cm from both edges of the film. This investigation was performed at three positions spread over the length of the film with a distance of 50 cm between the three positions and the samples were analyzed as mentioned in section 5.4.10.2.

5.3.4.3.5 Precision

The precision can be split up into three parts, repeatability, intermediate precision and reproducibility. Samples were produced in triplicates on the same day as mentioned in section 5.3.4.3.4 to determine repeatability. For intermediate precision, three films with a set WFT of 250 µm and a length of 1 m were produced each time on three different days over a time period of one month. Results of the measured caffeine content were calculated as coefficients of variation. The reproducibility determined as a comparison between different laboratories was not investigated in this study.

5.3.4.3.6 Robustness

The robustness of a method is evaluated by small, intentional changes in method parameters to obtain an idea of the reliability of the system during usage (ICH, 2005). Changes were made to the process and since the optical probe detects the WFT, the film formulation was also varied. The film formulations for the robustness study that differ from the basic formulation as described in section 5.3.4.3.1 are shown in Table 27. If not stated otherwise, the length of the produced films amounted to 1 m.

Table 27: Film formulations for robustness investigations. Values as percentage, referred to total formulation weight (w/w).

	Formulation				
	Viscosity1-a	**Viscosity2-a**	**Viscosity3-a**	**Viscosity4-a**	**Viscosity5-a**
HPMC	11	12.5	15	17.5	19
Citric acid * H_2O	3	3	3	3	3
Caffeine anhydrous	0.5	0.5	0.5	0.5	0.5
Dem. water	85.5	84	81.5	79	77.5
	Viscosity1-b	**Viscosity2-b**	**Viscosity3-b**	**Viscosity4-b**	**Viscosity5-b**
HPMC	11	12.5	15	17.5	19
Citric acid * H_2O	3	3	3	3	3
Caffeine anhydrous	1	1	1	1	1
Dem. water	85	83.5	81	78.5	77
	Polymer		**Color**		**Suspension**
HPMC	7.8		15		15
	PVA 5.2		**color** 15 drops		**MCC** 5
Citric acid * H_2O	2		3		3
Caffeine anhydrous	1		1		1
Dem. water	84		81		76

Films with two liner speed settings differing from the regularly used settings were produced. A slower setting (5 cm/min) than the basic setting (12.5 cm/min) and a faster setting (19.8 cm/min) were examined.

Furthermore, a different polymer matrix was considered as film formulation (Table 27, Polymer). The combination of PVA and HPMC was used showing an opaque appearance compared to the transparent appearance of the pure HPMC formulation. Three films were produced with the PVA and HPMC formulation.

A polymer solution containing red coloring agent (E 124, Table 27, Color) was investigated for in-line thickness measurements by producing three films as well.

The influence of different viscosities of the polymer solution was also investigated. For this reason, the adjustment of the caffeine content in the film by in-line thickness measurement as well as by calculating with the gap height of the coating knife as it was previously done was compared. Five polymer solutions were prepared for each method differing in the polymer content (11 – 19 %). For both methods, a target content of 1.2 mg per 6 cm² film was aimed for.

The caffeine content in the polymer solutions was calculated according to section 5.3.2.2. The gap height of 400 µm was applied as "coating thickness" as it was done before without the possibility of an in-line method. The caffeine content for this calculation resulted in 0.5 % for the polymer solutions (Table 27, Viscosity-a). For the in-line method, the WFT was adjusted to 200 µm, since preliminary studies revealed that the true WFT deviates from the gap height. Therefore, the caffeine content of 1 % for the in-line polymer solutions was the result (Table 27, Viscosity-b). All films were cast at same basic settings as mentioned in section 5.3.4.1 after measuring the viscosity of the solutions according to section 5.4.1.

Dispersed MCC was used to produce a polymer suspension (Table 27, Suspension) that was further investigated regarding the influence of particles for the in-line WFT measurement. The produced film was non-transparent because of the insoluble MCC in the aqueous polymer solution. The distance mode was used for measuring the in-line WFT in this case (refer to section 5.3.4.2). Three films were produced at basic settings. However, the temperature was reduced to 75/85 °C because of the lower solvent content of the film forming mass.

The caffeine content of all produced films was determined and evaluated regarding the impact of the changes made.

5.3.5 Cutting of orodispersible films

Precise cutting of ODF specimens for further characterizations was performed with a cutting plotter (Figure 60, Cameo® 3, Silhouette America, Lindon, USA). The samples of the drug-free films were cut from the whole width of the film except for two centimeters of the peripheral regions, which reduced differences in the film thickness due to surface effects of the polymer solutions. The samples from the API containing films were only cut from the point where the optical probe measured the thickness (refer to section 5.3.4.2). Besides, samples were cut over the whole length of the produced film to evaluate the homogeneity of the API content and other properties of the film throughout the process. The Silhouette Studio® software (version 4.0.837ss, Silhouette America, Lindon, USA) was used to create the shape of the samples, to enter the settings and to send the processed data to the plotter. The AutoBlade (Silhouette America, Lindon, USA) was used for the cutting, which is a blade that automatically adjusted the chosen blade settings entered in the software. The cutting thickness and cutting speed were selected matching the properties of the ODF. The lowest thickness level (1 out of 10) and a slow speed (3 out of 10) were sufficient to obtain good results for cutting the film without cutting the process liner (kiss-cut), and thus the cut samples were easy to remove from the liner.

Figure 60: Cameo® 3 cutting plotter with movable cutting unit (marked in red).

5.4 Analytical methods

5.4.1 Dynamic viscosity of the polymer mass

Rheological measurements were performed with a rheometer (Kinexus pro+, Malvern, Worcestershire, UK) by using a cone (1 °, 60 mm; CP1/60 SR2482 SS) and plate geometry (65 mm; PL65 S0520 SS). To investigate the rheological behavior of the polymer solutions, a shear ramp was recorded from 0.1 to 100 s^{-1} and 100 to 0.1 s^{-1}. To keep the measurement conditions constant, the temperature was set to 25 °C and each sample was measured three times. To compare the samples, the dynamic viscosity at a shear rate of 4 s^{-1} was determined. This value represented the settings of the pilot-scale film manufacturing process (gap height and liner speed). For the shear rate measurements, the viscosity was determined 60 times at the same shear rate. Each sample was measured three times and the mean and the standard deviation of the three measurements were calculated.

5.4.2 Refractive index of the polymer mass

The refractive index of the polymer solutions was determined using an Abbe refractometer (Carl Zeiss, Jena, Germany). The determination was performed three times at room temperature.

5.4.3 Particle size of MCC in the polymer suspension

Laser diffraction (Mastersizer 3000, Malvern, Worcestershire, UK) was used to investigate the particle size of MCC in the polymer suspension. The particle size distribution was determined from the measurement data. Measurements were performed using the wet dispersion unit Hydro MV with demineralized water as dispersant and a stirrer speed of 2500 rpm. Three repetitions were carried out for the measurement.

5.4.4 Visual and manual assessment

The film preparations were visual assessed after production as well as after storage. Especially the homogeneity of the film surface, the possible crystallization of components of the film and whether the film intensively curled after removing it from the process liner were surveyed. Furthermore, it was possible to get a first idea of the flexibility and the brittleness of a film after removing it from the process liner.

5.4.5 Mass

Weighing of the films was performed with an analytical balance (MC210P, Sartorius, Göttingen, Germany). The balance has a weighing capacity up to 210 g and a readability of 0.01 mg. Ten film samples were weighed and these samples were further used for the content uniformity determination. Mean, standard deviation and CI ($\alpha = 0.05$) were calculated.

5.4.6 Thickness

The thickness of the films was measured with a micrometer screw (Mitutoyo, Neuss, Germany) that was modified for the measurements of films by adding two plates to the measuring parts. The screw showed a measuring capacity area of 0 – 25 mm and a measuring accuracy of 0.001 mm. Ten film samples were measured and these samples were further used for content uniformity determination. Mean, standard deviation and CI ($\alpha = 0.05$) were calculated.

5.4.7 Disintegration time

To determine the disintegration time of the ODFs the "slide frame" method was used (Garsuch and Breitkreutz, 2010). The film (2x3 cm) was placed into a slide frame, which then was set horizontally on a little beaker. 200 µl of distilled water of 37 °C were dropped on the film using a pipette. The time until the film disintegrated, and the drop fell into the beaker was recorded. Measurements were repeated six times for each sample. Mean and standard deviation were calculated.

5.4.8 Dynamic vapor sorption

A dynamic vapor sorption system (SPS 11, ProUmid, Ulm, Germany) was used to investigate the water absorbency of the different film samples. The samples (2x3 cm) were dried at 0 % relative humidity. Subsequently, the relative humidity was increased in steps of 10 % until it reached 90 % relative humidity. For the films prepared with the pilot-scale coating bench, the measurement was further continued for relative humidities from 90 % to 0 %. Each step lasted until the weight of every sample was at equilibrium (weight change < 0.01 % / 30 min) but not less than 60 min. Measurements were performed once for every sample and the temperature was set to 25 °C.

5.4.9 Water content by Karl-Fischer titration

The residual water content of the produced films was determined by Karl-Fischer titration using a Volumetric KF Titrator (Mettler-Toledo, Giessen, Germany). As working medium,

Hydranal-Methanol dry (Honeywell, Offenbach, Germany) was used. The titration was performed with Hydranal-Composite 5 (Honeywell, Offenbach, Germany). Hydranal-Water Standard 10.0 (Honeywell, Offenbach, Germany) was used for calibration purposes. Measurements were performed three times for every sample.

5.4.10 Drug assay

5.4.10.1 Warfarin sodium

The warfarin sodium content of the film samples was determined using high performance liquid chromatography (HPLC) and a modified method from the United States Pharmacopoeia official monograph "Warfarin Sodium" (USP 39). An Elite® LaChrome System (Hitachi-VWR, Darmstadt, Germany) was used that consisted of a pump L-2130, an autosampler L-2200, an oven L-2300 and an ultraviolet (UV)-Detector L-2400. It was equipped with a 125 mm long Nucleosil® 120-3 RP-18 column (Machery-Nagel, Düren, Germany) that was operated at 40 °C oven temperature. A mixture of methanol/water/glacial acetic acid (64:36:1) served as mobile phase and the flow rate was set to 0.7 ml/min. The warfarin content of the ODF was determined by dissolving one film (2*2.5 cm) in 25.0 ml of distilled water to fit in the range of linearity. The sample was filtered through a 0.45 µm pore sized polypropylene membrane filter (VWR, Leuven, Belgium) and 15 µl were injected into the system. The API was detected at a wavelength of 280 nm. Each vial was measured three times and the mean was calculated. For each long film batch ten 2*2.5 cm films from the whole length of the long film were measured for evaluation of the content uniformity according to Ph.Eur. 2.9.40 (Ph.Eur 9.1, 2017). The acceptance value was calculated as shown in Equation 5:

Equation 5: Calculation of the acceptance value (AV). M is the reference value depending on $\bar{X}$, which is the mean of the ten individual contents, expressed as percentage of the label claim. k is the acceptability constant (k = 2.4 for n = 10) and s the standard deviation of the ten individual contents (Ph.Eur 9.1, 2017).

$$AV = |M - \bar{X}| + k * s$$

A system suitability test (CDER, 1994) was performed before every measurement with six samples of a 0.1 mg/ml warfarin solution, regarding the repeatability (CV of the area data < 1 %), the capacity factor (> 2) and the theoretical plate number (> 2000). The correct operation of the system was confirmed this way.

The HPLC method was validated according to the ICH guideline Q2 and the Reviewer Guidance (CDER, 1994; ICH, 2005). Figure 61 shows a characteristic chromatogram of the warfarin peak from a dissolved HPMC film containing 2.5 mg warfarin (0.1 mg / ml). The

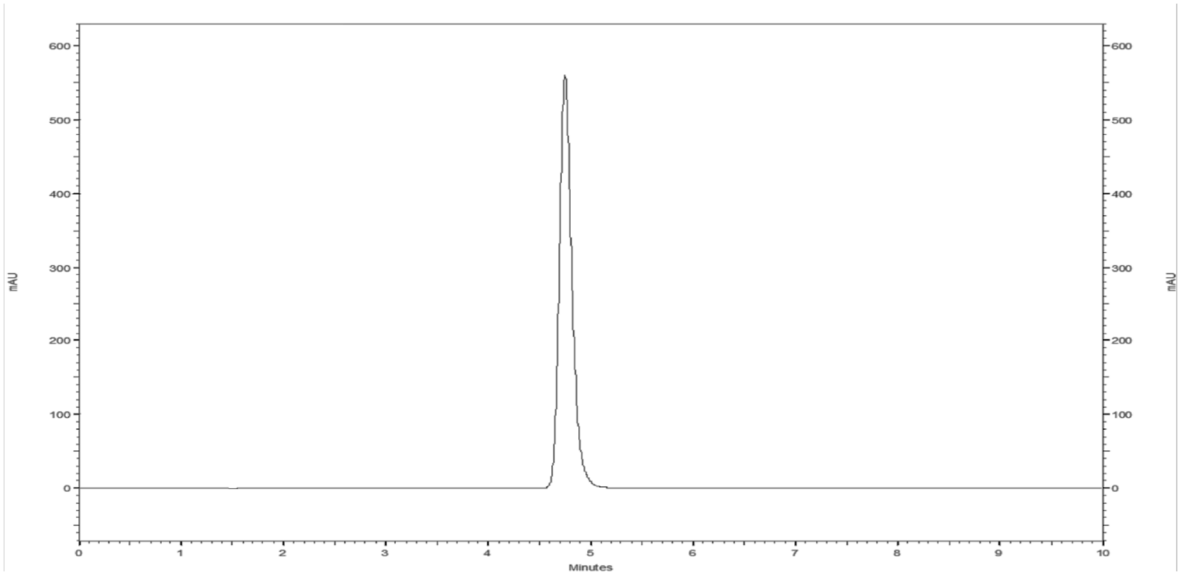

Figure 61: Chromatogram of a dissolved HPMC film containing warfarin.

retention time of the warfarin peak is at 4.75 min whereas the dead time for the system was determined with thiourea to be 1.54 min. A clear separation is given.

The HPLC method was validated regarding linearity, repeatability, intermediate precision and specificity. The linearity was demonstrated by calibration curves measured at seven consecutive days including five concentrations evenly spread over a range of 0.07 mg/ml to 0.13 mg/ml. The coefficients of determination were between 0.9995 and 0.9998. To test the repeatability a sample prepared once was measured ten times. It was performed at seven consecutive days and showed CVs between 0.13 % and 0.61 %. Furthermore, six separately prepared samples with the same concentrations were measured and showed a CV of 0.37 %. Intermediate precision was proven within different days. A solution containing 0.1 mg/ml warfarin was prepared at seven consecutive days and measured three times. The CV over the seven days was 0.77 %.

The specificity of the method was shown by measuring pure solvent that showed no absorption at a wavelength of 280 nm. Furthermore, a sample containing 0.1 mg/ml warfarin was exposed to light and measured three times at day number one and day number seven. The difference between the measured content was 0.36 % and within the range of the measurement error of the system. No change in the chromatogram was observed. The matrix influence of the ODF was tested with recovery investigations. A drug-free ODF in the size of the corresponding amount of API was added to warfarin solutions of 0.08, 0.095 and 0.12 mg/ml. The recovery rates were in the range of 98 – 102 % with values of 99.89, 99.53 and 99.57 %.

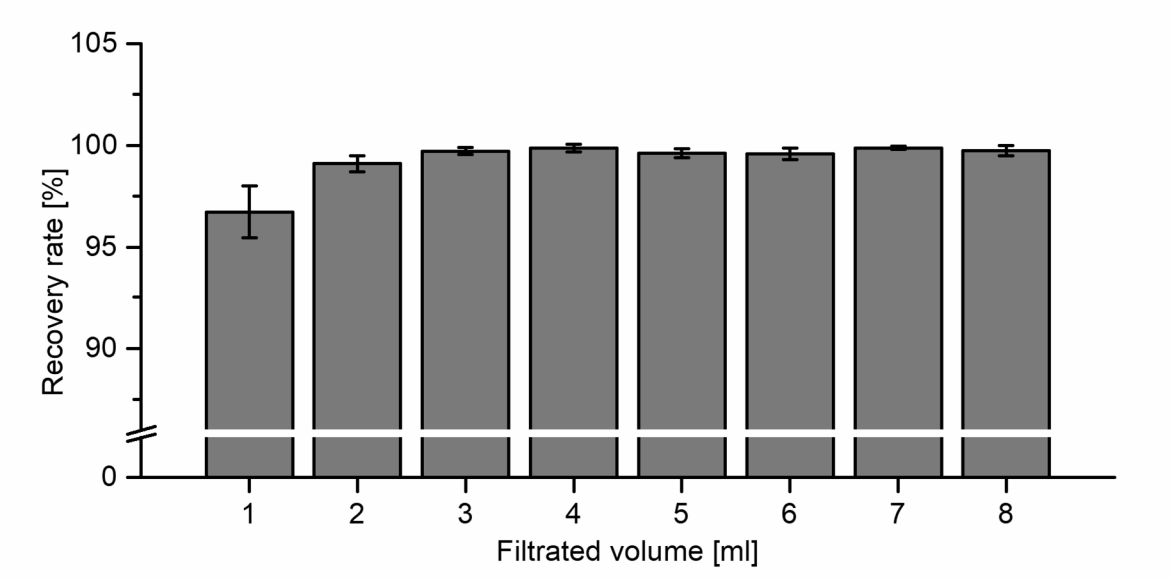

Figure 62: Recovery rate of a 0.1 mg/ml warfarin solution filtered through a 0.45 µm polypropylene membrane filter (mean ± sd, n = 3).

A filter adsorption test was performed to investigate the influence of the used polypropylene membrane filter with a pore size of 0.45 µm on the sample preparation for the HPLC measurements. The test was performed for three filters with each ten milliliters of 0.1 mg / ml warfarin solution. Each sample was measured with the above-mentioned HPLC method for warfarin. The first milliliter was sampled without being filtered. Then 1 ml was filtered into a vial and the next ml into the next vial and so on. The last milliliter was sampled again without being filtered. The recovery rate was calculated as shown in Equation 6:

Equation 6: Calculation of the recovery rate for the filter adsorption investigation.

$$Recovery\ rate\ [\%] = \frac{Peak\ area(X\ ml\ filtrated\ volume)}{Peak\ area(unfiltered\ sample)} * 100\ \%$$

The results from the filter adsorption investigation are shown in Figure 62 and point out that it was important to discard the first filtered 3 ml of the samples.

5.4.10.2 Caffeine

To determine the caffeine content in the film samples one sample (2*3 cm or 0.5*6 cm) was dissolved in 100.0 ml demineralized water to fit the calibrated range of 5 to 30 mg/l (Figure 63). The content was spectroscopically determined at a wavelength of 273 nm (n = 3) using a Lambda 25 UV/VIS spectrometer (Perkin-Elmer, Waltham, USA) after complete dissolution of the film matrix. The samples with MCC were filtered using a 0.45 µm polypropylene filter before analysis. The calibration was repeated once a month and was sensitive with a slope of

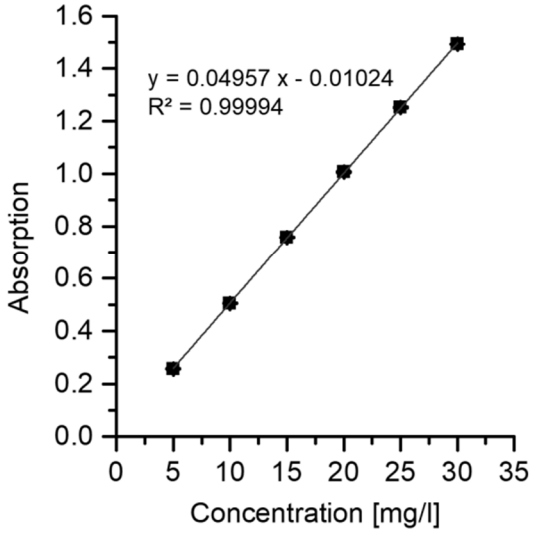

Figure 63: Linearity of the UV absorption of caffeine in demineralized water, measured at a wavelength of 273 nm; (mean ± sd, n = 3).

at least 0.0493 l/mg. The linear fit showed a coefficient of determination not less than 0.9995. Preliminary recovery tests showed that the film matrix as well as the filler MCC did not influence the spectroscopic quantification. Six samples were measured for each long film.

The caffeine content of the prepared film forming masses was determined by dissolving 750 mg of polymer solution in 500 ml of demineralized water. After complete dissolution of the polymer solution, the content was spectroscopically determined as mentioned above for the film samples. The determined content of the polymer solution was used to calculate the real target content for the film batches since the caffeine films were only used for the method validation of the optical probe (refer to section 5.3.4.3). The real target content was calculated because the results of the film content should only be dependent on the validated thickness measurement method and not on the preparation of the polymer mass.

5.4.11 Mechanical characterization

5.4.11.1 Puncture test

The puncture strength and the elongation of the films produced on the small-scale coating bench were investigated with the mechanical strength test of Preis et al. (2014b). A 2*3 cm film was placed in a horizontal position into a sample holder with a central hole of 9.9 mm diameter. Using a texture analyzer (TA.XTplus, Stable Micro Systems, Godalming, UK) the attached probe with a diameter of 5.0 mm moved down (speed: 1 mm/s) on the film and from the moment the probe touched the film the provided force and the distance the probe traveled were recorded. A force-distance diagram was obtained. The puncture strength was defined as

the maximum force applied at breakage of the film divided by the probe contact area of the film (for the 5.0 mm probe, the area is 19.64 mm²). The elongation to break was calculated according to Equation 7. Measurements were performed six times for each batch and the mean and the standard deviation were calculated.

Equation 7: Calculation of the elongation to break according to Preis et al. (2014b), where a' is the initial length of the sample not being punctured by the probe, b is the displacement of the probe, r is the radius of the probe and a the initial length of the sample holder opening radius.

$$elongation\ to\ break\ [\%] = \left(\frac{\sqrt{a'^2 + b^2} + r}{a} - 1\right) * 100\ \%$$

5.4.11.2 Tensile test

The mechanical properties of the films produced with the pilot-scale coating bench were investigated by performing a tensile test according to standard DIN EN ISO 527-1 and -3 (DIN, 2003, 2012). A texture analyzer (TA.XTplus, Stable Micro Systems, Godalming, UK) was used to characterize the test specimen (Figure 19, rectangular specimen with a length of 12 cm to match the equipment of the texture analyzer, refer to section 3.2.2.3). The clamps that hold the film sample were covered with sponge rubber to spare the film from the metal of the clamps. Convex metal clamps were used for the characterization of the films. The specimen was fixed between the upper and lower clamp with a distance of 10 cm. The test speed was set to 0.1 mm/s and the test lasted until the sample broke. The measurement was repeated five times.

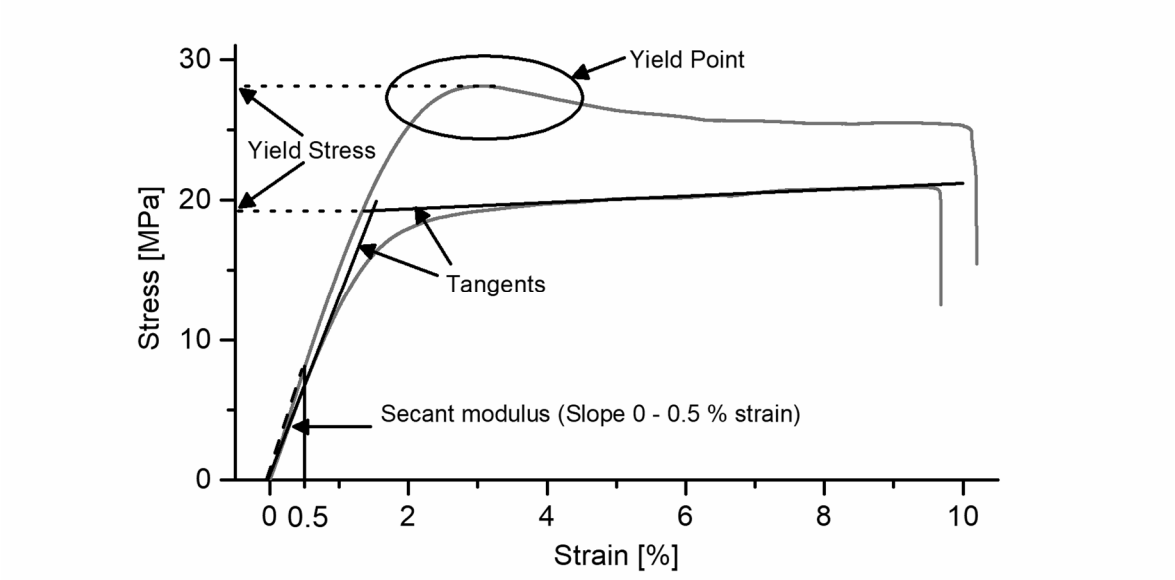

Figure 64: Exemplary diagram of two different stress-strain curves with and without yield point. Dotted line: yield stress determination. Dashed line: secant modulus determination. Used by courtesy of the European Journal of Pharmaceutics and Biopharmaceutics, Elsevier (Niese and Quodbach, 2019).

The force-distance diagram was recorded, transformed into a stress-strain diagram and the secant modulus, according to ASTM D882 (ASTM, 2012) as the slope of the linear region between 0 – 0.5 % strain and the yield stress as the stress at the transition from elastic to plastic deformation were determined. The yield stress was obtained from the stress-strain diagram by different ways depending on the shape of the curve. If the curve showed a yield point, the maximum stress at this point was used. If the curve did not show a yield point, the yield stress was visually identified, applying two tangents to the arms of the curve and determining the stress at the intercept of the tangents (Figure 64). The mean and the standard deviation were calculated.

5.4.12 90° Peel adhesion test

A texture analyzer (TA.XTplus, Stable Micro Systems, Godalming, UK) was used for 90° peel adhesion tests according to the FINAT (Féderation internationale des fabricants et transformateurs d'adhésifs et thermocollants sur papiers et autres supports) test method 2 (FINAT, 2001) that was modified for the intended purpose in this work. A 90° peel rig was applied to the basic assembly of the texture analyzer (Figure 65). The ODF, still attached to the process liner was cut into samples of 25*140 mm. The backside of the process liner was attached to the peel rig with double-sided tape. The initial part of the ODF was clamped into

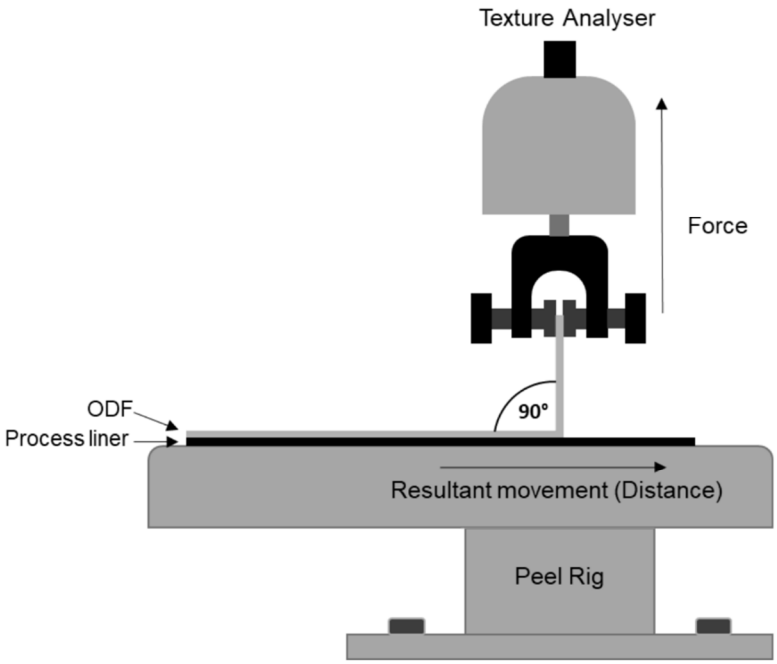

Figure 65: Texture analyzer assembly for the 90° peel adhesion test.

the upper arm of the texture analyzer with an angle of 90° to the peel rig. The upper arm of the texture analyzer then moved upwards with a speed of 2.5 mm/s and started the recording of the measured forces after reaching a trigger force of 1 g. The force was recorded over the length of the measurement distance of 100 mm. The measurement was repeated with six samples for each batch. Data analysis was performed by calculating the mean of the forces recorded within the range of 20 – 80 mm of a sample. Furthermore, the total mean, the standard deviation and the CI ($\alpha = 0.05$) of the six samples were calculated.

5.4.13 Surface tension

The surface tension was measured using a tensiometer (K100, Krüss, Hamburg, Germany) with an attached platinum plate according to the Wilhelmy method. Six samples were measured and the mean and the standard deviation were calculated. The platinum plate was cleaned from residues of the polymer solutions by flaming after rinsing.

5.4.14 Contact angle

Contact angle measurements were performed by drop shape analysis using a drop shape analyzer (DSA100, Krüss, Hamburg, Germany). The contact angle measurement was used to evaluate the wetting behavior of the polymer solution on the process liner. For this purpose, the process liner was fixed on the sample table with adhesive tape. The polymer solution was withdrawn by the syringe (1750 TLL, 500 µl, Hamilton, Bonaduz, Switzerland) and a drop of 15 µl was deposited on the process liner. The behavior of the drop was recorded with the integrated camera and pictures were saved at 0 and 30 s. The contact angle was determined after 30 s by using the supplied software (Drop Shape Analysis DSA1 version 1.90, Krüss, Hamburg, Germany). For ten drops the contact angles were measured and the mean, the standard deviation and the CI ($\alpha = 0.05$) were calculated.

Furthermore, the contact angle measurement was used to determine the SFE of the process liners by measuring the contact angles of water and diiodomethane on the liners. The drop volume was 6 µl for water and 2 µl for diiodomethane. Consulting the capillary length (Equation 8) a drop volume was determined that resulted in a maximum drop radius for that the contact angle was not influenced by the weight force of the liquid.

Twenty drops of the two test liquids were measured on every process liner and the mean, the standard deviation and the CI ($\alpha = 0.05$) were calculated. The polar and dispersive parts of the SFT of the polymer solutions were also determined by measuring a contact angle. At first, the

Equation 8: Capillary length (K^{-1}) of a liquid with a surface tension (σ), a density (ρ) and the gravitational constant (g).

$$\mathrm{K}^{-1} = \sqrt{\frac{\sigma}{\rho * g}}$$

contact angle of diiodomethane was measured on a smooth piece of Teflon® to calculate the SFE of the same. Then the contact angles of the polymer solutions on the Teflon® piece were measured to calculate the polar and dispersive parts of the SFT.

SFE and SFT calculations were performed as shown in section 5.4.15.

5.4.15 Surface free energy calculations

Calculations of the SFE of solid and liquid materials (also called SFT) were performed using the following equations. Young described the relation between the contact angle and the different SFEs at the three phase contact point:

Equation 9: Young's equation (1805) at the three phase contact point with the SFE of the solid phase (σ_s), the interfacial tension between the solid and liquid phase (σ_{sl}), the SFT of the liquid phase (σ_l) and the contact angle (θ).

$$\sigma_s = \sigma_{sl} + \sigma_l * \cos\theta$$

Since there are two unknown quantities in Equation 9 that cannot be directly measured ($\sigma_s \; and \; \sigma_{sl}$) the two-component model of Owens and Wendt was used to describe the interfacial tension between the solid and liquid phase:

Equation 10: Calculation of the interfacial tension between the solid and liquid phase (σ_{sl}) according to Owens and Wendt (1969) with the SFE of the solid phase (σ_s), the SFT of the liquid phase (σ_l) and their dispersive (D) and polar (P) interactions.

$$\sigma_{sl} = \sigma_l + \sigma_s - 2\left(\sqrt{\sigma_s^D \sigma_l^D} + \sqrt{\sigma_s^P \sigma_l^P}\right)$$

By this means, the SFE of the solid (σ_s) can be stepwise calculated from its dispersive (σ_s^D) and polar interaction fraction (σ_s^P) by solving both equations (Equation 9 and Equation 10) for the interfacial tension (σ_{sl}) and combining the remaining equations:

Equation 11: Combined Equation 9 (left side) and Equation 10 (right side).

$$\sigma_s - \sigma_l * \cos\theta = \sigma_l + \sigma_s - 2\left(\sqrt{\sigma_s^D \sigma_l^D} + \sqrt{\sigma_s^P \sigma_l^P}\right)$$

The transposition of Equation 11 leads to an equation only containing measurable quantities:

Equation 12: Final combination of Young's equation (Equation 9) with the model of Owens and Wendt (Equation 10) after transposition.

$$\sigma_l(1+\cos\theta) = 2\left(\sqrt{\sigma_s^D\sigma_l^D} + \sqrt{\sigma_s^P\sigma_l^P}\right)$$

The SFEs of the process liners as solid materials (σ_s) were calculated by using the mean values of the measured contact angles of diiodomethane and water on the liners. Since diiodomethane only interacts on a dispersive level (Ström et al., 1987), Equation 12 can be simplified by removing the polar interactions (*P*). The dispersive part of the SFT of diiodomethane (σ_l^D) is equal to the total SFT (σ_l) since the polar interactions do not exist. Therefore, the only unknown quantity remains the dispersive part of the SFE of the solid (σ_s^D) that can be easily calculated:

Equation 13: Calculation of the dispersive interaction of the SFE of the solid.

$$\sqrt{\sigma_s^D} = \frac{\sigma_l(1+\cos\theta)}{2\sqrt{\sigma_l^D}}$$

To obtain information about the polar interactions of the SFE of the solid (σ_s^P), the mean of the contact angles of water on the process liners was used for calculations. The SFT values for water, the contact angle and the before calculated dispersive part of the SFE of the solid are inserted in Equation 12 and the polar part of the SFE of the solid (σ_s^P) is the only unknown value and can be calculated. The absolute SFE of the solid is obtained by summing up the dispersive and the polar interactions.

The polar and dispersive interactions of the polymer solutions were determined by using a piece of Teflon® as a solid material showing only dispersive interactions. The SFE of Teflon® (σ_s) is therefore equal to the dispersive part of the SFE of the solid (σ_s^D). The SFE of Teflon® ($\sigma_s = \sigma_s^D$) was calculated according to Equation 13 using the mean of the measured contact angles of diiodomethane on Teflon® as well as the SFT data for diiodomethane. The mean of the contact angles of the polymer solution on Teflon®, the absolute SFT of the polymer solutions and the calculated SFE of Teflon® were used to calculate the dispersive part of the SFT (σ_l^D) of the polymer solution. For this purpose, Equation 13 was rearranged for the dispersive part of the SFT (σ_l^D). The polar part of the SFT (σ_l^P) was further calculated as the difference between the absolute SFT and the dispersive part (σ_l^D).

5.4.16 Storage

Samples were stored at 21 °C without humidity control after production.

5.4.17 Stability testing of unpacked ODFs

ODF samples for stability testing were stored over twelve weeks. The samples for the warfarin sodium assay (2x2.5 cm, 2.5 mg label claim, n = 10) and for testing of the mechanical properties performing the tensile test (2x12 cm, n = 5) were stored at 21 °C and 40 % relative humidity and at 21 °C and 60 % relative humidity. Content measurements (refer to section 5.4.10.1) and testing of the mechanical properties (refer to section 5.4.11.2) were performed before storing as well as after four, eight and twelve weeks. The differences between t0 and t12 were compared by calculation of a F-test (refer to section 5.2).

5.5 Rapid prototyping

5.5.1 3D-model processing

3D-CAD models were designed with the software Inventor® Professional 2016 (Autodesk®, San Rafael, USA). The obtained *.STL (stereolithography) files were prepared for 3D-printing using the open source slicing software Slic3r (Prusa Edition, version 1.39.1-prusa3d-win64). The slicing software prepared the layers of the model and converted it into kinematic instructions for the 3D-printer that were combined in the G-code (Figure 66).

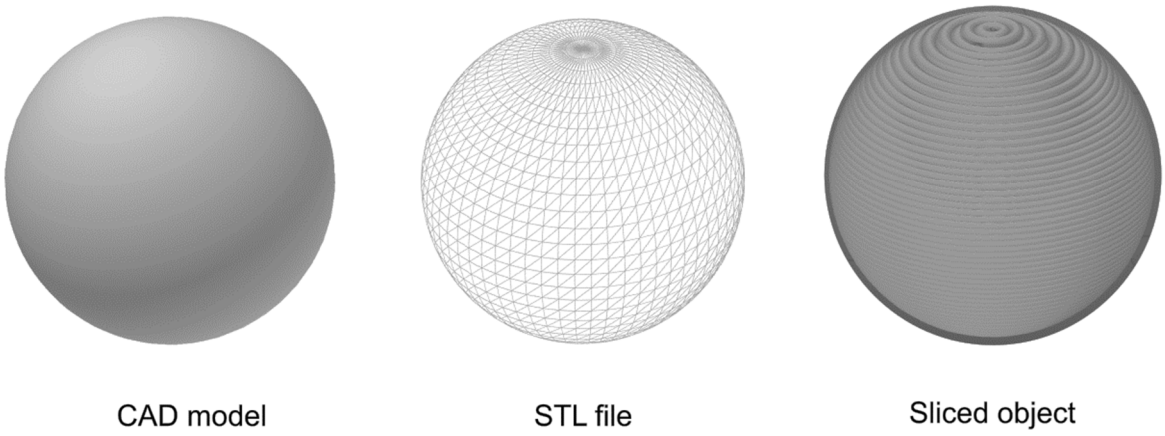

Figure 66: 3D-CAD-model (left), STL file (middle) and sliced object (right).

The applied settings in the slicer software for processing the models are shown in Table 28. Three different settings were used depending on the size of the printed object and the necessary level of precision for the component. Big objects were the housing parts of the device that tolerated faster speed settings. The middle-sized objects were e.g. the different rolls with attached teeth or toothed belt disks that require a higher level of precision to match the used toothed belt. Therefore, slower speed settings were applied. The small objects were e.g. the scale of the dosing indicator. Due to the small size and high level of precision, a slow speed and a smaller layer height were applied.

Table 28: Slicer settings for big, middle sized and small printed objects.

Settings	Big objects	Middle-sized objects	Small objects
layer height (first layer height) [mm]	0.2 (0.2)	0.2 (0.2)	0.1 (0.2)
perimeters	2	2	2
solid layers top - bottom	3 – 3	2 – 2	3 – 2
seam position	random	random	random
infill density [%]	15	20	20
fill pattern	rectilinear	rectilinear	rectilinear
fill angle [°]	45	45	45
solid infill threshold area [mm²]	0	0	25
skirt loops minimum	1	1	1
skirt distance from object [mm]	2	2	2
skirt height [layers]	1	1	1
skirt minimum extrusion length [mm]	4	4	4
brim width [mm]	3	3	4
support	no	no	no

Settings	Big objects	Middle-sized objects	Small objects
Speed [mm/s]			
perimeters	49.5	45	36
small perimeters (r < 6.5 mm)	22	20	16
external perimeter	38.5	35	28
infill (solid infill)	187 (187)	170 (170)	136 (136)
top solid infill	55	50	40
gap fill	44	40	32
travel	187	170	136
first layer	30	30	24
extrusion width [mm]	0.45	0.45	0.45
first layer	0.42	0.42	0.42
perimeters	0.45	0.45	0.45
external perimeters	0.45	0.45	0.45
infill (solid infill)	0.45 (0.45)	0.45 (0.45)	0.45 (0.45)
top solid infill	0.40	0.40	0.40
infill/perimeters overlap [%]	25	25	25
bridge flow ratio	0.8	0.8	0.8

5.5.2 3D-printing

3D-printing was performed using a Prusa i3 MK3 (Figure 67, Prusa research, Prague, Czech Republic). This printer uses the fused filament fabrication method where the extrusion head deposits a melted plastic strand on the print bed layer by layer to form the desired object. The commercial PLA filaments had a diameter of 1.75 mm and the printing nozzle had a diameter of 0.4 mm. They were printed with an extrusion head temperature of 215 °C for the first layer and 210 °C for all following layers. The print bed temperature was set to 60 °C. The fan of the print head was turned on except for the first layer to improve adherence of the printed object to the print bed that was made from polyetherimide.

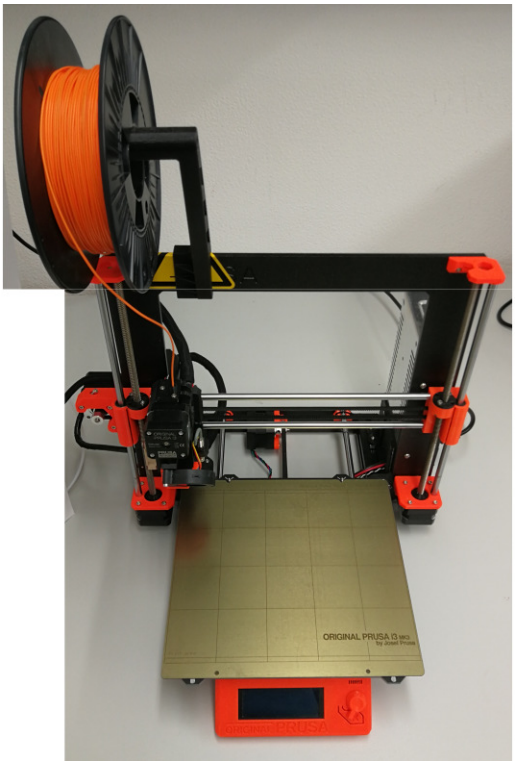

Figure 67: Prusa i3 MK3 3D printer.

5.6 Application of the dosing device prototype

5.6.1 Packaging of the long ODFs

The 2 cm wide cut long films were packed in sealing foil using a continuous sealing device (Figure 68, rotary sealer hm 500 DE, hawo, Obrigheim, Germany). The PE-foil (polyethylene) on one side and the RP-foil (rayopeel) on the other side (refer to Table 23 and section 5.1) were sealed at a temperature of 160 °C and a sealing time of 5 s resulting from the not-adjustable moving velocity of the conveyer belt. Using the RP-foil, an easy reopening was possible due to the special “Rayopeel” lamination of the foil.

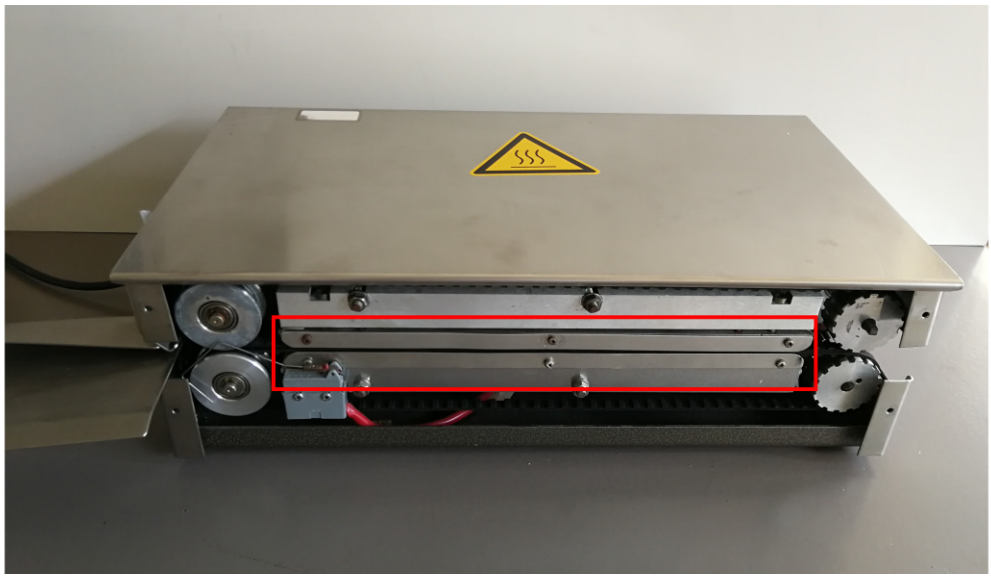

Figure 68: Rotary sealing device with the sealing area (marked in red).

5.6.2 Stability testing of packed long ODFs

Stability testing of packed long ODFs was performed over a period of 30 days. The mechanical properties (refer to section 5.4.11.2) were measured at the beginning of the test as well as after three, seven, 14 and 30 days. Content measurements were not performed because no changes were observed over storage for the unpacked ODFs (refer to section 5.4.17). For every measuring point, a long ODF (2 cm wide) was packed and stored at 21 °C and 60 % relative humidity. The stored length of the ODF was composed of five test specimens for the tensile test (2*12 cm; 60 cm) and additionally three, seven, 14 or 30 cm representing the daily dose of 1 mg warfarin used until the measuring point. The packed film was coiled up in the same manner as it would in the prototype of the dosing device and one side of the foil was left open to mimic the use in the dosing device (refer to Figure 37 and section 3.2.4.4). 1 cm film was cut off of each film every day to mimic the dosing by a patient.

5.6.3 Dosing with the dosing device prototype

The packed long ODF or the packed ribbon (as model film) were inserted in the 3D-printed prototype of the dosing device. Twenty doses of each 1, 2 and 5 cm length were cut subsequently. These lengths were corresponding to a warfarin content of 1, 2 and 5 mg per piece in case of the ODF.

5.6.4 Uniformity of mass of delivered doses from multidose container

According to Ph.Eur. 2.9.27, twenty doses of either the ribbon or the ODFs were dispensed by the 3D-printed prototype of the dosing device (refer to section 5.6.3), weighed and the average mass was calculated. The European Pharmacopoeia requires that not more than two individual masses deviate by more than 10 % and none by more than 20 % from the average mass (Ph.Eur 9.0, 2017b).

5.6.5 Dose uniformity of single-dose preparations

According to Ph.Eur. 2.9.6, the content of 10 doses of the ODFs, dispensed by the 3D-printed prototype of the dosing device (refer to section 5.6.3), were determined using HPLC (refer to section 5.4.10.1). The European Pharmacopoeia requires that not more than one individual content deviates by more than 15 % and none by more than 25 % from the average content. In the case of one value deviating by more than 15 % but less than 25 %, 20 more contents ought to be analyzed (Ph.Eur 9.0, 2017a). This step was not performed in this study.

5.6.6 Uniformity of dosage units

According to Ph.Eur. 2.9.40, the content of 10 doses of the ODFs, dispensed by the 3D-printed prototype of the dosing device (refer to section 5.6.3), were determined using HPLC (refer to section 5.4.10.1). The acceptance values (AV) were calculated according to the Ph.Eur. 2.9.40. The label claims were calculated depending on the length of the dispensed film and the content of the film forming mass used for production of the ODF. The European Pharmacopoeia requires an AV $\leq$ 15. If the AV is not met 20 more contents ought to be analyzed (Ph.Eur 9.1, 2017). This step has not been performed in this study.

6. Bibliography

Aithal, G.P., Day, C.P., Kesteven, P.J.L., Daly, A.K., 1999. *Association of polymorphisms in the cytochrome P450 CYP2C9 with warfarin dose requirement and risk of bleeding complications*. Lancet. 353, 717-719.

Aktories, K., 2005. *Allgemeine und spezielle Pharmakologie und Toxikologie*, 9. Ed. Elsevier, Urban & Fischer, Munich.

Alhnan, M.A., Okwuosa, T.C., Sadia, M., Wan, K.W., Ahmed, W., Arafat, B., 2016. *Emergence of 3D printed dosage forms: opportunities and challenges*. Pharm Res. 33, 817-1832.

Allen, J.D., Cobb, M.E., Hillman, R.S., Mungall, D.R., Ostoich, V.E., Stroy, G.H., 1985. *Integrated drug dosage form and metering system*. US 4712460.

Alomari, M., Mohamed, F.H., Basit, A.W., Gaisford, S., 2015. *Personalised dosing: Printing a dose of one's own medicine*. Int J Pharm. 494, 568-577.

Anderson, G.J.M., Bonney, S.G., Davies, M.B., Lintell, D.T.D.S., Wilson, A.A., 2003. *Medicament dispenser*. EP 2266650B1.

Arafat, B., Qinna, N., Cieszynska, M., Forbes, R.T., Alhnan, M.A., 2018. *Tailored on demand anti-coagulant dosing: An in vitro and in vivo evaluation of 3D printed purpose-designed oral dosage forms*. Eur J Pharm Biopharm. 128, 282-289.

Arens, E., 1953. *Strip dispenser*. US 2758710A.

Ashland, 2017. *Klucel™ hydroxypropylcellulose - Physical and chemical properties* [Accessed 12.08.2018]. https://www.ashland.com/file_source/Ashland/Product/Documents/Pharmaceutical/PC_11229_Klucel_HPC.pdf.

Ashley, S., 1991. *Rapid prototyping systems*. Mech Eng. 113, 34-43.

ASTM International, 2012. *ASTM D882 Standard test method for tensile properties of thin plastic sheeting*, ASTM International, West Conshohocken.

Avery, R.S., 1942. *Label dispenser*. US 2372245A.

Bala, R., Pawar, P., Khanna, S., Arora, S., 2013. *Orally dissolving strips: A new approach to oral drug delivery system*. Int J Pharm Invest. 3, 67-76.

Bauer, K.H., Frömming, K.H., Führer, C., Lippold, B.C., Müller-Goymann, C., Schubert, R., 2017. *Pharmazeutische Technologie : mit Einführung in Biopharmazie und Biotechnologie*, 10. Ed. Wissenschaftliche Verlagsgesellschaft, Stuttgart.

Berman, B., 2012. *3-D printing: The new industrial revolution*. Business Horizons. 55, 155-162.

Biss, T.T., Avery, P.J., Brandao, L.R., Chalmers, E.A., Williams, M.D., Grainger, J.D., Leathart, J.B., Hanley, J.P., Daly, A.K., Kamali, F., 2012. *VKORC1 and CYP2C9 genotype and patient characteristics explain a large proportion of the variability in warfarin dose requirement among children*. Blood. 119, 868-873.

Blomenkemper, M., Linn, M., Hackbarth, R., Bee, M., 2017. *Device and method for dispensing active ingredient-containing or active ingredient-carrying strips*. WO 2017186562A1.

Blum, M., 2000. *Dispenser for adhesive tape*. EP 1190973B1.

Boateng, J.S., Stevens, H.N.E., Eccleston, G.M., Auffret, A.D., Humphrey, M.J., Matthews, K.H., 2009. *Development and mechanical characterization of solvent-cast polymeric films as potential drug delivery systems to mucosal surfaces*. Drug Dev Ind Pharm. 35, 986-996.

Bontinick, W., 1972. *Heat-sealable film capable forming peelable seals*. US 3879492A.

Borges, A.F., Silva, C., Coelho, J.F.J., Simoes, S., 2015. *Oral films: Current status and future perspectives I - Galenical development and quality attributes*. J Controlled Release. 206, 1-19.

Breitkreutz, J., Boos, J., 2007. *Paediatric and geriatric drug delivery*. Expert Opin Drug Delivery. 4, 37-45.

Breitkreutz, J., Kleinebudde, P., Boos, J., 2002. *Arzneimittel für alle*. Pharm Ztg. 157, 16-24.

Buanz, A.B.M., Belaunde, C.C., Soutari, N., Tuleu, C., Gul, M.O., Gaisford, S., 2015. *Ink-jet printing versus solvent casting to prepare oral films: Effect on mechanical properties and physical stability*. Int J Pharm. 494, 611-618.

Cairns, D., 2012. *Essentials of pharmaceutical chemistry*, 4. Ed. Pharmaceutical Press, London.

CDER - Center for Drug Evaluation and Research, 1994. *Reviewer Guidance - Validation of chromatographic methods*.

D'Angelis, B.S., 2006. *Wound dressing dispenser*. US 2007/0068837A1.

Damikolas, G., 1998. *Portable sterile bandage dispenser*. US 6213343B1.

Dataphysics, 2018. *Understanding interfaces* [Accessed 13.08.2018]. https://www.dataphysics-instruments.com/knowledge/understanding-interfaces/#dispersivepolar.

Dave, R.N., Susarla, R., Khusid, B., Bhakay, A.A., Bilgili, E.A., Muzzio, F., 2013. *System and method for fabrication of uniform polymer films containing nano and micro particles via continuous drying process*. US 20160022599A1.

Davies, M.B., Hearne, D.J., Rand, P.K., Walker, R.I., 1990. *Inhalation device*. US 5860419A.

De Man, E.H., Boes, E., 1999. *Tape dispenser*. US 6659322B1.

Denter, U., Himmighofen, D., Schülein, R.G., 1986. *Nachfüllbarer Spender für Papier- und/oder Folienrollen*. EP 0265552B1.

DIN - Deutsches Institut für Normung, 2003. *DIN EN ISO 527-3 Kunststoffe - Bestimmung der Zugeigenschaften*, Teil 3: Prüfbedingungen für Folien und Tafeln. Beuth Verlag GmbH, Berlin.

DIN - Deutsches Institut für Normung, 2012. *DIN EN ISO 527-1 Kunststoffe - Bestimmung der Zugeigenschaften*, Teil 1: Allgemeine Grundsätze. Beuth Verlag GmbH, Berlin.

Dixit, R.P., Puthli, S.P., 2009. *Oral strip technology: Overview and future potential*. J Controlled Release. 139, 94-107.

El-Setouhy, D.A., El-Malak, N.S.A., 2010. *Formulation of a novel tianeptine sodium orodispersible film*. AAPS PharmSciTech. 11, 1018-1025.

EMA - European Medicines Agency, 2013. *Guideline on pharmaceutical development of medicines for paediatric use*, EMA/CHMP/QWP/805880/2012 Rev. 2.

Erichsen, 2016. *Film applicators*, TBE 284/286/288/358/360/411/421 - V/16.

Evans, C.T., Gieda, C., 2002. *Single dispensing film strip container*. US 7661555B1.

FDA - Food and Drug Administration - Center for Devices and Radiological Health, 1997. *Design control guidance for medical device manufacturers*.

FDA, 2008. *Guidance for industry - Orally disintegrating tablets* [Accessed 16.08.2018]. https://www.fda.gov/downloads/drugs/guidancecomplianceregulatoryinformation/guidances/ucm070578.pdf.

FINAT - Fédération Internationale des Fabricants et Transformateurs d'adhesifs et thermocollants sur papiers et autres support, 2001. *FINAT test method 2 Peel adhesion (90°) at 300mm per minute*, Den Haag.

Fowkes, F.M., 1962. *Determination of interfacial tensions, contact angles, and dispersion forces in surfaces by assuming additivity of intermolecular interactions in surfaces*. J Phys Chem. 66, 382.

Frampton, J.E., 2016. *Sublingual sufentanil: A review in acute postoperative pain*. Drugs. 76, 719-729.

Gardan, J., 2015. *Additive manufacturing technologies: state of the art and trends*. Int J Prod Res. 54, 3118-3132.

Garsuch, V., Breitkreutz, J., 2009. *Novel analytical methods for the characterization of oral wafers*. Eur J Pharm Biopharm. 73, 195-201.

Garsuch, V., Breitkreutz, J., 2010. *Comparative investigations on different polymers for the preparation of fast-dissolving oral films*. J Pharm Pharmacol. 62, 539-545.

Garsuch, V.I., 2009. *Preparation and characterization of fast-dissolving oral films for pediatric use*. Thesis, Heinrich Heine University, Düsseldorf.

Gebhardt, A., 2016. *Generative Fertigungsverfahren - Additive Manufacturing und 3D-Drucken für Prototyping – Tooling – Produktion*, 4. Ed. Carl Hanser Verlag, Munich.

Greenland, S.J., 1997. *Method of producing zone specific peelable heat seals for flexible packaging applications*. US 6245176B1.

Grellmann, W., 2007. *Polymer testing*, 1. Ed. Carl Hanser Verlag, Munich.

Groeneweg, G., 1998. *Manual stamp dispenser*. US 6171439B1.

Hariharan, M., Bogue, A., 2009. *Orally dissolving film strips (ODFS): the final evolution of orally dissolving dosage forms*. Drug Deliv Technol. 9, 24-29.

Hermes, M.F.K., 2012. *Kindgerechte, niedrigdosierte Zubereitungen mit Enalaprilmaleat*. Thesis, Heinrich Heine University, Düsseldorf.

Hoffmann, E.M., 2012. *Flexible Arzneistoffbeladung orodispersibler Filme durch Bedrucken*. Thesis, Heinrich Heine University, Düsseldorf.

Hoffmann, E.M., Breitenbach, A., Breitkreutz, J., 2011. *Advances in orodispersible films for drug delivery*. Expert Opin Drug Delivery. 8, 299-316.

ICH - International Council for Harmonisation of Technical Requirements for Pharmaceuticals for Human Use, 2003. *Stability Testing of New Drug Substances and Products*, Q1A(R2).

ICH - International Council for Harmonisation of Technical Requirements for Pharmaceuticals for Human Use, 2005. *Validation of analytical procedures: Text and methodology*, Q2 (R1).

Jansen, J., Horstmann, M., 2014. *Gut abschneiden-Feindosierung in oralen Filmen*. TechnoPharm. 4, 306-313.

Janßen, E.M., Schliephacke, R., Breitenbach, A., Breitkreutz, J., 2013. *Drug-printing by flexographic printing technology - A new manufacturing process for orodispersible films*. Int J Pharm. 441, 818-825.

Jones, D., 2007. *Steps on the road to personalized medicine*. Nat Rev Drug Discovery. 6, 770-771.

Karlsson, A., Singh, S.K., 1998. *Thermal and mechanical characterization of cellulose acetate phthalate films for pharmaceutical tablet coating: Effect of humidity during measurements*. Drug Dev Ind Pharm. 24, 827-834.

Khinast, J., Brenn, G., Zimmer, A., Eichinger, R., Bauer, W., 2009. *System and method for manufacturing a medication*. US 2011156315A1.

Kind, M., Dorfman, A., 1995. *Motorized dispenser for continous strip food product and method of dispensing the product*. US 5579669B1.

Klingmann, V., 2017. *Acceptability of mini-tablets in young children: results from three prospective cross-over studies*. AAPS PharmSciTech. 18, 263-266.

Klingmann, V., Spomer, N., Lerch, C., Stoltenberg, I., Fromke, C., Bosse, H.M., Breitkreutz, J., Meissner, T., 2013. *Favorable acceptance of mini-tablets compared with syrup: A randomized controlled trial in infants and preschool children*. J Pediatr. 163, 1728-1732.

Krampe, R., 2015. *Orodispersible Filme mit schwerlöslichem, hochdosiertem Arzneistoff: Herstellungstechniken und biorelevante Beurteilung*. Thesis, Heinrich Heine University, Düsseldorf.

Krampe, R., Visser, J.C., Frijlink, H.W., Breitkreutz, J., Woerdenbag, H.J., Preis, M., 2016. *Oromucosal film preparations: points to consider for patient centricity and manufacturing processes*. Expert Opin Drug Delivery. 13, 493-506.

Kulkarni, A., Deokule, H., Mane, M., Ghadge, D., 2010. *Exploration of different polymers for use in the formulation of oral fast dissolving strips*. J Curr Pharm Res. 2, 33-35.

Labrecque, N.F., 1990. *Cutting apparatus for wrap film*. US 5044241A.

Lee, S., 1999. *Adhesive tape dispenser*. US 6176409B1.

Lee, Y., Kim, K., Kim, M., Choi, D.H., Jeong, S.H., 2017. *Orally disintegrating films focusing on formulation, manufacturing process, and characterization*. J Pharm Invest. 47, 183-201.

Lehrke, I., Vollmer, U., Maier, S., 2004. *Primary packaging unit for flat administration forms*. EP 1824756B1.

Leichter, R.A., Blake, W.S., 2003. *Dispenser*. US 7040503B2.

Ligon, S.C., Liska, R., Stampfl, J., Gurr, M., Mülhaupt, R., 2017. *Polymers for 3D printing and customized additive manufacturing*. Chem Rev. 117, 10212-10290.

Lindert, S., 2016. *Entwicklung und Charakterisierung filmförmiger Zubereitungen zur oromukosalen Anwendung von Peptiden*. Thesis, Heinrich Heine University, Düsseldorf.

Ma, Q., Lu, A.Y.H., 2011. *Pharmacogenetics, pharmacogenomics, and individualized medicine*. Pharmacol Rev. 63, 437-459.

MacDonald, M.G., Getson, P.R., Glasgow, A.M., Miller, M.K., Boeckx, R.L., Johnson, E.L., 1987. *Propylene glycol: Increased incidence of seizures in low birth weight infants*. Pediatrics. 79, 622-625.

Messina, K., 2004. *Photo corner/mounting square dispenser box*. US 2006113423A1.

Mitra, B., Chang, J., Wu, S.J., Wolfe, C.N., Ternik, R.L., Gunter, T.Z., Victor, M.C., 2017. *Feasibility of mini-tablets as a flexible drug delivery tool*. Int J Pharm. 525, 149-159

Niese, S., Breitkreutz, J., Quodbach, J., 2019. *Development of a dosing device for individualized dosing of orodispersible warfarin films*. Int J Pharm. 561, 314-323.

Niese, S., Quodbach, J., 2018. *Application of a chromatic confocal measurement system as new approach for in-line wet film thickness determination in continuous oral film manufacturing processes*. Int J Pharm. 551, 203-211.

Niese, S., Quodbach, J., 2019. *Formulation development of a continuously manufactured orodispersible film containing warfarin sodium for individualized dosing*. Eur J Pharm Biopharm. 136, 93-101.

Owens, D.K., Wendt, R.C., 1969. *Estimation of the surface free energy of polymers*. J Appl Polym Sci. 13, 1741-1747.

Paediatric Formulary Committee, 2014. *British National Formulary for children - The authority on the selection and use of medicines in children*. BMJ Group, the Royal Pharmaceutical Society of Great Britain and RCPCH Publication Ltd., London.

Panchal, M.S., Patel, H., Bagada, A., Vadalia, K.R., 2012. *Formulation and evaluation of mouth dissolving film of ropinirole hydrochloride by using pullulan polymers*. Int J Pharmaceut Res Allied Sci. 1, 60-72.

Pardeike, J., Strohmeier, D.M., Schrödl, N., Voura, C., Gruber, M., Khinast, J.G., Zimmer, A., 2011. *Nanosuspensions as advanced printing ink for accurate dosing of poorly soluble drugs in personalized medicines*. Int J Pharm. 420, 93-100.

Patel, A.R., Prajapati, D.S., Raval, J.A., 2010. *Fast dissolving films (FDFs) as a newer venture in fast dissolving dosage forms*. Int J Drug Dev Res. 2, 232-246.

PDCO - Paediatric Committee at the European Medicines Agency, 2013. *Inventory of paediatric therapeutic needs - Cardiovascular therapeutic area*, EMA/PDCO/246339/2013.

Ph.Eur 9.0, 2017a. *2.9.6 Uniformity of content of single-dose preparations*, in: European Pharmacopoeia Comission (Ed.), European Pharmacopoeia. European Directorate for the Quality of Medicines & Healthcare (EDQM), Strasbourg, France.

Ph.Eur 9.0, 2017b. *2.9.27 Uniformity of mass of delivered doses from mutidose containers*, in: European Pharmacopoeia Comission (Ed.), European Pharmacopoeia. European Directorate for the Quality of Medicines & Healthcare (EDQM), Strasbourg, France.

Ph.Eur 9.0, 2017c. *Warfarin-sodium*, in: European Pharmacopoeia Comission (Ed.), European Pharmacopoeia. European Directorate for the Quality of Medicines & Healthcare (EDQM), Strasbourg, France.

Ph.Eur 9.1, 2017. *2.9.40 Uniformity of Dosage Units*, in: European Pharmacopoeia Comission (Ed.), European Pharmacopoeia. European Directorate for the Quality of Medicines & Healthcare (EDQM), Strasbourg, France.

Ph.Eur 9.3, 2018a. *Oromucosal Preparations*, in: European Pharmacopoeia Comission (Ed.), European Pharmacopoeia. European Directorate for the Quality of Medicines & Healthcare (EDQM), Strasbourg, France.

Ph.Eur 9.3, 2018b. *Tablets*, in: European Pharmacopoeia Comission (Ed.), European Pharmacopoeia. European Directorate for the Quality of Medicines & Healthcare (EDQM), Strasbourg, France.

PMC, 2017. *The Personalized Medicine Coalition. The personalized medicine report 2017* [Accessed 02.10.2018]. http://www.personalizedmedicinecoalition.org/Userfiles/PMC-Corporate/file/The-Personalized-Medicine-Report1.pdf.

Precitec, 2018. *Precitec GmbH, Measurement principle* [Accessed 02.07.2018]. http://www.precitec.de/produkte/optische-messtechnik/so-funktionierts/#tab2.

Preis, M., Breitkreutz, J., Sandler, N., 2015. *Perspective: Concepts of printing technologies for oral film formulations*. Int J Pharm. 494, 578-584.

Preis, M., Gronkowsky, D., Grytzan, D., Breitkreutz, J., 2014a. *Comparative study on novel test systems to determine disintegration time of orodispersible films*. J Pharm Pharmacol. 66, 1102-1111.

Preis, M., Knop, K., Breitkreutz, J., 2014b. *Mechanical strength test for orodispersible and buccal films*. Int J Pharm. 461, 22-29.

Preis, M., Pein, M., Breitkreutz, J., 2012. *Development of a taste-masked orodispersible film containing dimenhydrinate*. Pharmaceutics. 4, 551-562.

Preis, M., Woertz, C., Kleinebudde, P., Breitkreutz, J., 2013. *Oromucosal film preparations: classification and characterization methods*. Expert Opin Drug Delivery. 10, 1303-1317.

Repka, M.A., Gutta, K., Prodduturi, S., Munjal, M., Stodghill, S.P., 2005. *Characterization of cellulosic hot-melt extruded films containing lidocaine*. Eur J Pharm Biopharm. 59, 189-196.

Repka, M.A., Prodduturi, S., Stodghill, S.P., 2003. *Production and characterization of hot-melt extruded films containing clotrimazole*. Drug Dev Ind Pharm. 29, 757-765.

Reynolds, K.K., Valdes, R., Hartung, B.R., Linder, M.W., 2007. *Individualizing warfarin therapy*. Pers Med. 4, 11-31.

Roche Registration, 2018. *Summary of product characteristics of Herceptin® i.v. Approval number: EU/1/00/145/001* [Accessed 10.10.2018]. https://www.roche.de/dok/Herceptin-reg-150-mg-fachinfo-0-na-attach.pdf.

Rosenberg, J.M., Nathan, J.P., Plakogiannis, F., 2002. *Weight variability of pharmacist-dispensed split tablets*. J Am Pharm Assoc. 42, 200-205.

Ross, N., 2003. *Powered dispenser for interconnected strip bandages*. US 7077289B2.

Rudawska, A., Jacniacka, E., 2009. *Analysis for determining surface free energy uncertainty by the Owen–Wendt method*. Int J Adhes Adhes. 29, 451-457.

Sakanishi, Y., 2006. *Coating film transfer tool*. US 7784517B2.

Saša, B., Odon, P., Stane, S., Julijana, K., 2006. *Analysis of surface properties of cellulose ethers and drug release from their matrix tablets*. Eur J Pharm Sci. 27, 375-383.

Schellekens, H., Aldosari, M., Talsma, H., Mastrobattista, E., 2017. *Making individualized drugs a reality*. Nat Biotechnol. 35, 507-513.

Schoemakers, J., Grummel, A., 2002. *Dosing stick containing rod-shaped tablets*. WO 02/102296A1.

Shastry, B.S., 2006. *Pharmacogenetics and the concept of individualized medicine*. Pharmacogenomics J. 6, 16-21.

Sheffield, W., 2011. *Dispenser for an orally dissolvable strip*. US 8499965B2.

Shimoda, H., Taniguchi, K., Nishimura, M., Matsuura, K., Tsukioka, T., Yamashita, H., Inagaki, N., Hirano, K., Yamamoto, M., Kinosada, Y., Itoh, Y., 2009. *Preparation of a fast dissolving oral thin film containing dexamethasone: A possible application to antiemesis during cancer chemotherapy*. Eur J Pharm Biopharm. 73, 361-365.

Sobhani, P., Christopherson, J., Ambrose, P.J., Corelli, R.L., 2008. *Accuracy of oral liquid measuring devices: Comparison of dosing cup and oral dosing syringe*. Ann Pharmacother. 42, 46-52.

Speer, I., Steiner, D., Thabet, Y., Breitkreutz, J., Kwade, A., 2018. *Comparative study on disintegration methods for oral film preparations*. Eur J Pharm Biopharm. 132, 50-61.

Spomer, N., Klingmann, V., Stoltenberg, I., Lerch, C., Meissner, T., Breitkreutz, J., 2012. *Acceptance of uncoated mini-tablets in young children: Results from a prospective exploratory cross-over study*. Arch Dis Child. 97, 283-286.

Standing, J.F., Tuleu, C., 2005. *Paediatric formulations - Getting to the heart of the problem*. Int J Pharm. 300, 56-66.

Stanković, M., Frijlink, H.W., Hinrichs, W.L.J., 2015. *Polymeric formulations for drug release prepared by hot melt extrusion: application and characterization*. Drug Discovery Today. 20, 812-823.

Stegemann, S., Ecker, F., Maio, M., Kraahs, P., Wohlfart, R., Breitkreutz, J., Zimmer, A., Bar-Shalom, D., Hettrich, P., Broegmann, B., 2010. *Geriatric drug therapy: Neglecting the inevitable majority*. Ageing Res Rev. 9, 384-398.

Stegemann, S., Gosch, M., Breitkreutz, J., 2012. *Swallowing dysfunction and dysphagia is an unrecognized challenge for oral drug therapy*. Int J Pharm. 430, 197-206.

Steiner, D., Finke, J.H., Kwade, A., 2018. *Instant ODFs – Development of an intermediate, nanoparticle-based product platform for individualized medication*. Eur J Pharm Biopharm. 126, 149-158.

Sternberger-Rützel, E., Daffner, R., Urbanetz, N.A., 2018. *What does individualized medicine mean in drug product development and manufacturing?* Pharm Ind. 80, 770-784.

Stoltenberg, I., Breitkreutz, J., 2011. *Orally disintegrating mini-tablets (ODMTs) – A novel solid oral dosage form for paediatric use*. Eur J Pharm Biopharm. 78, 462-469.

Ström, G., Fredriksson, M., Stenius, P., 1987. *Contact angles, work of adhesion, and interfacial tensions at a dissolving hydrocarbon surface*. J Colloid Interface Sci. 119, 352-361.

Susarla, R., Sievens-Figueroa, L., Bhakay, A., Shen, Y., Jerez-Rozo, J.I., Engen, W., Khusid, B., Bilgili, E., Romañach, R.J., Morris, K.R., Michniak-Kohn, B., Davé, R.N., 2013. *Fast drying of biocompatible polymer films loaded with poorly water-soluble drug nano-particles via low temperature forced convection*. Int J Pharm. 455, 93-103.

Tanner, S., Wells, M., Scarbecz, M., McCann, B.W., 2014. *Parents' understanding of and accuracy in using measuring devices to administer liquid oral pain medication*. J Am Dent Assoc. 145, 141-149.

Teng, J., Song, C.K., Williams, R.L., Polli, J.E., 2002. *Lack of medication dose uniformity in commonly split tablets*. J Am Pharm Assoc. 42, 195-199.

Thabet, Y., Breitkreutz, J., 2018. *Orodispersible films: Product transfer from lab-scale to continuous manufacturing*. Int J Pharm. 535, 285-292.

Thabet, Y., Klingmann, V., Breitkreutz, J., 2018a. *Drug formulations: standards and novel strategies for drug administration in pediatrics*. J Clin Pharmacol. 58, 26-35.

Thabet, Y., Lunter, D., Breitkreutz, J., 2018b. *Continuous inkjet printing of enalapril maleate onto orodispersible film formulations*. Int J Pharm. 546, 180-187.

Thabet, Y., Lunter, D., Breitkreutz, J., 2018c. *Continuous manufacturing and analytical characterization of fixed-dose, multilayer orodispersible films*. Eur J Pharm Sci. 117, 236-244.

Upcraft, S., Fletcher, R., 2003. *The rapid prototyping technologies*. Assembly Automation. 23, 318-330.

van Riet-Nales, D.A., de Neef, B.J., Schobben, A.F.A.M., Ferreira, J.A., Egberts, T.C.G., Rademaker, C.M.A., 2013. *Acceptability of different oral formulations in infants and preschool children*. Arch Dis Child. 98, 725-731.

van Santen, E., Barends, D.M., Frijlink, H.W., 2002. *Breaking of scored tablets: A review*. Eur J Pharm Biopharm. 53, 139-145.

Visser, J.C., Dohmen, W.M.C., Hinrichs, W.L.J., Breitkreutz, J., Frijlink, H.W., Woerdenbag, H.J., 2015a. *Quality by design approach for optimizing the formulation and physical properties of extemporaneously prepared orodispersible films*. Int J Pharm. 485, 70-76.

Visser, J.C., Weggemans, O.A.F., Boosman, R.J., Loos, K.U., Frijlink, H.W., Woerdenbag, H.J., 2017a. *Increased drug load and polymer compatibility of bilayered orodispersible films*. Eur J Pharm Sci. 107, 183-190.

Visser, J.C., Woerdenbag, H.J., Crediet, S., Gerrits, E., Lesschen, M.A., Hinrichs, W.L.J., Breitkreutz, J., Frijlink, H.W., 2015b. *Orodispersible films in individualized pharmacotherapy: The development of a formulation for pharmacy preparations*. Int J Pharm. 478, 155-163.

Visser, J.C., Woerdenbag, H.J., Hanff, L.M., Frijlink, H.W., 2017b. *Personalized medicine in pediatrics: The clinical potential of orodispersible films*. AAPS PharmSciTech. 18, 267-272.

Vuddanda, P.R., Alomari, M., Dodoo, C.C., Trenfield, S.J., Velaga, S., Basit, A.W., Gaisford, S., 2018. *Personalisation of warfarin therapy using thermal ink-jet printing*. Eur J Pharm Sci. 117, 80-87.

Walsh, J., Bickmann, D., Breitkreutz, J., Chariot-Goulet, M., EuPFI, 2011. *Delivery devices for the administration of paediatric formulations: overview of current practice, challenges and recent developments*. Int J Pharm. 415, 221-231.

Wening, K., Breitkreutz, J., 2010. *Novel delivery device for monolithical solid oral dosage forms for personalized medicine*. Int J Pharm. 395, 174-181.

Wening, K., Breitkreutz, J., 2011. *Oral drug delivery in personalized medicine: Unmet needs and novel approaches*. Int J Pharm. 404, 1-9.

Wong, K.V., Hernandez, A., 2012. *A review of additive manufacturing*. ISRN Mechanical Engineering. 2012, 1-10.

Wörtz, C., 2015. *Entwicklung und Charakterisierung von orodispersiblen Polymerfilmen mit suspendiertem Arzneistoff*. Thesis, Heinrich Heine University, Düsseldorf.

Young, T., 1805. *An essay on the cohesion of fluids*. Philos Trans R Soc London. 95, 65-87.

Yu, H.C.M., Chan, T.Y.K., Critchley, J.A.J.H., Woo, K.S., 1996. *Factors determining the maintenance dose of warfarin in chinese patients*. Q J Med. 89, 127-136.

Yuan, X., 2013. *Drug dispensing and dosing method and device*. US 2014242098A1.

7. Danksagung

Die vorliegende Arbeit entstand unter der Leitung von Prof. Jörg Breitkreutz und der Betreuung von Dr. Julian Quodbach im Rahmen meiner Tätigkeit als wissenschaftliche Mitarbeiterin am Institut für Pharmazeutische Technologie und Biopharmazie der Heinrich-Heine-Universität Düsseldorf.

Mein besonderer Dank gilt Dr. Julian Quodbach, der durch seine umfassende Betreuung einen wesentlichen Anteil zum Entstehen dieser Arbeit beigetragen hat. Besonders dankbar bin ich für die vielen motivierenden und aufbauenden Gespräche zu Zeiten der Verunsicherung und Verzweiflung meinerseits. Sein immerwährender Glaube an mich und meine Arbeit haben mir auch in den frustrierenden Momenten der letzten Jahre das nötige Durchhaltevermögen gegeben. Dazu kommen seine ständige Ansprechbarkeit und Diskussionsbereitschaft bei unerwarteten Ergebnissen sowie aber auch die gemeinsame Freude bei erreichten Erfolgen. Vielen Dank Julian, dass Du einfach immer ein offenes Ohr hattest!

Meinem Doktorvater Prof. Jörg Breitkreutz danke ich für die freundliche Aufnahme am Institut und die Möglichkeit sehr frei an der eigenen Arbeit zu forschen. In Erinnerung werden mir besonders Ihre kreativen Ideen bleiben. Außerordentlich dankbar bin ich Ihnen für die Ermöglichung und Ermutigung zur Teilnahme an diversen Konferenzen, Symposien und Seminaren, die neben dem für die Arbeit relevanten Inhalten auch meinen persönlichen Horizont erweitert haben.

Prof. Peter Kleinebudde danke ich für die vielen konstruktiven und kritischen Fragen und Anregungen in Fokusgruppen-Sitzungen sowie bei Vorträgen, die dazu beitrugen auch mal mit einem anderen Blickwinkel auf die Problempunkte der Arbeit zu schauen. Vielen Dank Ihnen, auch für die Übernahme des Koreferats dieser Arbeit.

Den guten Seelen des Instituts, Dorothee Eikeler, Dorothee Hetkämper-Flockert, Dr. Klaus Knop, Lisa Long, Karin Matthée, Annemarie Schmitz und Stefan Stich danke ich für die Unterstützung bei allen alltäglichen Fragen und Problemen.
Dorothee Eikeler und Karin Matthée danke ich besonders für ihre Unterstützung bei der Auswertung zahlreicher Spannungs-Dehnungs-Kurven sowie Karin Matthée auch für die Durchführung von Karl-Fischer-Titrationen und ein lustiges gemeinsames AFL-Praktikum. Außerdem denke ich gerne an die netten Gespräche in Eurem Büro zurück.

Dr. Klaus Knop danke ich für das Lösen diverser Knoten in meinem Kopf sowie seine immerwährende Ansprechbarkeit. Vielen Dank auch für das Korrekturlesen dieser Arbeit.
Lisa Long danke ich dafür, dass sie einfach immer da war, uns zuverlässig mit Kaffee und Eis versorgt hat und mit ihrer fröhlichen Art immer für ein Pläuschchen zu haben war.
Stefan Stich danke ich für die Anfertigung der Halterung für den optischen Sensor an der kontinuierlichen Filmziehbank.

Allen Doktorandinnen und Doktoranden aus dem Institut danke ich für eine schöne gemeinsame Zeit, gesprächige Kaffeepausen, spaßige Abende und unvergessliche Reisen zu Konferenzen und Seminaren. Mein besonderer Dank gilt Dr. Elisabeth Lenz, die mir den Einstieg am Institut und in die Promotion sehr erleichtert hat und mir zu Beginn immer mit einem Rat zur Seite stand. Außerdem danke ich Dr. Yasmin Thabet, die mich in die Geheimnisse der oralen Filme und der kontinuierlichen Filmziehbank eingeweiht hat.

Für die engagierte Mitarbeit während des Wahlpflichtpraktikums danke ich Valentine Elezaj und Julia Matros.

Dem Stammtisch Pottwal bin ich sehr dankbar für die Zeit, die wir auch außerhalb der Uni und der Arbeit miteinander verbracht haben und für die Freundschaften, die in den letzten drei Jahren neu entstanden sind oder sich weiter gefestigt haben. Letzteres gebührt Carolin Korte, der ich sehr dankbar bin, dass wir nach der einmaligen Zeit im Studium in Münster auch im AK Q die Promotion gemeinsam durchgezogen haben.

Ein ganz besonderer Dank gilt vor allem den Menschen, die mich außerhalb des Institutes auf dem Weg zu dieser Arbeit begleitet haben und immer Verständnis für meine begrenzte Freizeit gezeigt haben.
Stefan, Anika, Lara und Yannick Bartholomé danke ich für ihre teils schon ewig währende Freundschaft und das Bewusstsein, dass ich mich immer auf Euch verlassen kann.
Meiner Familie danke ich für die bedingungslose Unterstützung beim Verfolgen meiner Ziele sowie den Rückhalt und die Motivation, die ich immer zu Hause bei meinen Eltern und Großeltern erhielt.
Meinem Bruder danke ich für seine Hilfestellungen im Umgang mit der CAD-Software besonders zu Beginn der Promotion und seinen Tipps und Tricks bei jeglichen Fragestellungen technischer Art. Vielen Dank auch für die Hilfe bei der Anfertigung der Klingen für das Dosiergerät.

A special thanks goes to my parents and my American family for the possibility to spend a high school exchange year in the USA. This great experience remarkably influenced my personal development and improved my language skills, which allowed me to prepare this thesis in English.

Zum Schluss gilt mein Dank Martin, der wohl am meisten unter den turbulenten und stressigen Zeiten der letzten Jahre leiden musste, die im Rahmen dieser Arbeit auftraten und teilweise bis nach Hause anhielten. Von Herzen danke ich Dir für die Unterstützung diese Arbeit erfolgreich zu Ende zu bringen, für die Gin Tonics nach langen Tagen in der Uni, um die angespannte und gestresste Laune zu verbessern und für die vielen geopferten Wochenenden.

8. Eidesstattliche Erklärung

Hiermit erkläre ich gemäß §5 Absatz 1 der Promotionsordnung der Mathematisch-Naturwissenschaftlichen Fakultät der Heinrich-Heine-Universität Düsseldorf an Eides Statt, dass die Dissertation von mir selbstständig und ohne unzulässige fremde Hilfe unter Beachtung der „Grundsätze zur Sicherung guter wissenschaftlicher Praxis an der Heinrich-Heine-Universität Düsseldorf“ erstellt worden ist und dass ich diese in der vorgelegten oder in ähnlicher Form noch bei keiner anderen Fakultät eingereicht habe.

Düsseldorf, den

_____

Svenja Niese